AGENCE NATIONALE DE LA RECHERCHE ANR	Compte-rendu de fin de projet	

Projet ANR-15-CE09-0009

3DCLEAN (3D CataLytic Environmental lAb at the Nanoscale)

Programme CE09 2015

Ce document est à remplir par le coordinateur en collaboration avec les partenaires du projet. L'ensemble des partenaires doit avoir une copie de la version transmise à l'ANR.

Ce modèle doit être utilisé uniquement pour le compte-rendu de fin de projet.

A IDENTIFICATION

Acronyme du projet	3DCLEAN
Titre du projet	**3D C**ata**L**ytic **E**nvironmental l**A**b at the **N**anoscale
Coordinateur du projet (société/organisme)	Thierry Epicier INSA Lyon (MATEIS, umr CNRS 5510)
Période du projet (date de début – date de fin)	30/11/2015 29/05/2019 prolongé au 30/11/2019
Site web du projet, le cas échéant	http://www.clym.fr/3DCLEAN_web/3DCLEAN-ANR.html

Rédacteur de ce rapport	
Civilité, prénom, nom	M. Thierry Epicier
Téléphone	0687883069
Adresse électronique	Thierry.epicier@insa-lyon.fr
Date de rédaction	28/11/2019

Si différent du rédacteur, indiquer un contact pour le projet	
Civilité, prénom, nom	
Téléphone	
Adresse électronique	

Liste des partenaires présents à la fin du projet (société/organisme et responsable scientifique)	MATEIS (T.E.) IFPEN (A-S. Gay) IPCMS (O. Ersen) CREATIS (V. Maxim)

B RESUME CONSOLIDE PUBLIC

Il est nécessaire de respecter les instructions ci-dessous.

B.1 INSTRUCTIONS POUR LES RESUMES CONSOLIDES PUBLICS

B.2 RESUME CONSOLIDE PUBLIC EN FRANÇAIS

Titre d'accroche du projet *(environ 80 caractères espaces compris)*

Microscopie Electronique en Transmission environnementale operando de nanocatalyseurs

Titre 1 : situe l'objectif général du projet et sa problématique (150 caractères max espaces compris)

Vers une caractérisation chimique quantitative et 3D in situ et operando de nanoparticules métalliques pour la catalyse hétérogène

Paragraphe 1 : *(environ 1200 caractères espaces compris)*

Dans le contexte énergétique et environnemental mondial du 21° siècle, la production industrielle doit être meilleure, plus propre/efficace/économique. Des efforts sont ainsi requis dans le domaine de la catalyse qui joue un rôle prépondérant dans plus de 80 % des procédés chimiques. 3DCLEAN s'appuie sur la Microscopie Electronique en Transmission operando ou "Environnementale" (ETEM) pour améliorer la compréhension de procédés catalytiques et promouvoir le développement de nouveaux catalyseurs. Il s'agit d'étudier des nanomatériaux sous gaz et en température directement in situ dans le microscope, du point de vue de l'évolution morphologique, chimique et structurale jusqu'à l'échelle atomique. 2 équipements spécifiques, à Lyon (MATEIS) et à Strasbourg (IPCMS) sont utilisés pour mettre en œuvre de nouvelles approches : (i) un microscope ETEM dédié pour le suivi de l'évolution 3D de catalyseurs quasiment en temps réel, et (ii) un microscope équipé d'une cellule environnementale pour l'analyse des gaz réactionnels des réactions étudiées. 2 systèmes sont fournis par IFPEN : des nanocatalyseurs Pd de réactions d'hydrogénation (sélective, production CH_4), et des catalyseurs base Co pour la synthèse Fischer-Tropsch. Des traitements d'image spécifiques nécessaires à la quantification morphologique seront assurés par CREATIS.

Titre 2 : précise les méthodes ou technologies utilisées (150 caractères max espaces compris)

Tomographie rapide 'temps réel' et analyse des gaz de réaction lors du conditionnement des catalyseurs ou en cours de fonctionnement

Paragraphe 2 : *(environ 1200 caractères espaces compris)*

Lors du conditionnement (étuvage, calcination, réduction) de nanocatalyseurs métalliques (nanoparticules NPs), diverses évolutions peuvent amorcer une future dégradation (désactivation) de leurs propriétés catalytiques lors de leur utilisation future en conditions réelles. Ainsi, la coalescence de particules ou leur empoisonnement conduisent à une réduction des surfaces actives. Comprendre ces processus pour les contrôler requiert d'observer les NPs in situ en ETEM. Les évolutions morphologiques doivent idéalement être suivies en 3D : ceci fait l'objet du développement d'une approche de tomographie rapide, où l'acquisition de la série de projections nécessaires s'opère en quelques secondes afin que l'évolution soit négligeable au cours de l'enregistrement. Un logiciel spécifique de reconstruction adapté à des images bruitées permet d'optimiser la reconstruction 3D à partir de micrographies à faible rapport signal-sur-bruit (temps d'acquisition très courts). Par ailleurs, l'analyse des gaz de la réaction catalytique est fondamentale pour prouver son occurrence et quantifier son efficacité notamment lors de la désactivation des nanocatalyseurs. Pour ce faire, un spectromètre de masse a été adapté à une cellule environnementale utilisée dans un microscope conventionnel fonctionnant sous haut vide.

Résultats majeurs du projet *(environ 600 caractères espaces compris)*

La tomographie rapide appliquée aux catalyseurs en conditions réactionnelles a permis de suivre l'évolution d'un même objet lors de traitements in situ tels la réduction sous hydrogène en température (catalyseurs $Pd@SiO_2$) ou la calcination de catalyseurs Pd/Al_2O_3 sous air ou sous oxygène. L'analyse chimique par spectrométrie de masse a été rendue opérationnelle grâce au système $Ni@Al_2O_3$ (méthanation du CO_2). L'activité de traitement d'image offre de nouvelles perspectives : quantification des facettes cristallographiques des NPs (capitale par rapport à leur activité), suivi de trajectoires de NPs, optimisation de routines grâce à l'intelligence artificielle (*machine learning*).

Production scientifique et brevets depuis le début du projet (environ 500 caractères espaces compris)

La production scientifique repose sur un grand nombre de **communications en congrès** et plusieurs **publications** (respectivement **43** et **16** - doublons congrès/RCL compris -), la plupart multipartenaires. La synergie 3DCLEAN a également été à l'origine d'un atelier "Défi CNRS" en 2016 : GLEEM (Gas & Liquid Environmental Electron Microscopy, www.cnrs.fr/mi/spip.php?article953), lui-même impliqué dans la création en 2018 du GDR 2015 national Nanoperando associant les communautés 'X' (i.e. synchrotron) et microscopies (AFM/STEM, électronique) sur la thématique environnemental / operando de nano-objets.

Illustration

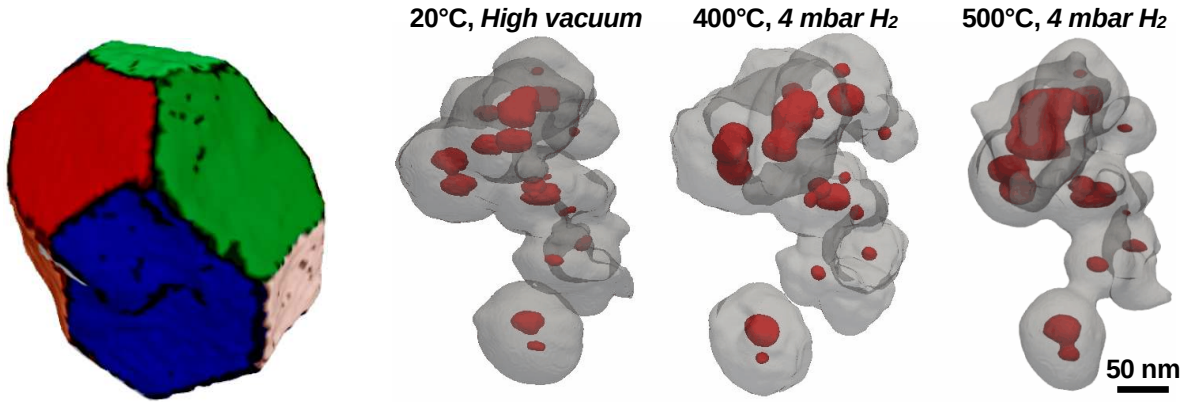

Tomographie de catalyseurs $Pd@SiO_2$ en évolution dynamique sous conditions de gaz et de température en Microscopie Electronique en Transmission Environnementale (ETEM) : à gauche, analyse 3D quantitative des facettes cristallographiques d'une NP de Pd (ETEM en cellule ; IPCMS-CREATIS) ; à droite : suivi en 'in situ rapide' dans l'ETEM dédié (MATEIS-IFPEN).

Informations factuelles

3DCLEAN (*3D Catalytic Environmental Lab at the Nanoscale*) est un projet PRC de 42 mois (étendu à 48 mois) regroupant le laboratoire coordonnateur MATEIS (Université de Lyon, INSA de Lyon, UCBL Lyon 1, UMR CNRS 5510), IFPEN (centre de recherches de Solaize), IPCMS (Université de Strasbourg, UMR CNRS 7504) et CREATIS (Université de Lyon, INSA de Lyon, UMR CNRS 5220, INSERM U1206, UCBL Lyon 1, UJM St-Etienne). Il a porté sur un développement expérimental en microscopie électronique environnementale dans le domaine de la catalyse (recherche fondamentale à visée applicative). Le projet a débuté le 30/11/2015 et a bénéficié d'une aide ANR de 618 488 € pour un coût global d'environ 1 950 k€.

B.3 RESUME CONSOLIDE PUBLIC EN ANGLAIS

Titre d'accroche du projet *(environ 80 caractères espaces compris)*

Operando Environmental Electron Microscopy of nanaocatalysts

Titre 1 : situe l'objectif général du projet et sa problématique (150 caractères max espaces compris)

Towards a quantitative chemical 3D, in situ and operando characterization of metallic nanoparticles for heterogeneous catalysis

Paragraphe 1 : *(environ 1200 caractères espaces compris)*

In the energetic and environmental context of the 21st century, the industrial production has to be better, cleaner, more efficient and cost-effective. Efforts are thus required in the domain of catalysis, which plays a preponderant role in more than 80% of chemical processes. 3DCLEAN relies on operando or 'environmental' Transmission Electron Microscopy (ETEM) to improve the understanding of catalytic processes and promote the development of new catalysts. The aim is to study nanomaterials under gas and temperature directly in situ in the microscope, from the point of view of their morphological, chemical and structural evolution down to the atomic level. 2 specific instrument in Lyon (MATEIS) and Strasbourg (IPCMS) are used to implement new approaches: (i) a dedicated ETEM unit of the tracking of 3D evolution of nanocatalysts almost in real time, and (ii) a microscope equipped with an environmental close cell for the analysis of reactants during gas reactions.
2 systems are provided by IFPEN: Pd nanocatalysts for hydrogenation (selective, CH4 production) and Co-based nanocatalysts for the Fischer-Tropsch synthesis. Specific image processing required to the morphological quantification will be performed by CREATIS.

Titre 2 : précise les méthodes ou technologies utilisées (150 caractères max espaces compris)

Fast 'real time' tomography and gas analysis during the conditioning of catalysts or under working conditions

Paragraphe 2 : *(environ 1200 caractères espaces compris)*

During conditioning metallic catalysts (drying, calcination, reduction), various evolutions can lead to a future degradation of their catalytic properties (e.g. de-activation) when they are used under real working conditions. Coalescence of nanoparticles (NPs), poisoning induce a decrease of active surfaces. Understanding these processes in order to control them require to observe NPs in situ in ETEM. Ideally, their morphological evolution must be followed in 3D: this is the objective of our fast tomography approach, where the acquisition of the series of required projections is realized in a few seconds, so that the evolution remain negligible during recording.
A specific software optimized for noisy images allows to improve the 3D reconstruction using micrographs with a weak SNR, as a consequence of their short exposure time. Moreover, the analysis of gases during a catalytic reaction is of a fundamental interest in order to prove their occurrence and quantify their efficiency, especially when de-activation occurs. For this purpose, a residual gas analyzer has been adapted to an environmental close cell used in a conventional (high vacuum) microscope.

Résultats majeurs du projet *(environ 600 caractères espaces compris)*

Fast tomography applied to catalysts in reaction conditions a allowed to follow the evolution of a single object during in situ treatments, like reduction under hydrogen ($Pd@SiO_2$ catalysts) or the calcination of Pd/Al_2O_3 catalysts under air or oxygen.
The chemical analysis through mass spectroscopy with the RGA has been tested with the $Ni@Al_2O_3$ system used for CO_2 methanation. Image processing activities have open new perspectives for the quantification of crystallographic facets of NPs (an important topic regarding their activity), the tracking of NPs trajectories, or the optimization of routines through machine learning.

Production scientifique et brevets depuis le début du projet (environ 500 caractères espaces compris)

The scientific production consists in a large number of communications in conferences and articles in journals (respectively 43 and 16), most of them associating at least 2 partners.
The 3DCLEAN synergy has also helped in the organization of a "Défi CNRS" workshop in 2016 : GLEEM (Gas & Liquid Environmental Electron Microscopy, *www.cnrs.fr/mi/spip.php?article953*). This initiative is also linked to the creation of the national GDR Nanoperando (GDR2015) in 2018, which associates the 'X-Ray' communities (i.e. synchrotron) with microscopists (AFM/STEM, electron M.) on the thematic 'environmental / operando' study of nano-objects.

Illustration

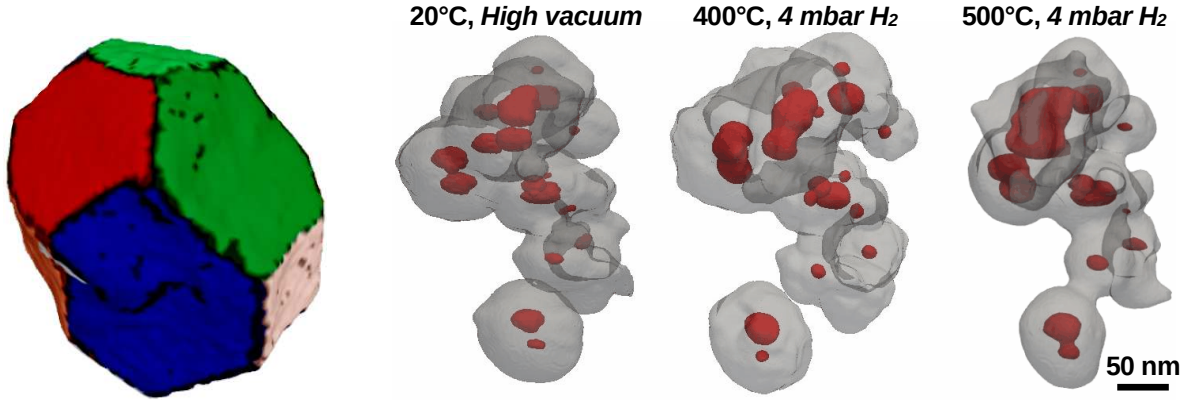

Tomography of Pd@SiO_2 catalysts during their dynamic evolution under gas and temperature in Environmental Transmission Electron Microscopy (ETEM). On the left: 3D quantitative analysis of crystallographic facets of the Pd NP (ETEM in a close-cell, IPCMS-CREATIS). On the right: fast in situ tracking of the same Pd@SiO_2 aggregate during reduction in a dedicated ETEM (MATEIS-IFPEN).

Informations factuelles

3DCLEAN (*3D Catalytic Environmental Lab at the Nanoscale*) is a Collaborative Research Project (PRC) of 42 months (extended to 48 months) associating the coordinator laboratory MATEIS (Université de Lyon, INSA de Lyon, UCBL Lyon 1, UMR CNRS 5510), IFPEN (centre de recherches de Solaize), IPCMS (Université de Strasbourg, UMR CNRS 7504) and CREATIS (Université de Lyon, INSA de Lyon, UMR CNRS 5220, INSERM U1206, UCBL Lyon 1, UJM St-Etienne). The project concerned an experimental development in environmental electron microscopy applied to heterogeneous catalysis (fundamental research for application purposes). It has started on November, 30 2015 and received an aid from the ANR of 618 488 € for a global cost of about 1 950 k€.

C MEMOIRE SCIENTIFIQUE

Mémoire scientifique confidentiel : ~~oui /~~ non

C.1 RESUME DU MEMOIRE

Dans le contexte énergétique et environnemental mondial du 21° siècle, la production industrielle doit être meilleure, plus propre/efficace/économique. Des efforts sont ainsi requis dans le domaine de la catalyse qui joue un rôle prépondérant dans plus de 80 % des procédés chimiques. 3DCLEAN s'appuie sur la Microscopie Electronique en Transmission operando ou "Environnementale" (ETEM) pour améliorer la compréhension de procédés catalytiques et promouvoir le développement de nouveaux catalyseurs. Il s'agit d'étudier des nanomatériaux sous gaz et en température directement in situ dans le microscope, du point de vue de l'évolution morphologique, chimique et structurale jusqu'à l'échelle atomique. 2 équipements spécifiques, à Lyon (MATEIS) et à Strasbourg (IPCMS) sont utilisés pour mettre en œuvre de nouvelles approches : (i) un microscope ETEM dédié pour le suivi de l'évolution 3D de catalyseurs quasiment en temps réel, et un microscope équipé d'une cellule environnementale pour l'analyse des gaz réactionnels des réactions étudiées. 2 systèmes sont fournis par IFPEN : des nanocatalyseurs Pd de réactions d'hydrogénation (sélective, production CH_4), et des catalyseurs base Co pour la synthèse Fischer-Tropsch. Des traitements d'image spécifiques nécessaires à la quantification morphologique seront assurés par CREATIS.
Lors du conditionnement (étuvage, calcination, réduction) de nanocatalyseurs métalliques (nanoparticules NPs), diverses évolutions peuvent amorcer une future dégradation (désactivation) de leurs propriétés catalytiques lors de leur utilisation future en conditions réelles. Ainsi, la coalescence de particules ou leur empoisonnement conduisent à une réduction des surfaces actives. Comprendre ces processus pour les contrôler requiert d'observer les NPs in situ en ETEM. Les évolutions morphologiques doivent idéalement être suivies en 3D : ceci a fait l'objet du développement de la tomographie rapide, où l'acquisition de la série de projections nécessaires s'opère en quelques secondes afin que l'évolution soit négligeable au cours de l'enregistrement. Un logiciel spécifique de reconstruction adapté à des images bruitées permet d'optimiser la reconstruction 3D à partir de micrographies à faible rapport signal-sur-bruit (temps d'acquisition très courts). Par ailleurs, l'analyse des gaz de la réaction catalytique est fondamentale pour prouver son occurrence et quantifier son efficacité notamment lors de la désactivation des nanocatalyseurs. Pour ce faire, un système d'analyse des gaz 'RGA' très sensible couplé à un spectromètre de masse a été adapté à une cellule environnementale dans le microscope.
La tomographie rapide appliquée aux catalyseurs en conditions réactionnelles a permis de suivre l'évolution d'un même objet lors de traitements in situ tels la réduction sous hydrogène en température (catalyseurs $Pd@SiO_2$), ou la calcination sous oxygène ou sous air de catalyseurs Pd/Al_2O_3. L'analyse chimique opérationnelle grâce au RGA a été testée sur plusieurs systèmes dont $Ni@Al_2O_3$ (méthanation du CO_2). Divers traitements d'image ont été développés classiquement pour des mesures de tailles ou de trajectoires de NPs, mais aussi pour le défloutage, le débruitage et la tomographie. De nouvelles perspectives sont apparues : quantification des facettes cristallographiques des NPs (capitale par rapport à leur activité), suivi de trajectoires de NPs, optimisation grâce à l'intelligence artificielle (*machine learning*).

C.2 ENJEUX ET PROBLEMATIQUE, ETAT DE L'ART

Le projet 3DCLEAN se situe dans la problématique de l'expansion de la population mondiale et de ses conséquences importantes du point de vue social, écologique, énergétique, et leurs effets pour l'industrie. Plus spécifiquement sur les aspects de la production énergétique, il est clairement établi que la mise à disposition de nouvelles sources d'énergie 'verte' ne pourra répondre à la demande dans la décennie à venir (pour le transport notamment). En parallèle néanmoins, le déclin progressif des ressources fossiles conventionnelles impose le développement de nouveaux procédés industriels pour la production de biocarburants, les intermédiaires chimiques et l'énergie, par la transformation de sources renouvelables et de biomasse particulière. Cette stratégie combat opportunément l'effet de serre.

Tous ces éléments impactent très fortement les sciences de la catalyse qui dessinent de nombreuses voies de synthèse, conversion et traitement de matières premières (biocarburants, valorisation biochimique ou thermochimique, pyrolyse…) au plan industriel. Une classe importante de nanomatériaux utilisés dans ces procédés correspond aux catalyseurs hétérogènes. Ceux-ci sont constitués d'une phase active, principalement des nanoparticules (NPs) à base de métaux nobles ou des sulfures de métaux de transition, dispersés à la surface d'un support d'oxyde poreux, tel que l'alumine ou la silice-alumine. Il est crucial de bien maîtriser les étapes du conditionnement des catalyseurs. Partant de supports imprégnés par des solutions contenant des complexes à base des métaux catalytiques, il convient de brûler les résidus organiques et de réduire les oxydes métalliques nécessairement formés durant cette calcination, tout en veillant au contrôle de la taille des NPs (la phase active).
Ce contexte nous oriente naturellement vers la Microscopie Electronique en Transmission Environnementale *(ETEM : Environmental Transmission Electron Microscopy)*, une des approches développées dans un rythme exponentiel durant ces 2 dernières décennies. Microscopie électronique, car les NPs sont de taille généralement comprises entre 2 et quelques nanomètres, voire moins pour les agrégats en direction de la catalyse de l'atome isolé. Environnemental, car les avancées technologiques récentes permettent d'introduire du gaz et de chauffer les échantillons in situ, permettant une microscopie in situ, voire operando d'intérêt fondamental pour les nanocatalyseurs.
Ainsi, 3DCLEAN ambitionne d'une part de permettre une microscopie chimiquement quantitative en permettant l'analyse des gaz réactionnels par l'adjonction d'un spectromètre de masse sur une cellule environnementale fermée d'origine commerciale et d'autre part de développer une approche tridimensionnelle in situ aussi rapide que possible pour suivre en quasi-temps réel l'évolution morphologique du système catalytique NPs@support.

C.3 APPROCHE SCIENTIFIQUE ET TECHNIQUE

C.3.1. PRESENTATION DU PROGRAMME GLOBAL DU PROJET 3DCLEAN

Le projet 3DCLEAN est organisé autour des tâches *(Work Packages)* suivantes (plus scientifiquement décrites en ANNEXES (sections F à J) :

WP 1: Preparation of catalysts, catalytic tests and preliminary TEM characterization

Les systèmes catalytiques initialement prévus pour les différentes applications en microscopie environnementale (cf. sous-sections suivantes) ont été fournis par le responsable IFPen *(Pd/alumina, Shape-controlled Co nanoparticles, Pd@silica)* et les tests préliminaires effectués en interne par ce même partenaire. Les 2 premiers systèmes ont notamment été étudiés respectivement lors des thèses de Siddardha Koneti (soutenue le 05/12/2017 à MATEIS, Lyon) et Kassiogé DEMBELE (soutenue le 20/12/2017 à IPCMS, Strasbourg ; ces 2 thèses partiellement impliquées dans le projet n'étaient pas financées par l'ANR). Un quatrième système servant à la réaction de méthanation du CO_2 a été utilisé pour l'analyse des gaz réactionnels et pour la comparaison ETEM/Ecell) : il était constitué de particules de Ni supportées sur alumine delta (δ-alumina). La **Figure 1** illustre les microstructures de ces 4 catalyseurs, et leur évolution en conditions d'études en microscopie environnementale est reportée en ANNEXE F.1.1. Des échantillons d'origine extérieure ont été utilisés ; ils ne seront pas spécialement documentés dans le présent rapport mais se retrouvent dans plusieurs des publications associées au projet (et accréditant 3DCLEAN et le soutien de l'ANR).

WP 2: Purchase, set-up and testing of the RGA analyzer on the HPEC device

Cette tâche était dévolue à l'achat et l'installation d'un spectromètre de masse *(RGA : Residual Gas Analyzer)* sur un porte-objet environnemental 'gaz' (*E-cell*, ou *HPEC : High Pressure Environmental Cell*) disponible sur le microscope JEOL2100F du partenaire IPCMS. L'opération a été réalisée auprès de la société Protochips©(www.protochips.com), fournisseur de l'*Ecell*. Il s'agit du premier système de ce type installé dans le monde, il reste à ce jour l'unique équipement disponible sur l'hexagone.

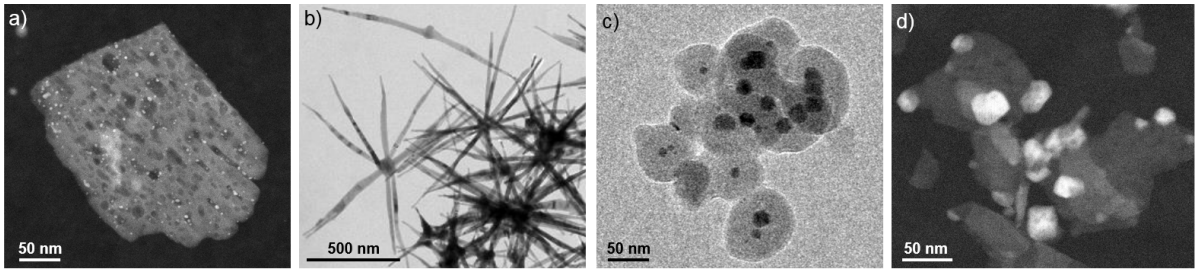

Figure 1 : microstructures 'TEM' des catalyseurs IFPen étudiés au cours du projet. a): nanoparticules de palladium (Pd NPs) sur alumina delta ; ETEM 300 kV, MATEIS-CLYM (image en mode STEM). b) : "nano-oursins" de filaments de Cobalt ; TEM 200 kV, IPCMS. C): agrégats Pd@SiO_2 (TEM 300kV, MATEIS-CLYM). d): NPs de nickel (partiellement oxydées) sur alumine δ ; STEM 200 kV, IPCMS.

WP3: Environmental 2D/3D image processing (fast tomography and morphological analysis)

Cette tâche concernait principalement l'amélioration de l'acquisition et du traitement des séries d'images (projections sous différents angles de vue) nécessaires à la reconstruction tomographique en microscopie électronique (mode TEM).

Un préliminaire était de pouvoir piloter (et accélérer) l'acquisition des données afin d'espérer 'suivre' en 3D l'évolution d'un système nanométrique soumis à une évolution morphologique (structural, chimique) sous l'effet de la température et du gaz en mode environnemental. Cette tâche a été accomplie au travers d'un développement logiciel grâce au protocole de contrôle du microscope ETEM et fourni par son constructeur FEI (*TEMScripting*©). Des acquisitions fiables de quelques secondes (typiquement 10 à 5 secondes) ont ainsi pu être réalisées tout en gardant la zone d'intérêt dans le champ de vue de la caméra (correction des déplacements erratiques en cours de rotation du porte-échantillon). La méthode utilisée (illustrée en ANNEXE H, §.1.3) repose sur une calibration ultra-rapide des mouvements de l'objet (programmation C++ et Visual Basic pour l'interface avec le microscope).

L'acquisition rapide a par ailleurs été rendue possible par l'équipement principal du partenaire MATEIS, financée par l'ANR : une caméra 'Oneview™ Gatan' CMOS optimisé, permettant des acquisitions 2k×2k à 100 images/seconde (ou *frames per second fps*). Grâce à cette caméra à la fois rapide et sensible, nous avons pu faire l'économie quasi-complète du développement de méthodes de 'défloutage' initialement prévues dans le projet, et d'autres pistes de traitements d'image adaptés à la problématique ont pu être explorées, voir §. C.4.

WP 4: Environmental microscopy on selected catalytic systems

Dans le cas des catalyseurs à base de cobalt, le développement de l'approche "operando" en combinant la microscopie électronique et la spectroscopie de masse a été testé pour la première fois ; elle a permis de déterminer les conditions dans lesquelles le fonctionnement des catalyseurs *Fischer-Tropsch* est optimum, et d'étudier l'influence de l'environnement de gaz autour de ces nanoparticules sur leur réactivité de surface par rapport aux processus de décomposition et de recombinaison des molécules correspondantes.

Pour les catalyseurs à base de Ni, cette approche "operando" a permis d'obtenir des informations essentielles sur le déroulement de la réaction catalytique de méthanation du CO_2. La mesure des produits de réaction simultanément au suivi des caractéristiques structurales et morphologiques des particules a démontré que la réaction se produit en deux étapes, avec la génération du CO, et que la présence des molécules d'eau dans la réaction conduit à une restructuration du catalyseur qui peut avoir un rôle bénéfique, dans certains cas, sur le rendement catalytique de ces nanoparticules.

En bénéficiant de l'expertise du partenaire CREATIS dans le développement de nouveaux algorithmes mathématiques de traitement des données, les travaux réalisés sur le système constitué de particules de Pd encapsulées dans une couche mésoporeuse de silice ont permis de mettre en place une approche méthodologique d'un grand intérêt pour les catalyseurs nanométriques ; il s'agit d'une quantification des facettes cristallographiques d'une NP à partir de sa reconstruction tomographique de manière quasi-automatique, ce qui permet de traiter un grand nombre de particules pour obtenir des valeurs représentatives, du point de vue statistique, de la proportion de différentes facettes qui

influence les propriétés catalytiques de l'ensemble. Sur ce même système, une analyse de type "étude d'objet unique" (*Identical Location* **[MAY08]**), en combinant le suivi environnemental à la tomographie électronique, a pu être réalisée à l'échelle de la cellule environnementale, en effectuant des acquisitions tomographiques en début et en fin de suivi in-situ des particules choisies. Cette approche, très complémentaire de la 'tomographie rapide' développée dans un ETEM dédié au cours du projet, a permis de mettre en évidence des changements structuraux fins au niveau de la surface des NPs, induits par le traitement in-situ dans l'environnement de gaz spécifique à l'étape d'activation des catalyseurs, ou à la réaction catalytique proprement dite.
Enfin, en ce qui concerne le système constitué des particules de Pd déposées sur alumine, une étude couplée ETEM/E-cell TEM a pu être réalisée au travers de suivis in-situ dans des conditions d'environnement similaires en ETEM et E-cell. Elles ont fourni des informations sur l'influence de la pression du gaz sur le comportement dynamique des nanoparticules et les processus physico-chimiques impliqués et, de manière plus générale, sur les avantages et les inconvénients des deux approches pour l'étude des nanomatériaux catalytiques, approches qui se sont avérées par ailleurs parfaitement complémentaires.

WP 5: meetings, presentations in congresses, reports / publications / patents

Ce dernier *WorkPackage* est classique comme son titre l'indique. Il présente néanmoins quelques points intéressants et est décrit de manière exhaustive dans l'ANNEXE 5.

C.3.2. GESTION DES TACHES : ANALYSE TECHNIQUE DES PROBLEMES ET SOLUTIONS RETENUES

Dans l'ensemble, le projet s'est déroulé conformément à nos attentes et nous ne mentionnerons ici qu'un seul 'problème' lié au défloutage complet des images acquises en tomographie rapide (WP3, détails en ANNEXE H : §.H.2 et H.3). Cet écueil a été assez rapidement et 'naturellement' réglé du fait de l'achat de la caméra rapide (microscope ETEM lyonnais), dont la vitesse d'acquisition en mode dynamique s'est avérée suffisamment rapide pour pouvoir assez valablement négliger les problèmes de bougé et de flou des micrographies (100 *fps* en format 2k).

C.4 RESULTATS OBTENUS

L'ensemble des livrables du projet ont été respectés, soit pour l'acquisition et la mise en service des équipements demandés (MATEIS, IPCMS), soit pour la valorisation des résultats au travers de publications et de communications à congrès. Nous avons essentiellement apporté une modification aux objectifs initiaux : le problème de flou induit par la rotation des objets lors d'acquisitions continues en tomographie rapide s'est avéré très mineure du fait de la caméra rapide ('Oneview Gatan'), et ce sujet n'a pas été développé autant que nous pensions devoir le faire. Ceci nous a permis d'aborder d'autres aspects du traitement d'images pour la tomographie environnementale, qui sont repris en ANNEXES H et I et ré-évoqués en section C6. Les principaux résultats sont liés aux équipements acquis dans le cadre du projet et aux objectifs s'y référant :

- D'une part, la démonstration d'une analyse quantitative des gaz produits lors d'une réaction catalytique positivement opérante dans une cellule environnementale grâce au spectromètre de masse installé à Strasbourg (e.g. méthanation du CO_2, cf. ANNEXE G).
- D'autre part, la démonstration d'une acquisition tomographique de quelques secondes permettant de suivre en temps 'réel' l'évolution d'un système catalytique sous gaz et en température dans l'ETEM 'dédié' lyonnais **[KON19]**.

Dans les 2 cas, l'apport du partenaire IFPen au travers de la fourniture de catalyseurs modèles bien contrôlés, et celle du partenaire CREATIS en matière de traitement d'images 3D ont permis de positionner ces résultats à l'état de l'art : le RGA de l'IPCMS est l'un des seuls systèmes installés à ce jour, et la tomographie environnementale pratiquée à MATEIS-CLYM ne l'est par aucun groupe dans le monde dans de telles conditions temporelles[1].

[1] On notera cependant des approches intéressantes récentes mais sur des nanoparticules individuelles menées à l'échelle atomique en conditions environnementales **[ALT19]**.

C.5 EXPLOITATION DES RESULTATS

Les résultats obtenus dans le projet 3DCLEAN sont à la hauteur des attendus initiaux. La plupart a été publiée ou présentée en congrès, mais plusieurs publications sont à venir, en l'occurrence sur la méthode 'Fastomo' (cf. ANNEXE H, §.H.2.3) et sur l'utilisation du RGA pour l'analyse des gaz réactionnels (ANNEXE G). D'autres publications seront issues des travaux de 3DCLEAN dans les années qui viennent. De plus, les équipements acquis au CLYM (caméra rapide Oneview) et à l'IPCMS (RGA monté sur porte-objet 'Ecell') sont déjà couramment utilisés par de nombreux microscopistes (voir ANNEXE J, §.J.3.2 liée au WP5) et contribueront significativement, de par leurs performances, à de nombreuses nouvelles publications dans les prochaines années.

C.6 DISCUSSION

3DCLEAN a atteint ses objectifs ; le projet a permis une avancée significative dans le domaine de la Microscopie Electronique en Transmission Environnementale, sous gaz en température, notamment pour l'étude de nanocatalyseurs. D'une part, le Spectromètre de masse (RGA) installé sur la cellule *High Pressure Environmental Cell* de l'IPCMS est à notre connaissance le premier opérationnel dans le monde. D'autre part, la tomographie rapide in situ est à l'heure actuelle la seule approche de ce type développée en conditions environnementales. En l'occurrence, ajoutant une approche 3D 'pendant', elle comble le 'gap' entre les approches 'avant' / 'après' réalisées soit avec transfert de l'échantillon hors du microscope pour traitement ex-situ (par exemple, **[Yu12]**), soit in situ en mode environnemental (e.g. **[BAZ18]**).
En complément des approches méthodologiques en MET Environnementale, ce travail a permis d'explorer quelques pistes de grand intérêt en matière de traitement d'images qui offrent donc de nouvelles perspectives au niveau de la recherche avec, compte-tenu du contexte énergétique global et de l'importance de la catalyse dans les procédés chimiques industriels, un impact sociétal certain à moyen terme :

(i) Pour la tomographie en conditions difficiles, de nouveaux algorithmes sont possibles, mêlant approches de débruitage (MAP-EM, §.H.3.3) et *Machine Learning* (§.H.3.4).
(ii) Pour la catalyse, l'analyse quantitative des facettes (cf. §.I.4.2) se développant à la surface des NPs sera d'un apport capital pour comprendre le fonctionnement des catalyseurs (identification des faces actives) ainsi que de leur possible désactivation.
(iii) Egalement, des travaux préliminaires concernant le suivi de trajectoires de NPs ont pu être menés (cf. ANNEXE I, section I.5) qui donnent lieu à des projets locaux en cours.

Au-delà des aspects purement scientifiques, 3DCLEAN a joué un rôle notable dans la dynamisation et la structuration de la communauté française dans le domaine de la Microscopie Electronique in situ et operando :

- d'une part, l'atelier GLEEM : *Gas and Liquid Environmental Electron Microscopy*, tenu en décembre 2016 dans le cadre du Défi CNRS 'Instrumentation aux Limites' (cf. §.J.2.2, www.cnrs.fr/mi/spip.php?article953)
- d'autre part, la participation active de MATEIS et de l'IPCMS (notamment au travers des responsables scientifiques au sein de 3DCLEAN, membres du bureau) dans le GDR NanOperando crée par le CNRS en 2018 (www.nanoperando.org). Cette structure regroupant plus de 150 chercheurs dans le pays et dédiée à l'étude operando et in situ, notamment par microscopie électronique, des nanomatériaux, a notamment tenu sa première réunion nationale à Lyon en Novembre 2018 (cf. §.J.2.3, https://nanoperando.sciencesconf.org/).

C.7 CONCLUSIONS

Le projet 3DCLEAN s'est déroulé dans d'excellentes conditions tant en termes de collaborations scientifiques que de complémentarité et de pluridisciplinarité des expertises réunies. De nombreux travaux restent à publier, qui n'ont pu être soumis avant la remise du présent rapport.

C.8 REFERENCES

[ALT19] T. Altantzis et al., *Nano Lett.* **19** (2019) 477.
[BAZ18] W. Baaziz et al., Nanoscale, **10** (2018) 20178
[KON19] S. Koneti et al., *Materials Characterization*, **151** (2019) 480; doi.org/10.1016/j.matchar.2019.02.009; https://hal.archives-ouvertes.fr/hal-02151235.
[MAY08] K.J. Mayrhofer et al., *Electrochem. Commun.* **10** (2008) 1144.
[YU12] Y. Yu et al., *Nano Lett.* **12** (2012) 4417.

D LISTE DES LIVRABLES

Quand le projet en comporte, reproduire ici le tableau des livrables fourni au début du projet. Mentionner l'ensemble des livrables, y compris les éventuels livrables abandonnés, et ceux non prévus dans la liste initiale.

Date de livraison	N°	Titre	**Nature** (rapport, logiciel, prototype, données, …)	**Partenaires** (souligner le responsable)	Commentaires
mi-2016	1.a	WP1: catalysts	Échantillons (données)	IFPEN-MATEIS-IPCMS	
mi-2017	1.b	WPI: characterization and catalytic results	Rapport	IFPEN-MATEIS-IPCMS	
03/2017	2.a	WP2: RGA analyser: operating system	Prototype	IPCMS	
2018	2.b	WP2: quantitative measurements of gas (reactants)	Données expérimentales	IPCMS-IFPEN-MATEIS	1ers résultats fin 2017
Mi-2019	3.a	WP3: improved acquisition of tomographic series in the ETEM	Protocole de pilotage d'un microscope	CREATIS-MATEIS	Prototype disponible dès 2017 ; finalisation mi-2019
09/2018	3.b	WP3: optimized processing of the series for the reconstruction	Logiciel	CREATIS-MATEIS	Logiciel déposé sur plateforme *free access* en 2018 (Github)
2019	3.c	WP3: quantitative morphological analysis of ETEM/HPEC results	Données expérimentales	IPCMS-CREATIS	Résultats en continu entre 2017 et 2019 (dépouillement d'expériences in situ)
2019	4.a	WP4: ETEM / HEPC experiments	Données expérimentales	MATEIS-IPCMS-CREATIS	Résultats en continu entre 2017 et 2019 (dépouillement d'expériences in situ)
2017, 2018	4.b	WP4: ETEM / HEPC experiments : comparison	Données expérimentales sur le même système en ETEM et E-Cell (HEPC)	MATEIS-IPCMS-CREATIS	Expériences croisées en 2017 et 2018
2019	5	WP5: common meetings, presentations in congresses, reports / publications / patents		MATEIS-IPCMS-IFPEN-CREATIS	
2017	3.d	WP3: optimized processing of the series for the reconstruction	Méthodologie de défloutage	CREATIS-MATEIS	Approche abandonnée du fait de sa non-nécessité (justifiée)
2018	4.b	WP4: Quantitative morphological analysis of results obtained on catalysts followed in environmental microscopy (ETEM and HPEC).	Traitement 3D du facetage des NPs	MATEIS-IPCMS-CREATIS	Sous-tâche non anticipée dans le projet initial

E IMPACT DU PROJET

Ce rapport rassemble des éléments nécessaires au bilan du projet et plus globalement permettant d'apprécier l'impact du programme à différents niveaux.

E.1 INDICATEURS D'IMPACT

Nombre de publications et de communications (à détailler en E.2)

		Publications multipartenaires	Publications monopartenaires
International	Revues à comité de lecture	**10**	**6**
	Ouvrages ou chapitres d'ouvrage		
	Communications (conférence)	**19**	**14**
France	Revues à comité de lecture		
	Ouvrages ou chapitres d'ouvrage		
	Communications (conférence)	**5**	**5**
Actions de diffusion	Articles vulgarisation		
	Conférences vulgarisation		
	Autres		

Autres valorisations scientifiques (à détailler en E.3)

Ce tableau dénombre et liste les brevets nationaux et internationaux, licences, et autres éléments de propriété intellectuelle consécutifs au projet, du savoir-faire, des retombées diverses en précisant les partenariats éventuels. Voir en particulier celles annoncées dans l'annexe technique).

	Nombre, années et commentaires (valorisations avérées ou probables)
Brevets internationaux obtenus	
Brevet internationaux en cours d'obtention	
Brevets nationaux obtenus	
Brevet nationaux en cours d'obtention	
Licences d'exploitation (obtention / cession)	
Créations d'entreprises ou essaimage	
Nouveaux projets collaboratifs	
Colloques scientifiques	En marge du projet 3DCLEAN mais initialement prévu dans le programme (non financé par l'ANR) : DEFI CNRS 2016 'GLEEM' : *Gas and Liquid Environmental Electron Microscopy* (co-organisateurs : O. Ersen (IPCMS) et T. Epicier (MATEIS). Workshop tenu au CNRS (Paris, Michel-Ange) les 13-14/12/2016 ; 100 participants. http://www.cnrs.fr/mi/spip.php?article953 **(voir §.J.1.2.)**
Autres (préciser)	

E.2 LISTE DES PUBLICATIONS ET COMMUNICATIONS

Nous rapportons ici la liste des travaux publiés en précisant les partenaires co-auteurs pour identifier les réalisations multi-ou mono-partenaires à la fois dans des revues (RCL) ou présentés en conférences internationales (Int) ou nationales (Nat), y compris **invitée**s.
Le décompte fait état de 16 publications RCL et 43 communications à congrès, dont 20 invitées. 58 % des travaux associent au moins 2 partenaires.

Publications RCL multipartenaires

1. **MATEIS-CREATIS** : L. Roiban, S. Koneti, K. Tran, Y-M Feng, T. Grenier, V. Maxim, T. Epicier, Rapid Tomography in Environmental TEM: How Fast Can We Go to Follow the 3D Evolution of Nanomaterials in situ?, Microsc. Microanal. 22, 5, (2016), 8; doi:10.1017/S143192761601206X
2. **MATEIS- IFPEN** : S. Koneti, L. Roiban, A-S. Gay, P. Avenier, F. Dalmas, T. Epicier, Calcination of Pd Nanoparticles on Delta Alumina : Ex-situ Analysis versus In-situ Environmental TEM, Microsc. Microanal. 22 S5, (2016), 56. DOI: 10.1017/S1431927616012319
3. **IPCMS-IFPEN** : K. Dembele, S. Moldovan, C. Hirlimann, J. Harmel, K. Soulantica, P. Serp, B. Chaudret, A.-S. Gay, S. Maury, A. Berliet, A. Fecant, O.Ersen, Reactivity and structural evolution of urchin-like Co nanocrystals under controlled environments, J. of Microscopy, 269, 2 (2018), 168.
4. **MATEIS-CREATIS-IFPEN** : H. Banjak, T. Grenier, T. Epicier, S. Koneti, L. roiban, A-S. gay, I. Magnin, F. Peyrin, V. Maxim, Evaluation of noise and blur effects with SIRT-FISTA-TV reconstruction algorithm: Application to fast environmental transmission electron tomography, Ultramicroscopy, 189, (2018), 109.
5. **IPCMS-IFPEN** : M. Bahri, K. Dembélé, C. Sassoye, D.P. Debecker, S. Moldovan, A. S. Gay, C. Hirlimann, C. Sanchez, O. Ersen, In situ insight into the unconventional ruthenium catalyzed growth of carbon nanostructures, Nanoscale, 10 31 (2018), 14957. DOI: 10.1039/c8nr01227j. https://hal.archives-ouvertes.fr/hal-01912233v1.
6. **IPCMS-IFPEN-CREATIS** : W. Baaziz, M. Bahri, A-S. Gay, A. Chaumonnot, D. Uzio, S. Valette, C. Hirlimann, O. Ersen, Thermal behavior of Pd@SiO_2 nanostructures in various gas environments: a combined 3D and in situ TEM approach, Nanoscale, 10 (2018), 20178. DOI: 10.1039/c8nr06951d. https://hal.archives-ouvertes.fr/hal-01991904v1.
7. **MATEIS-CREATIS-IFPEN** : T. Epicier, H. Banjak, A-S. Gay, T. Grenier, S. Koneti, V. Maxim, L. Roiban, Very Fast Tomography in the (E)TEM to Probe Dynamics in Materials during Operando and In Situ Experiments, Microsc. Microanal., 24, 1 (2018), 1814. Doi : 10.1017/S1431927618009558
8. **IPCMS-IFPEN** : K. Dembélé, M. Bahri, G. Melinte, C. Hirlimann, A. Berliet, S. Maury, A-S. Gay, O. Ersen, Insight by In Situ Gas Electron Microscopy on the Thermal Behaviour and Surface Reactivity of Cobalt Nanoparticles, ChemCatChem 18 (2018), DOI: 10.1002/cctc.201801445.
9. **MATEIS-IFPEN** : T. Epicier, S. Koneti, P. Avenier, A. Cabiac, A-S. Gay, L. Roiban, 2D & 3D in situ study of the calcination of Pd nanocatalysts supported on delta-Alumina in an Environmental Transmission Electron Microscope, Catalysis Today, 334, 15 (2019), 68-78. DOI: 10.1016/j.cattod.2019.01.061, https://hal.archives-ouvertes.fr/hal-02151239.
10. **MATEIS-IFPEN-CREATIS** : S. Koneti, L. Roiban, F. Dalmas, C. Langlois, A-S Gay, A. Cabiac, T. Grenier, H. Banjak, V. Maxim, T. Epicier, Fast electron tomography: applications to beam sensitive samples and in situ TEM or operando Environmental TEM studies, Materials Characterization, 151 (2019) 480-495. DOI: 10.1016/j.matchar.2019.02.009, https://hal.archives-ouvertes.fr/hal-02151235.

Publications RCL mono-partenaires

11. **MATEIS** : T. Epicier, Nanoparticles in The ETEM: From Gas-Surface Interactions of Single Objects to Collective Behavior of Nanocatalysts, Microscopy and Microanalysis, 23 S1(2017), 898-899; DOI: 10.1017/S1431927617009916, https://hal.archives-ouvertes.fr/hal-01612811.
12. **MATEIS** : S. Koneti, J. Borges, L. Roiban, M.S. Rodrigues, N. Martin, T. Epicier, F. Vaz, P. Steyer, Electron Tomography of Plasmonic Au Nanoparticles Dispersed in a TiO2 Dielectric Matrix, ACS Appl. Mater. Interfaces, 10, 49, (2018), 42882-42890, DOI: 10.1021/acsami.8b16436, https://hal.archives-ouvertes.fr/hal-02151266.
13. **MATEIS** : L. Roiban, S. Li, M. Aouine, A. Tuel, D. Farrusseng, T. Epicier, Fast "Operando" Electron Nano-Tomography, J. of Microscopy, 269 2 (2018), 117-126; DOI: 10.1111/jmi.12557, https://hal.archives-ouvertes.fr/hal-01612818.

14. **CREATIS** : V. Maxim, Enhancement of Compton camera images reconstructed by inversion of a conical Radon transform, Inverse Problems 35 014001 (2019); DOI: 10.1088/1361-6420/aaecdb, https://hal.archives-ouvertes.fr/hal-01932981v1
15. **MATEIS :** A. Monpezat, S. Topin, V. Thomas, C. Pagis, M. Aouine, L. Burel, L. Cardenas, A. Tuel, A. Malchère, T. Epicier, D. Farrusseng, L. Roiban, Migration and Growth of Silver Nanoparticles in Zeolite Socony Mobil 5 (ZSM-5) Observed by Environmental Electron Microscopy: Implications for Heterogeneous Catalysis, ACS Appl. Nano Mater. 2, 10, (2019), 6452-6461. DOI : 10.1021/acsanm.9b01407; https://hal.archives-ouvertes.fr/hal-02354958.
16. **CREATIS** : Y. Feng, A. Etxebeste, D. Sarrut, J-M. Létang, V. Maxim, 3D reconstruction benchmark of a Compton camera against a parallel hole gamma-camera on ideal data, IEEE Transactions on Radiation and Plasma Medical Sciences, in press, (2019).

Communications Multi-partenaires

1. ***Int.*** **MATEIS-CREATIS-IFPEN :** L. Roiban, S. Koneti, V. Maxim, T. Grenier, P. Avenier, A. Cabiac, A-S Gay, F. Dalmas, T. Epicier, Fast Electron Microscopy 3D analysis of nano-materials in operando mode, **conference invitée** à EMN Meeting on Mesoporous Materials Prague, Czech Republic June 13-17th, (2016).
2. ***Int.*** **CREATIS-MATEIS :** Y-M. Feng, K. Tran, S. Koneti, L. Roiban, A-S Gay, C. Langlois, T. Epicier, T. Grenier, V. Maxim, Image deconvolution for fast Tomography in Environmental Transmission Electron Microscopy, Proceed. EMC2016, doi: 10.1002/9783527808465.EMC2016.6973.
3. ***Int.*** **IPCMS-IFPEN :** K. Dembélé, S. Moldovan, J. Harmel, K. Soulantica, P. Serp, B. Chaudret, A.-S Gay, S. Maury, A. Fecant. O. Ersen, Stability and reactivity of anisotropic cobalt nanostructures under inert and reactive environments investigated by in-situ TEM, Proceed. EMC2016, doi: 10.1002/9783527808465.EMC2016.6180
4. ***Int.*** **MATEIS-CREATIS-IFPEN :** S. Koneti, L. Roiban, V. Maxim, T. Grenier, P. Avenier, A. Cabiac, A-S. Gay, F. Dalmas, T. Epicier, Proceed. EMC2016, doi: 10.1002/9783527808465.EMC2016.6438
5. ***Int.*** **MATEIS-CREATIS-IFPEN :** S. Koneti, L. Roiban, T. Grenier, V. Maxim, A.-S. Gay, F. Dalmas, T. Epicier, P. Vernoux, Rapid Tomography in Environmental TEM: Solutions for a Fast Analysis of Nano-Materials in 3D under In-Situ conditions, communication orale à MRS Spring Meeting, April 17-21 2017, Phoenix, AZ, USA.
6. ***Int.*** **MATEIS-IFPEN :** S. Koneti, L. Roiban, A-S. Gay, P. Avenier, F. Dalmas, T. Epicier, Calcination of Pd Nanoparticles on Delta Alumina : Ex-situ Analysis versus In-situ Environmental TEM, communication orale à MRS Spring Meeting, April 17-21 2017, Phoenix, AZ, USA.
7. ***Int.*** **CREATIS-MATEIS :** H. Banjak, T. Grenier, V. Maxim, S. Koneti, L. Roiban, T. Epicier, Towards One Hertz Electron Tomography Of Dynamic Processes Under Environmental Conditions: Expectations And Limitations Due To Blur Effects, communication orale à ICTMS (3rd International Conference on Tomography of Materials and Structure), Lund, Sweden, 26-30 June 2017 (http://ictms2017.lth.se).
8. ***Int.*** **MATEIS-CREATIS-IFPEN :** S. Koneti, L. Roiban, T. Grenier, V. Maxim A-S. Gay, F. Dalmas, T. Epicier, Rapid Tomography in Environmental TEM: Solutions for a Fast Analysis of Nano-Materials in 3D under In-Situ conditions, poster à Microscopy & Microanalysis 2017 in St. Louis, Missouri, USA, August 6-10, 2017.
9. ***Int.*** **IFPEN-IPCMS :** A.-S. Gay, K. Dembélé , M. Bahri , S. Maury; L. Lemaitre, M. Rivallan, O. Ersen, Microstructural evolution of Co catalysts during activation and Fischer-Tropsch reaction investigated by operando Transmission Electron Microscopy, Europacat, Florence, Italie, août 2017
10. **Int IPCMS-IFPEN:** M. Bahri, O. Ersen, K. Dembélé, A.-S. Gay, W. Baaziz, G. Melinte, Environmental Gas TEM for Catalysis in Operando Conditions, Protochips Workshop, February 2018, Prague, (**invited conference**).
11. ***Int.*** **IPCMS-IFPEN :** S. Maury, A.-S. Gay, K. Dembélé , M. Bahri, L. Lemaitre, M. Rivallan, O. Ersen, Microstructural evolution of Co catalysts during activation and

Fischer-Tropsch reaction investigated by operando Transmission Electron Microscopy, *'Syngas convention'*, Cape Town, Afrique du Sud, mars 2018

12. ***Int.*** **IPCMS-IFPEN :** K. Dembélé, M. Bahri1, C. Hirlimann, G. Melinte, S. Moldovan, A. Berliet, A.-S. Gay, S. Maury, O. Ersen, Insight by operando tem on the thermal behaviour of cobalt-based Fischer-Tropsch catalysts, poster à Solid Liquid Interfaces: Challenging Molecular Aspects for Industrial Applications [SLIMAIA), Rueil-Malmaison, F, 27-29 mars 2018.
13. ***Int.*** **IPCMS-IFPEN :** M. Bahri, A-S. Gay, K. Dembélé A.-C. Dubreuil, O. Ersen, The investigation of Ni/alumina catalysts by Operando TEM: direct insights on the catalyst activation and operation during the CO_2 methanation reaction, poster à Operando VI, 6° Int. Congress on Operando Spectroscopy, 11-19 Avril, 2018, Estepona, Málaga (Spain).
14. ***Int.*** **MATEIS- IFPEN :** T. Epicier, S. Koneti, L. Roiban, A-S. Gay, P. Avenier, Why Don't we Follow the Calcination and Reduction Stages of Pd Nanocatalysts Supported on Alumina In Situ Directly in an Environmental Transmission Electron Microscope?, présentation orale à PREPA12, 12th International Symposium, 8-12 Juillet 2018, Louvain-la-Neuve, Belgique, www.ldorganisation.com/v2/page/prepa/products.html.
15. ***Int.*** **MATEIS- CREATIS :** T. Epicier, H. Banjak, A-S. Gay, T. Grenier, S. Koneti, V. Maxim, L. Roiban, Very Fast Tomography in the (E)TEM to Probe Dynamics in Materials during Operando and In Situ Experiments, **conférence invitée** à M&M2018: Microscopy & Microanalysis meeting (www.microscopy.org/MandM/2018/), 5-9 Août 2018, Baltimore, MD, USA. Microsc. Microanal. 24 (Suppl 1), (2018), 1814; DOI : 10.1017/S1431927618009558, https://hal.archives-ouvertes.fr/hal-01934140.
16. ***Int.*** **IPCMS-MATEIS-IFPEN :** M. Bahri, L Roiban, A.-S. Gay, O. Ersen, T. Epicier, Gaseous Environmental TEM: a complementary study of nanocatalysts using a combined "dedicated ETEM vs E-cell" approach, oral à IMC19, 19th International Microscopy Conference, Sidney, Australia, 9-14 September 2018, imc19.com.
17. **Int IPCMS-IFPEN-CREATIS :** C. Hirlimann, W. Baaziz, M. Bahri, A.-S. Gay, S. Valette, O. Ersen, Combining environmental gas TEM and electron tomography, oral à IMC19, 19th International Microscopy Conference, Sidney, Australia, 9-14 September 2018, imc19.com.
18. ***Int.*** **CREATIS-MATEIS :** T. Grenier, L. Roiban, H. Banjak, S. Koneti, V. Maxim, T. Epicier, A robust method to acquire tilt series in a few seconds for Fast Operando Nano-Tomography in ETEM, oral à IMC19, 19th International Microscopy Conference, Sidney, Australia, 9-14 September 2018, imc19.com.
19. ***Int.*** **CREATIS-MATEIS :** H. Banjak, T. Grenier, T. Epicier, L. Roiban, V. Maxim, Deep Neural Network for Iterative Image Reconstruction with Application to Fast Environmental Transmission Electron Tomography, mini-oral à IMC19, 19th International Microscopy Conference, Sidney, Australia, 9-14 September 2018, imc19.com.
20. ***Nat.*** **MATEIS-IFPEN :** T. Epicier, S. Koneti, L. Roiban, A-S. Gay, A. Cabiac, 2D and fast 3D in situ calcination and reduction of pd nanocatalysts supported on alumina in Environmental Transmission Electron Microscopy, oral à Matériaux 2018, 19-23 Nov. 2018, www.materiaux2018.fr/, https://hal.archives-ouvertes.fr/hal-01934081v1.
21. ***Nat.*** **IPCMS-MATEIS :** M. Bahri, L. Roiban, O. Ersen, T. Epicier, A Converging gaseous Environmental TEM study in a dedicated 'open cell' ETEM microscope and an Environmental 'close' Ecell, présentation orale à la 1ère réunion nationale du GDR Nanoperando, Colloque de Lyon, 28-30 Novembre 2018 (https://nanoperando.sciencesconf.org).
22. **Nat IPCMS-IFPEN :** O. Ersen, M. Bahri, D. Ihiawakrim, W. Baaziz, A.-S. Gay, C. Hirlimann, TEM for catalysis under operando conditions in an environmental cell, présentation orale à la 1ère réunion nationale du GDR Nanoperando, Colloque de Lyon, 28-30 Novembre 2018 (https://nanoperando.sciencesconf.org).
23. ***Nat.*** **MATEIS-CREATIS :** T. Epicier, T. Grenier, H. Banjak, V. Maxim, S. Koneti, L. Roiban, Fast acquisition of tilt series in environmental tem tomography: tips and tricks, oral au Colloque 2019 de la Soc. Française des Microscopies (SFμ), 2-5 Juillet 2019, Poitiers, F.

24. ***Nat.*** **MATEIS-IFPEN :** L. Roiban, S. Koneti, B. Chal, A. Monpezat, S. Topin, D. Farrusseng, A-S. Gay, F. Dalmas, G. Foray, T. Epicier, Fast electron tomography and its application to the study of beam sensitive samples of materials in environmental conditions, **conférence invitée** au Colloque 2019 de la Soc. Française des Microscopies (SFμ), 2-5 Juillet 2019, Poitiers, F.

Communications Mono-partenaires

25. ***Int.*** **CREATIS** : V. Maxim, Compton camera imaging and Radon transforms on the cone: From data to images**, conférence invitée** à 100 Years of the Radon Transform, Mar 2017, Linz, Austria. https://hal.archives-ouvertes.fr/hal-02359629.
26. ***Int.*** **MATEIS** : T. Epicier, The TEM nanolab: towards operando microscopy of nanomaterials under gaseous environments, **conférence invitée** à NANOMAT 2017; May 16-19, 2017, Fukuoka, Japan.
27. ***Int.*** **MATEIS** : T. Epicier, S. Koneti, L. Roiban, D. Lopez-Gonzalez, P. Vernoux, Real time 3D Environmental TEM in-depth study of catalytic soot combustion on Zirconia-based catalysts, presentation orale à MMC2017: Microscience Microscopy Congress 3-7 July 2017, Manchester, UK.
28. ***Int.*** **MATEIS** : S. Koneti, F. Dalmas, L. Roiban, T. Epicier, Fast high resolution 3d microstructural characterization of nanoplatelet-filled polymer nanocomposites, EPFLyon 2017: 16th European Polymer Federation Congress, 02-07 July 2017, Lyon, F.
29. ***Int.*** **MATEIS** : T. Epicier, Nanoparticles in The ETEM: From Gas-Surface Interactions of Single Objects to Collective Behavior of Nanocatalysts, **conférence invitée** à Microscopy & Microanalysis 2017 in St. Louis, Missouri, USA, August 6-10, 2017.
30. ***Int.*** **MATEIS** : S. Koneti, L. Roiban, D. Lopez-Gonzalez, P. Vernoux, T. Epicier, Real time 3D Environmental TEM in-depth study of catalytic soot combustion on Zirconia-based catalysts, poster à Microscopy & Microanalysis 2017 in St. Louis, Missouri, USA, August 6-10, 2017.
31. **Nat IPCMS :** O. Ersen, M. Bahri, D. Ihiawakrim, N. Ortiz, W. Baaziz, G. Melinte, K. Dembélé, Apport de techniques de microscopie électronique 3D et environnementale à l'étude de nanostructures, Réunion annuel du Groupe Français d'Etude des Composées d'Insertion (GFECI), Mars 2018, Touquet (**conférence invitée**).
32. ***Int.*** **CREATIS** : V. Maxim, Practical considerations for Compton camera analytic image reconstruction, **conference invitée** à 9th International Conference "Inverse Problems: Modeling and Simulation" (IPMS-2018), May 2018, Malta. https://hal.archives-ouvertes.fr/hal-02359645.
33. **Int IPCMS :** O. Ersen, Advanced electron microscopy techniques applied to carbon nanomaterials and composites, CIMTEC 2018, 8th Forum on New Materials, June 2018, Peruggia (Italia) (**invited conference**).
34. **Nat IPCMS :** O. Ersen, M. Bahri, D. Ihiawakrim, N. Ortiz, W. Baaziz, G. Melinte, K. Dembélé, S. Moldovan, C. Hirlimann, Combinaison de techniques de microscopie électronique pour l'étude de la croissance, des propriétés structurales et de la réactivité de nanomatériaux, Journée IRMA, Novembre 2018, Caen (**conférence invitée**).
35. ***Nat.*** **MATEIS** : T. Epicier, Nanomaterials 'alive' under gas in the Environmental Transmission Electron Microscope (ETEM), **keynote invitée** au colloque annuel 2018 du C'Nano (symposium 'Advanced Characterization'), Toulon, 11-13 déc. 2018 (https://cnano2018.sciencesconf.org/).
36. **Int IPCMS :** O. Ersen, Advanced electron microscopy techniques for the study of the properties and dynamical behaviour of the nanomaterials, Sixth International Conference on Multifunctional, Hybrid and Nanomaterials (HYMA), March 2019, Sitges (Spain) (**invited conference**).
37. **Int IPCMS :** O. Ersen, Advanced electron microscopy applied to nanomaterials and nano-objects: the contribution of the 3D imaging and in-situ operando TEM, Congress of Romanian Society for Electron Microscopy (CREMS), October 2019, Bucarest (Romania) **(invited conference)**.
38. **Nat IPCMS :** O. Ersen, M. Bahri, D. Ihiawakrim, N. Ortiz, W. Baaziz, G. Melinte, Microscopie électronique in-situ environnementale pour l'étude des propriétés

dynamiques de nanomatériaux, Journée Sol-Gel, Octobre 2019, Tours (**conférence invitée**).

39. **Nat IPCMS :** O. Ersen, M. Bahri, D. Ihiawakrim, N. Ortiz, W. Baaziz, G. Melinte, Advanced electron microscopy techniques applied to nanomaterials and nano-objects, 7th LCS Workshop, May 2019, Deauville (**conférence invitée**).
40. ***Int.* CREATIS** : V. Maxim, E. Bretin, Dual approach for TV-regularized Maximum Likelihood Expectation Maximization in tomography with Poisson data**, conférence invitée** à ICIAM, Jul 2019, Valencia, Spain. https://hal.archives-ouvertes.fr/hal-02359496v1.
41. ***Int.* CREATIS** : V. Maxim, Total variation regularization in tomography with Poisson distributed data**, conférence invitée** à Applied Inverse Problems (AIP), Jul 2019, Grenoble, France. https://hal.archives-ouvertes.fr/hal-02359404.
42. ***Int.* MATEIS** : T. Epicier, Nanomaterials 'Alive' under Gas in the Environmental Transmission Electron Microscope (ETEM), **conférence invitée** à ICMAT 2019, 23 - 28 June 2019, Marina Bay Sands, Singapore.
43. ***Int.* CREATIS** V. Maxim, Challenges in Compton camera imaging for medical applications Modern Challenges in Imaging, **conférence invitée** à In the Footsteps of Allan MacLeod Cormack, Aug 2019, Tufts University, United States, https://hal.archives-ouvertes.fr/hal-02359478v1.

E.3 LISTE DES ELEMENTS DE VALORISATION

*La liste des éléments de valorisation inventorie les retombées (autres que les publications) décomptées dans le deuxième tableau de la section **E.1**.*

E.3.1. LOGICIELS ET MISE A DISPOSITION SUR PLATEFORMES

Les principaux éléments de valorisation outre la production scientifique usuelle (publications, conférences) résident dans le développement d'un **logiciel de reconstruction tomographique, SIRT-FISTA-TV**, associé aux travaux 4 et 19 de la liste E.2 précédente. Ce produit sera décrit en ANNEXE H (section H.3) ; comme il y est indiqué, le logiciel est disponible pour la communauté de 2 manières :

1) il est référencé sur la plateforme de logiciels libres Github (https://github.com/CSET-Toolbox/CSET).
2) Il est également disponible sur une plateforme locale mise en place par le laboratoire CREATIS, permettant aux utilisateurs de faire tourner des algorithmes par internet sur un cloud distant GPU (Virtual Imaging Platform VIP, https://www.creatis.insa-lyon.fr/vip/).

Les partenaires de ce projet sont CREATIS (initiateur) et MATEIS.

Dans le même esprit, 3DCLEAN a contribué par certains aspects à la plateforme similaire développée en interne par IFPen pour le traitement d'images en ligne : **PLUG-IM** (https://www.plugim.fr).

E.3.2. AUTRES ELEMENTS D'OUVERTURE

En parallèle des précédentes actions 'logiciel' abouties, MATEIS et CREATIS ont entrepris une ouverture au travers d'une extension scientifique du projet 3DCLEAN, visant à une meilleure caractérisation et compréhension des mécanismes d'interactions de nanoparticules catalytiques supportées sur une surface. Il s'agit à ce jour de projets collaboratifs locaux au sein de l'Université de Lyon - Lyon-St-Etienne – (évoqués en ANNEXE I : contextes locaux de la FR CNRS IngéLySe - ingelyse.com - et de l'EUR MANUTECH-SLEIGHT - https://eur-manutech-sleight.universite-lyon.fr/ -). Ils portent sur le développement de codes spécifiques à la détection et au suivi de trajectoires des nanoparticules à partir de séquences d'images dynamiques enregistrées en mode Environnemental en TEM (ETEM). Cette démarche associe le Laboratoire Hubert Curien de l'Université Jean Monnet de St-Etienne, également spécialiste dans le traitement d'images et l'étude des surfaces, et est porteuse de possibilités de futures collaborations.

Comme autres éléments d'ouverture (mais plus spécifiquement au niveau national), on peut également citer le rôle joué par le projet 3DCLEAN dans la **structuration d'une communauté autour de la thématique de la microscopie électronique environnementale** et Operando, avec d'une part l'Atelier 'GLEEM' qui s'est tenu au CNRS en décembre 2016 (Tableau 'Autres valorisations scientifiques' du paragraphe E.1), et d'autre part sa contribution au GDR national NanOperando créée en 2018 par le CNRS (INP). Ces actions sont détaillées en ANNEXE J, §.J.2.

Enfin, 2 illustrations de travaux issus des recherches 3DCLEAN ont fait l'objet de **couvertures de revues scientifiques** :

- D'une part, l'article 13 de la liste E.2, à l'occasion d'un numéro spécial du Journal of Microscopy (https://onlinelibrary.wiley.com/loi/13652818) coédité par Thierry Epicier suite à la tenue du 16° Congrès Européen de Microscopie à Lyon en 2016 (EMC : *European Microscopy Congress* www.emc2016.fr, où d'ailleurs plusieurs travaux des partenaires ont été présentés - liste E.2, 2, 3, 4)
- la référence 8 de la liste E.2 (travail collaboratif IPCMS – IFPen)

Figure 2 : couvertures de journaux illustrées par des travaux directs de 3DCLEAN. A gauche, *J. of Microscopy* (MATEIS) ; A droite : *ChemCatChem* (IPCMS-IFPen).

E.4 BILAN ET SUIVI DES PERSONNELS RECRUTES EN CDD (HORS STAGIAIRES)

Ce tableau dresse le bilan du projet en termes de recrutement de personnels non permanents sur CDD ou assimilé.

Identification				Avant le recrutement sur le projet			Recrutement sur le projet				Après le projet				
Nom et prénom	Sexe H/F	Adresse email (1)	Date des dernières nouvelles	Dernier diplôme obtenu au moment du recrutement	Lieu d'études (France, UE, hors UE)	Expérience prof. antérieure, y compris post-docs (ans)	Partenaire ayant embauché la personne	Poste dans le projet (2)	Durée missions (mois) (3)	Date de fin de mission sur le projet	Devenir professionnel (4)	Type d'employeur (5)	Type d'emploi (6)	Lien au projet ANR (7)	Valorisation expérience (8)
BAHRI Mounib	H	Mounib.bahri@ipcms.unistra.fr	2019/11	Doctorat	France	0	IFPEN	Post-doctorant	Embauché le 13/06/2016 pour 18 mois	Déc. 2017	Prolongation de post-doctorat	EPST	Chercheur contractuel	Employeur IPCMS (partenaire)	oui
BANJAK Hussein	H	Hussein.Banjak@creatis.insa-lyon.fr	2019/05	doctorat	France	0	CREATIS	Post-doctorant	Embauché le 18/10/2016 pour 24 mois	10/2018	Embauché dans une startup suisse (Intom Gmbh, 2019/01)	Société privée	R&D engineer	non	oui : responsable développement 'software' en reconstruction tomographique

F APPENDIX 1: WP 1 - PREPARATION OF CATALYSTS, CATALYTIC TESTS AND PRELIMINARY TEM CHARACTERIZATION

Note: all texts reported in the Appendices (sections F to J) are written in English.

F.1 RECALL OF THE DEFINITION OF THE TASKS

Duration	1 year
Objective	. Supply model catalysts for the project, with appropriate characterization and catalytic tests results performed on fresh and spent catalysts as much as possible. . Some operando characterizations will be performed (XRD-DRIFT, EXAFS at synchrotron facilities). . Complementary conventional TEM
Responsable	Anne-Sophie Gay (IFPEN)
Partners	MATEIS / IPCMS
Deliverables	. Catalysts . Characterizations and catalytic tests results - report
Contribution	IFPEN internal resources and facilities; MATEIS / IPCMS equipments; about 10 Person.Months (P.M)
Risks and failback solutions	*Low risk: the techniques for catalysts synthesis, characterization and tests are known and controlled by IFPEN.*

For this project, model heterogeneous catalysts have been studied. They consist on simplified systems compared to industrial catalysts, thus they are more appropriate to highlight characterization challenges.

F.2 PD CATALYSTS

F.2.1. CONTEXT AND AIM OF THE STUDY

A first system studied in the 3DCLEAN project concerns Pd catalysts. Pd is known to be catalytically active for different hydrogenation process. It is used for:

- selective hydrogenation in petrochemistry. For example in gasoline pyrolysis a naphta cracking by-product contains highly reactive species such as conjugated dialkenes, styrene and indene that needs to be hydrogenated before being blended to the gasoline pool. This hydrogenation should not be completed to maintain a good octane number. Other important applications occur in polymer synthesis. For polyethylene or polypropylene synthesis, the feedstock needs to be rid of alkynes (acetylene) compound without transforming the desired products, ethylene or propylene **[SOR12]**.
- CO_2 hydrogenation for methane production, so called the Sabatier reaction. Low temperature methanation has been investigated on different noble metals, among which Pd is one of the most active and selective to CH4 formation **[SAS11, KAR12]**.

Depending on applications, Pd nanoparticles can be supported on different types of supports. It is usually alumina for selective hydrogenation in petrochemistry **[SOR12]**. For this process, it is known that interaction between the support and the particle is a key parameter for catalyst activity and stability. The crystallographic nature of alumina can modify interactions and catalyst stability. Selectivity of catalyst is strongly linked to the nature of the exposed facets of the particles. Controlling the shape of NPs, quantifying the interaction with the support during the activation step and catalytic reaction are important parameters for designing catalysts with high activity, selectivity and stability **[BER07, BIS09, ARG02]**.

For these samples, the aim of the work is to study the role of the support on the formation of Pd NP during the genesis step (comprising impregnation / drying / calcination and reduction).
Other more innovative supports are developed by IFPEN, for example the innovative synthesis of the catalyst proposed by MARTINS et al. **[MAR15]** for CO_2 methanation: shape-controlled Pd nanocubes and polyedra NPs were embedded in mesoporous silica shells. This core-shell structure presents several advantages for catalysis like preventing thermal sintering of NPs during catalysis and then delays deactivation.
For these samples, the aim of the work is to study the stability of encapsuled Pd NP during heat treatments and the sensibility of NP shapes to gaseous environments.

These systems were studied during Sid Koneti's PhD at MATEIS-CLYM **[KON17]** and Mounib Bahri's Post-doc (in collaboration with IPCMS).

F.2.2. CATALYSTS PREPARATION AND PRELIMINARY CHARACTERIZATION

Pd/alumina catalysts
Pd supported catalyst is prepared by colloidal synthesis. The detailed protocol has been previously described **[RAM07, DID98]**. An aqueous acid Pd solution ($Pd(NO_3)_2$ solution provided by HERAUS with 8.22 wt. % Pd concentration, pH of 1) is stabilized with sodium nitrite (0.4 mol $NaNO_2$ by 1 mol of Pd). Further NaOH addition by pH adjustment to 2 allows to obtaining the colloidal Pd solution. Initial mean particle sizes of 1.7 nm (for a similar acid PH) and around 2 nm were respectively measured in previous works **[RAM07, DID98]**.
After 5 min maturation, the solution is used for dry impregnation of an alumina support consisting in 2–4mm beads. Two different alumina supports were used:

- A mesoporous δ-alumina, SBET = 70m^2/g
- A mesoporous δ-alumina, SBET = 7 m^2/g

The Pd concentration of the catalyst extrudates is 0.3 wt. % for Pd/δ-Al_2O_3 and 0.05 wt% for α-Al_2O_3, however since Pd NPs are located in a shell of few hundred of µm thickness the resulting Pd concentration in such a shell is significantly larger than the nominal amount. After completion of this process called 'impregnation', the material is dried at 120 °C under ambient air and calcined at 425°C for 2 h. The final reduction to insure the metallic state of Pd NPs is performed under hydrogen at atmospheric pressure during 2 h at 150°C.
Catalysts were characterized by TEM to measure nanoparticle size at the last step of catalyst activation and by CO-chemisorption to measure the Pd dispersion.
Pd/ δ-alumina consists of large and globular aggregates of well crystallized δ-alumina **(Figure 3)**. The size of the alumina nodules is about few dozens to hundreds of nm. Pd NPs are dispersed on the surface of alumina. Time to time, some NP are agglomerated but most of them are isolated.

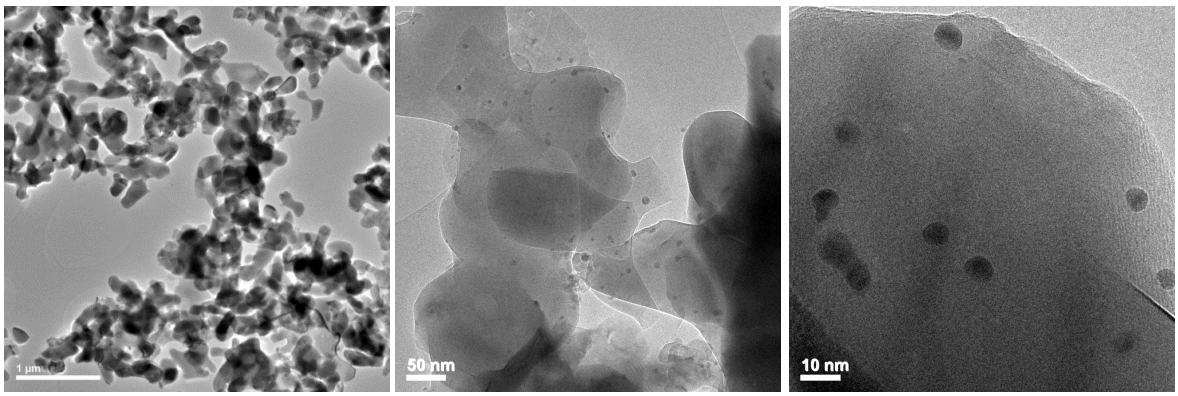

Figure 3: TEM images of Pd/α-alumina.

Pd/δ-alumina consists of a mixture of large well crystallized mesoporous alumina platetets (hundreds of nm) and aggregated small nanoparticles (few nm). Pd NPs are dispersed on the surface of alumina (**Figure 4**). Time to time, some NP are agglomerated but most of them are isolated.

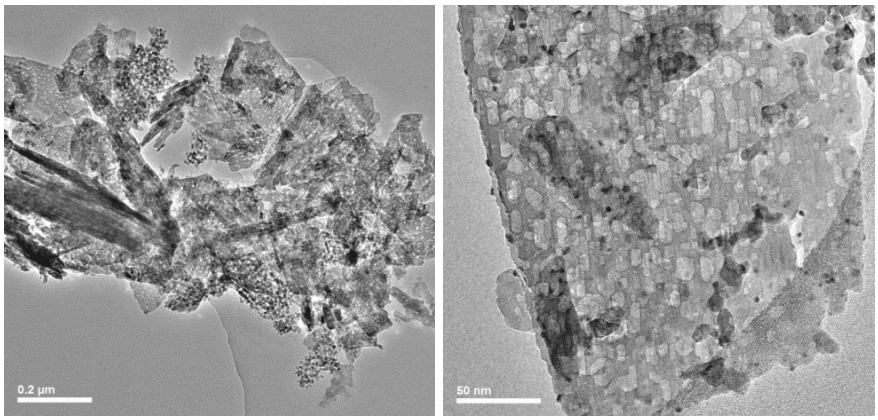

Figure 4: TEM images of Pd/δ-alumina.

Size distribution and dispersions are indicated in the table below; NP diameters increase slightly after calcination, indication that some NP sintering appear during high temperature heat treatment.

Sample	Preparation step	CO-chemisorption Dispersion (%)	TEM Mean diameter (nm)	TEM size standard deviation (nm)
0.3%Pd/δ-Al_2O_3	IMPR+DRY	-	2.03	0.77
0.3%Pd/δ-Al_2O_3	IMPR+DRY+CALC	28.6	2.41	0.91
0.05%Pd/α-Al_2O_3	IMPR+DRY	-	1.73	0.70
0.05%Pd/α-Al_2O_3	IMPR+DRY+CALC	35,5	2.17	0.82

Core-shell Pd@SiO_2

The Pd@SiO_2 nanostructures were synthesized following the procedure detailed **[MAR15]** which consists of three steps:

(1) a seed mediated growth of Pd particles from isotropic colloids of 3–4 nm following the Nikoobakht method **[NIK03]**. Pd nanocubes and Pd nano-polyhedra are synthesized using K_2PdCl_4 as Pd precursor, in presence of various proportions of CTAB and sodium ascorbate, and maturation conditions in order to obtain the final colloidal solution **[BER07, BIS09]**.

(2) the Pd encapsulation by a mesoporous silica shell. In order to obtain core@shell Pd nanoparticles with a mesoporous silica shell (Pd@m-SiO_2), 1 g of tetraethylorthosilicate (TEOS) is added afterwards drop-wise under strong magnetic stirring and the mixture is left overnight for maturation under moderate stirring at room temperature. After maturation and EtOH addition, the suspension was centrifuged (20 min, 14 000 rpm) to recover the precipitate.

(3) the thermal treatment. The black solid is then dried under air at room temperature and finally treated with a hydrogen flow at 250°C for 12 h (heating rate of 2°C min^{-1}).

Two different catalysts were studied:

- one consisting in cubic Pd NPs exposing mostly (100) facets
- one consisting in octahedra but also pyramids or icosahedra NP of Pd giving a combination of (111) and (100) facets.

A reference catalyst was prepared by incipient wetness impregnation of Pd precursor on SiO_2.

Fresh cubic Pd@SiO_2 were characterized by TEM and electron tomography (**Figure 5**). Pd nanoparticles are mainly cubic, even if some round particles are also observed. Between one and two particles are present in each SiO_2 shell. Pd NPs are between 5 and 30 nm. SiO_2 shells are between 40 and 70 nm. Silica presents a very small porosity. Further results on this system will be exposed in the next ANNEXES (H, section H.4 - contribution from MATEIS - and I, section I.4.2 - contribution from IPCMS -).

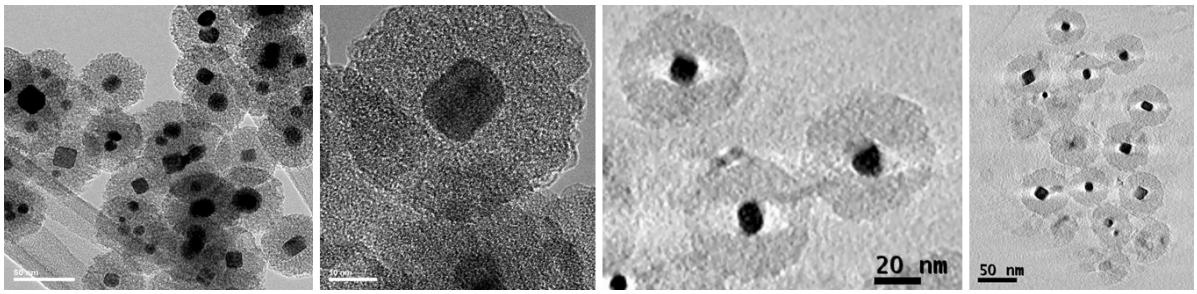

Figure 5: TEM images (Left) and electron tomography (right) of cubic Pd@SiO_2.

These systems were studied during Mounib Bahri's Post-doc **[BAA18]**.

F.2.3. Operando Infrared spectroscopy characterization

Operando Infrared spectroscopy characterization was performed on the reference catalyst described above. Indeed, quantities of core-shell materials were too low to perform other characterizations than TEM. The purpose was to apply an alternative technique to operando TEM to compare results. Complementary information can be obtained:

- Reaction products can be more easily detected by IR in as much the sample quantity is larger than in operando TEM (80 mg vs 1 µg)
- The NP size evolution can be qualitatively estimated by following the evolution of the "stoichiometric factor".

The IFPEN equipment consists of two IR analytical chains connected in series and connected to a mass spectrometer. Everything is supplied by a gas mixer. The DRIFT cell allows IR analysis of the catalyst surface during H_2 reduction and CO_2 / H_2 reaction.

Surface analysis is only qualitative. The gas cell allows to analyze by IR the gases consumed or produced during the reduction under H_2 and the reaction under CO_2 / H_2.The analysis of the gas phase is quantitative, the quantification depending on the Beer Lambert law:

$A = \varepsilon l c$

(Where ε is the absorbance, l the path in the media and c the speed of light)

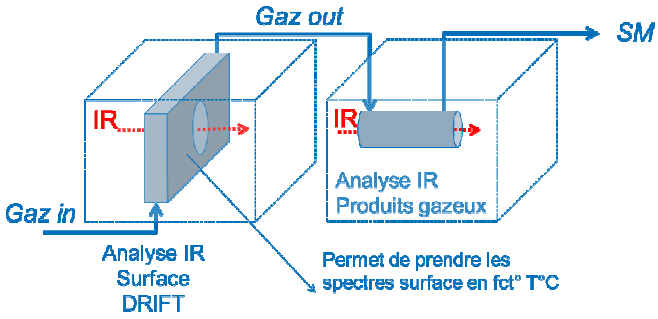

Figure 6: **IR equipment.**

It is complementary to the information given by the mass spectrometer. The IR equipment is described in **Figure 6**; the sample is mounted in a transmission Linkam reactor. The conditions for CO_2 methanation were: reduction under H_2/Ar at 400°C, methanation of CO_2 under CO_2/H_2/Ar at different temperatures: 400, 443, 436 and 454°C (**Figure 7**).

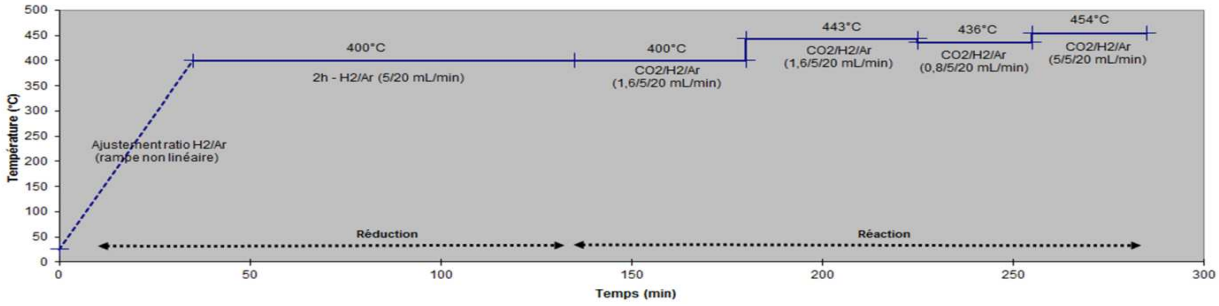

Figure 7: Diagram showing the heat treatment and gas applied to the samples.

The detection of both CH_4 and CO in the products (**Figure 8**) show that two competitive mechanisms take place:

$CO_2 + 4H_2 \leftrightarrow CH_4 + 2H_2O$ (methanation reaction)
$CO_2 + H_2 \leftrightarrow CO + H_2O$ (Water Gas Shift)

CO can be an intermediate of CO_2 reaction since it can also be hydrogenated to form CH_4. Conversion increases with temperature. Ratio CH_4/CO is favored with higher temperature.

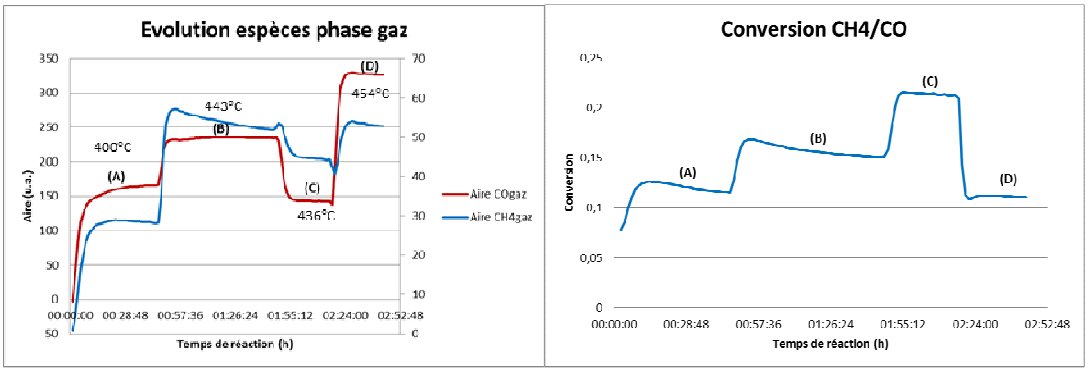

Figure 8: products detected by IR in the gas phase during methanation reaction. *Left*: amounts of CH_4 and CO; *right*: ratio CH_4/CO.

Thanks to CO adsorption on Pd particles, it is possible to estimate the change of size of nanoparticles thanks to the "stoichiometric factor (FS)" (see **Figure 9**):

- For small NP, CO is linked with a carbon down position to the NP, FS is equal to 1
- For larger NP, CO is linked with a bridge position to the NP, FS is equal to 0.5

Thus, an increase of FS corresponds to an increase of NP size. The evolution of FS according to the reaction parameters is presented on **Figure 9**. NP size clearly increases during change from 400°C to 443°C. It seems to stay constant after.

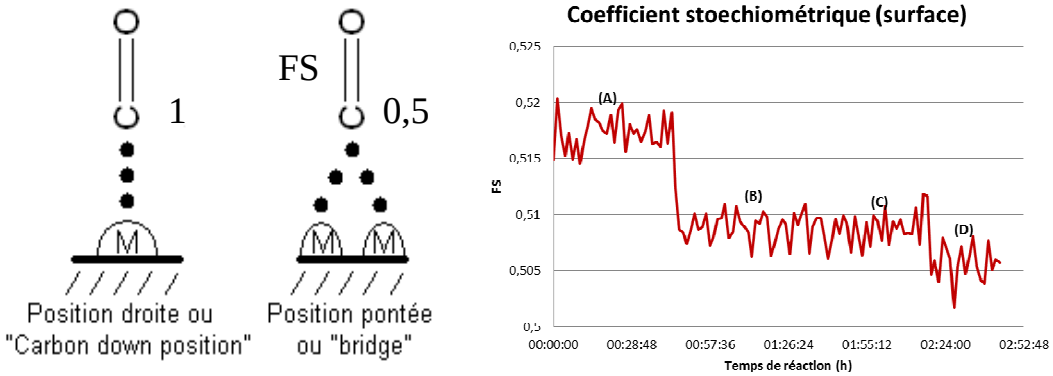

Figure 9: Description of the stoechiometric factor and its evolution with the reaction time.

F.3 CO/ALUMINA CATALYSTS

F.3.1. CONTEXT AND AIM OF THE STUDY

Cobalt-based catalysts are used for the Fischer-Tropsch synthesis (FTS) **[KHO07]**. This well-known process enables the production of transportation fuels through the catalytic conversion of syngas (CO and H_2) coming from various resources such as natural gas, biomass or coal. The following reaction is concerned:

$(2n+1)H_2 + nCO \rightarrow C_nH_{2n+2} + nH_2O$

The objective is to realize the FTS inside the microscope to follow simultaneous the morphological changes of nanoparticles (Co NPs) and the reactants. Lots of assumption exist concerning catalyst deactivation: sintering of NPs, surface reconstruction, coking, surface oxidation by water produced during the reaction. For this study, model catalysts with size controlled nanoparticles of Co have been prepared. This study requires both imaging and chemical analysis, the spectroscopic analysis being performed in order to detect H_2O, CH_4 and paraffins as produced compounds (EELS and/or RGA).

These systems were studied during Kassoigé Dembele's PhD **[DEM17]** and Mounib Bahri's Post-doc.

F.3.2. CATALYSTS PREPARATION AND PRELIMINARY CHARACTERIZATION

Co catalysts have been prepared according to **[BRA13]**. The catalysts were synthesized by wetness incipient impregnation of a cobalt nitrate precursor [$Co(NH_3)_2$, $6H_2O$] on gamma alumina (Puralox) or silica-alumina supports. Ethylene glycol (EG) was added to the precursor in solution to obtain a narrow particle size distribution of cobalt and limit the formation of cobalt aggregates. The addition of all the cobalt (between 11 and 14% by weight) is done in two successive impregnations. After each impregnation, the following steps are carried out: i) the maturation (1 h 30) allowing the capillary migration of the precursor in the pores of the support; ii) drying in air at 85°C overnight to remove water from the impregnating solution; iii) and calcination under air at 400°C for 4h to decompose the cobalt nitrate and generate Co_3O_4 crystallites. They are then reduced to form active Co° phase. Three samples were specially studied during ANR project, their main characteristics are presented in the Table below.

Sample name	**Co_3O_4 wt% (XRF)**	**Pt ppm**	**Co_3O_4 crystallites mean size (nm) (XRD)**
Co/A_2O_3-15nm	14 ± 5	/	15
Co-Pt/A_2O_3-15nm	13,2 ± 3	355	15
Pt-Co/γ-Al_2O_3-SiO_2-16nm	15 ± 3	1000	16

In industrial reactors, process is operated at 230°C and 30 bar. For technical reasons, this high pressure cannot be applied to operando TEM. Some results on these catalysts were obtained on lab equipments to estimate CO conversion and CH_4 selectivity at low pressures (Laure Braconnier and Edouard Rebman's theses at IFPen). Results are presented in the Table below.

Catalyseur	**Co/Al_2O_3-15nm**	**Co-Pt/A_2O_3-15nm**
H2/CO	2	2
Syngas pressure (bar)	6	1.7
Temperature (°C)	230	235
Conversion CO	33 %	11.6
Sélectivité méthane	15 %	34

It can be noticed that by lowering the pressure, the total conversion of CO is largely decreased and the CH_4 selectivity increases.

F.3.3. OPERANDO INFRARED SPECTROSCOPY CHARACTERIZATION

Operando Infrared spectroscopy characterization was performed on the 3 catalysts described above. Complementary information can be obtained:

- Reaction products can be more easily detected by IR in as much the sample quantity is larger than in operando TEM (80 mg vs 1 µg)
- NP size evolution can be qualitatively followed via that of the stoichiometric factor.
- Species formed and adsorbed at the surface of the catalyst can be measured.

The IR equipment has been described on **Figure 6**; the sample is mounted in a Harrick DRIFT cell. The conditions of FT synthesis were applied. Same protocols (reduction time and temperature, operation conditions: temperature 220-250°C, pressure 1 bar, H2/CO ratio = 2) was applied in operando IR and operando TEM. The temperature/gas steps are described below (**Figure 10**).

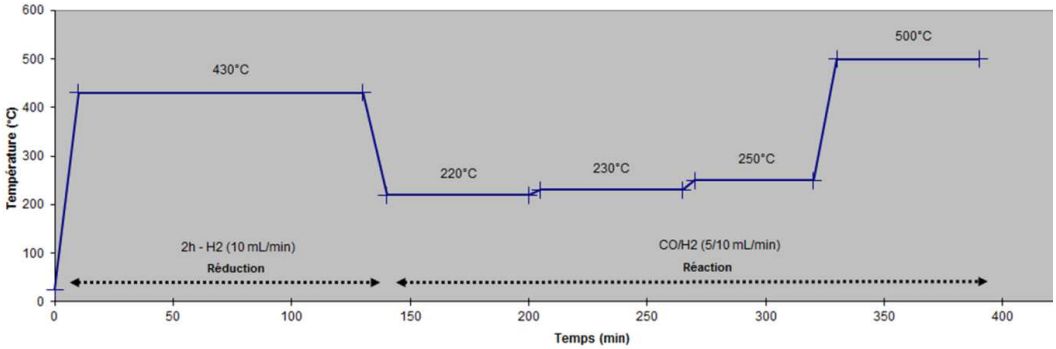

Figure 10: Heat treatment / gas applied to the samples

As an example, **Figure 11** describes the nature of species detected in the gaseous phase according to the reaction temperature for the Co-Pt/SiO_2-Al_2O_3 catalyst. Between 220° and 250°C, FT synthesis takes place in as much C_nH_{2n+2} paraffins and water are detected. Even if the method is not qualitative, we can observe that the main product formed is methane, confirming the high selectivity to CH_4 at low pressure.
Conversion is increasing with temperature. At very high temperature, 500°C, CO conversion is strongly increased but product reactions are methane and CO_2, showing that a water-gas- shift reaction is occurring. For the two other catalysts, the reactions are quite similar, only the CO conversion level differs: conversion is largely lower for the catalyst without Pt. It is higher for Co-Pt/Al_2O_3 than Co-Pt/SiO_2- Al_2O_3.

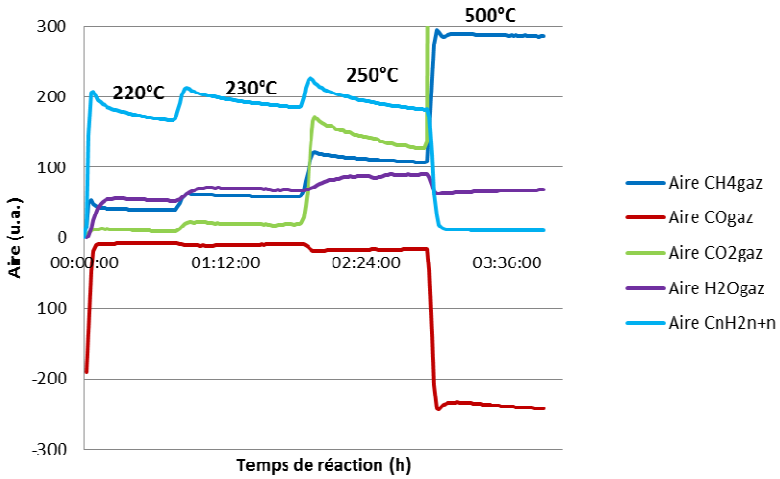

Figure 11: products detected by IR in the gas phase during FT synthesis

The following graph (**Figure 12**) compares the evolutions of the stoichiometric factor for the 3 catalysts. It can be interpreted as a size measure of the Co nanoparticle. If FS is decreasing, it means than the proportion of bridge CO is increasing, corresponding to a larger proportion of bigger particles.
We can observe different behaviors according to the catalysts:

- For Co/ Al_2O_3 catalyst, FS is increasing with reaction temperature between 220 and 250°C. It can be associated to the reduction of Co_3O_4 with is not achieved at the end of the reduction step. In particular, in catalysts supported on alumina and without Pt doping, reduction of small particles is difficult. It is achieved during FT synthesis. This result also explains why CO conversion on this catalyst is lower

- Both Co-Pt catalysts do not show changes in size during the first part of the reaction.
- At 500°C, all catalysts present an important increase in size. This is due to sintering favored by high temperature.

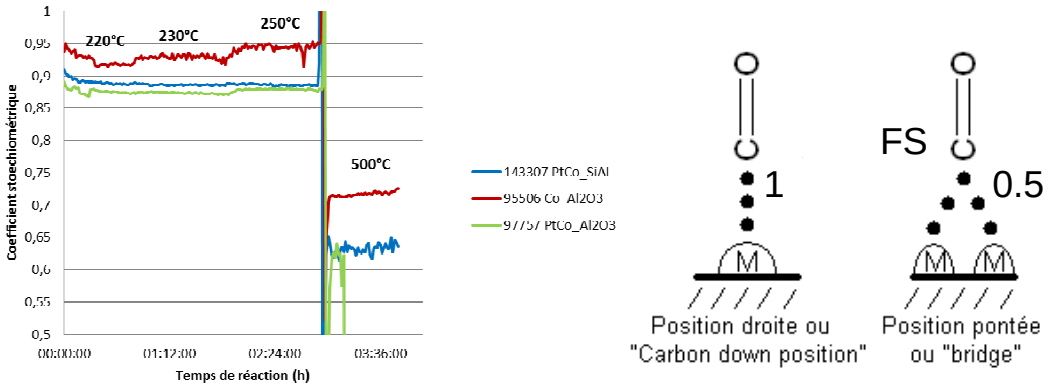

Figure 12: evolution of the stoechiometric factor according to reaction time.

F.4 Ni/alumina catalysts

F.4.1. Context and aim of the study

Another system of catalysts was studied during 3DCLEAN project: Ni/alumina. This family of catalyst can be used for CO_2 methanation. In this topic, selectivity of the reaction of CO_2 methanation vs Water gas shift is a main issue. It could be linked with NP size.
In a more general context of heterogeneous catalysis, there is also a big deal with NiO reduction for Ni active phase formation.
These systems were studied during Mounib Bahri's Post-doc and for crossed-experiments between IPCMS and MATEIS.

F.4.2. Catalysts preparation and preliminary characterization

Two different catalysts were studied:
- Ni/δ-alumina containing 10% NiO, obtained by incipient wetness impregnation of Ni precursor. Catalysts are dried and calcined at 280°C. NPs on oxide form are of small size, with weak interaction with the support. It is referred as "Ni-Small"
- Ni/δ-alumina containing 15% NiO, obtained by incipient wetness impregnation of Ni precursor. Catalysts are dried and calcined at 450°C. NPs on oxide form are of large size, with strong interaction with the support. It is referred as "Ni-large"

Figure 13 confirms that the first preparation "Ni-Small" leads to very small NiO particles, hardly visible. Their size is of few nm.
In situ XRD was performed on calcined samples to follow the reduction process under H_2 during temperature increase.

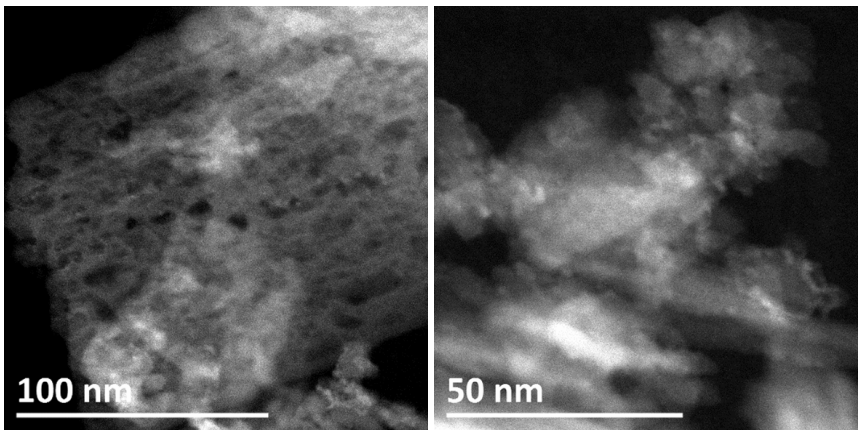

Figure 13 : ADF-STEM images of "Ni-Small" under oxide form.

On **Figure 14**, it can be seen that at the beginning of the step at 400°C, most of NiO is converted to Ni° nanoparticles. The reduction on "Ni-small" sample is quite easy. The crystallite size at 400°C is 4 nm at 400°C.
Figure 15 confirms that the second preparation "Ni-large" leads to larger NiO particles. Their size is of dozens of nm. They present a hollow structure.

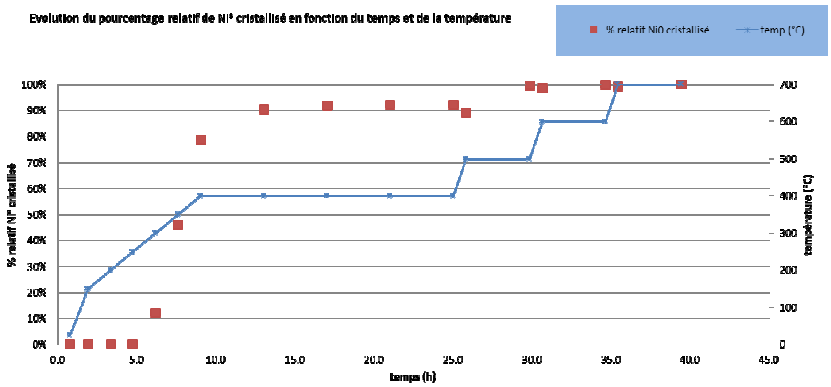

Figure 14: In situ XRD reduction under H_2 of "Ni-small" sample.

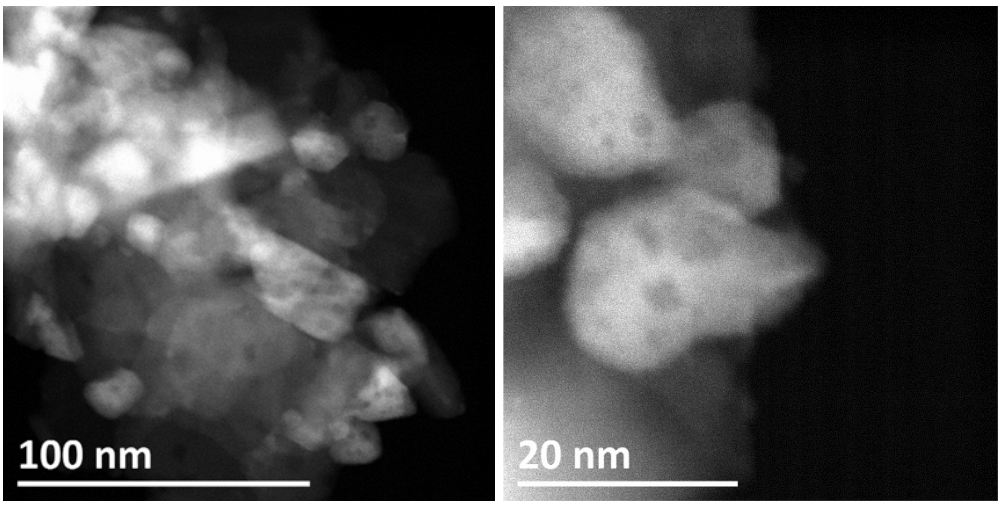

Figure 15: ADF-STEM images of "Ni-large" under oxide form.

In situ XRD was performed on calcined samples to follow the reduction process under H_2 during temperature increase. On **Figure 16**, it can be seen that NiO is difficult to reduce to Ni°. Even after several hours at 400°C, only 40% of Ni is in the metallic form. It needs to increase temperature up to 700°C to complete the reduction of "Ni-large" sample.

F.4.3. OPERANDO INFRARED SPECTROSCOPY CHARACTERIZATION

The experiment was performed on "Ni-large" sample. The aim was to use an alternative technique to operando TEM to compare results (see ANNEXE G, section G.2.2). The conditions of CO_2 methanation were applied. Complementary information can be obtained:

- Reaction products can be more easily detected by IR in as much the sample quantity is larger than in operando TEM (80 mg vs 1 µg)
- NP size evolution can be qualitatively estimated by evolution of the stoichiometric factor.

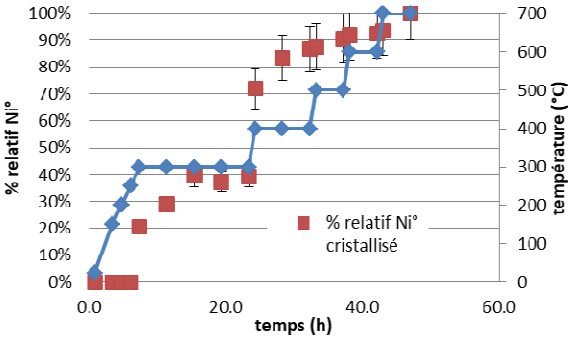

Figure 16: In situ XRD reduction under H_2 of "Ni-large" sample.

The temperature/gas steps are described on **Figure 17** below.

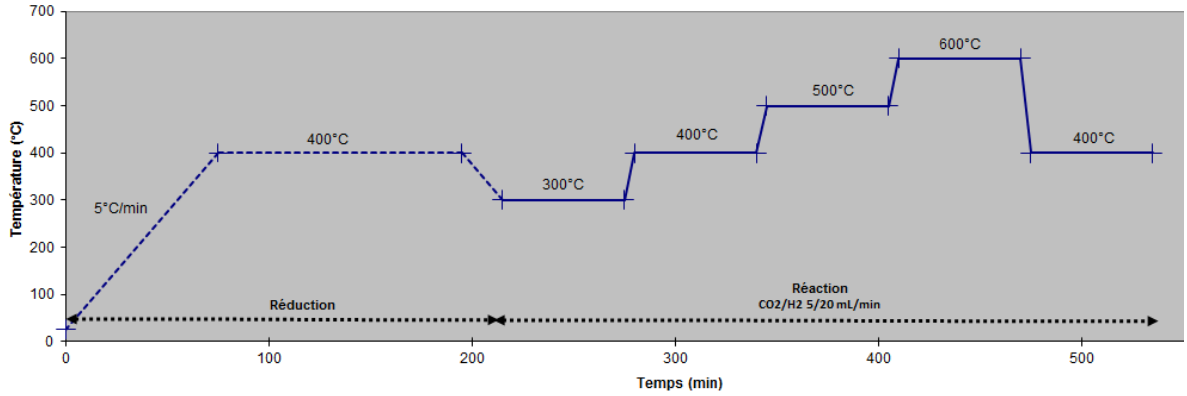

Figure 17 : Heat treatment / gas applied to the samples

After reduction under H_2 at 400°C and under a CO_2/H_2 reaction mixture, a CO_2 consumption, a formation of CH_4 and CO_2 and water are observed in the gas phase (**Figure 18**). This is reflected on the surface of the catalyst by linear or bridged nickel carbonyl species. At 300°C, a chemisorption of alkanes and carbonate species is also observed. Analysis of the gas phase by mass spectrometry confirms these observations as well as H_2 consumption during the reaction. It should also be noted that the $Ni(CO)_4$ gas was not observed.

The reaction system highlights the following reactions:

(1) $CO_2 + 4H_2 \leftrightarrow CH_4 + 2H_2O$ or $CO + 3H_2 \rightarrow CH_4 + H_2O$ (methanation reactions)
(2) $CO_2 + H_2 \leftrightarrow CO + H_2O$ (Water Gas Shift)
(3) $n\,CO + 2\,(n + 1)\,H_2 \rightarrow C_2H_2 + 2 + n\,H_2O$ (Fischer Tropsch reaction only at 300°C)

The modulation of the reaction temperature from 300 to 600°C strongly impacts the CH_4 conversion rates as well as the competitive equilibrium between the 3 reactions identified. Moreover, the carbonyl formation of Ni at the surface of the catalyst makes it possible to probe the nature of the active phase at the various reaction temperatures. Indeed the monitoring of the stoichiometric factor (FS) calculated from the areas of the linear / bridged carbonyls is a good indicator for qualitatively evaluating the evolution of the size of the nanoparticles of Ni over time and as a function of the reaction temperature.

The stoichiometric factor (between 0.5 and 1 assuming the hypothesis of the formation of two-sided carbonyls μ^2) is determined by the following relation:

$$FS = \frac{(\text{linear} + \text{bridged})}{(\text{linear} + 2 \times \text{bridged})}$$

This result (**Figure 19**) shows a great increase of Ni NP size during CO_2 methanation at high temperature. It does not seem to influence CH_4 formation, but decreases CO formation (cf. **Figure 18**). Thus CO_2 methanation is favored vs water gas shift on larger NPs.

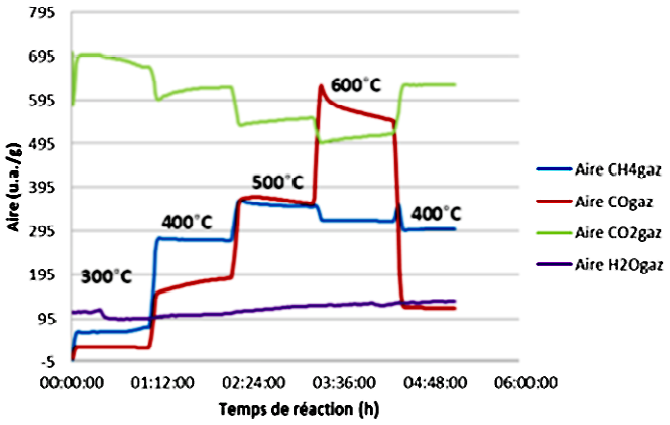

Figure 18: Evolution of products concentration in the gas phase.

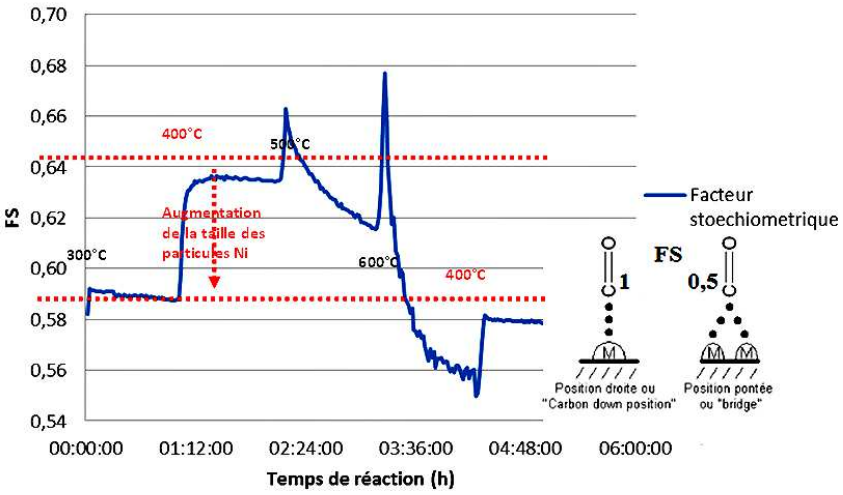

Figure 19: evolution of the stoechiometric factor according to reaction time.

F.5 REFERENCES

[ARG02] A.M. Argo, J.F. Odzak, F.S. Lai, B.C. Gates, *Nature* **415** (2002), 623.
[BAA18] W. Baaziz, M. Bahri, A S Gay, A. Chaumonnot, D. Uzio, S. Valette, C. Hirlimann, O. Ersen, *Nanoscale*, **10** (2018) 20178.
[BER07] G. Berhault et al., *Appl. Catal. A* **327** (2007), 32.
[BIS09] L. Bisson et al., *Chem. Mater*. **21** (2009), 2668.
[BRA13] L. Braconnier et al., *Catalysis Today* **215** (2013) 18.
[DEM17] K. Dembelé, thesis, U. Strasbourg, F, 20/12/20187. http://www.theses.fr/2017STRAE008
[DID98] D. Didillon, E. Merlen, T. Pagès, D. Uzio, *Stud. Surf. Sci. Catal.* **118** (1998) 41.
[KAR12] A. Karelovic, P. Ruiz, *Appl. Catal. B Environ*. **113–114** (2012) 237.
[KHO07] A.Y. Khodakov et al., *Chemical Reviews* **107** (2007) 1692.
[KON17] S. Koneti, thesis, UDL – INSA-Lyon, 05/12/2017. http://www.theses.fr/2017LYSEI123
[MAR15] J. Martins et al., *Catalysis Communications* **58** (2015) 11.
[NIK03] B. Nikoobakht, M. A. El-Sayed, *Chem. Mater.*, **15** (2003) 1957.
[RAM07] M. Ramos-Fernandez et al., *Oil & Gas Science and Technology – Rev. IFP,* **62** 1 (2007), 101.
[SAS11] C. Sassoye et al., *Green Chem.* **13** (2011) 3230.
[SOR12] L Sorbier et al., *IOP Conf. Series: Materials Science and Engineering,* **32** (2012) 012023.

G APPENDIX 2: WP 2 - PURCHASE, SET-UP AND TESTING OF THE RGA ANALYZER ON THE HPEC DEVICE

G.1 RECALL OF THE DEFINITION OF THE TASKS

Duration	6 months
Objective	. Development of the RGA system, in collaboration with *Protochips* . Installation, technical setp-up, test on model systems, sensibility range. . correlation with EELS (in HPEC and ETEM)
Responsable	Ovidiu Ersen (IPCMS)
Partners	MATEIS (ETEM comparison / checks within the compatible pressure ranges)
Deliverables	. operational system . quantitative measurements of gas (reactants)
Contribution	IPCMS internal resources and facilities; support from *Protochips*; about 24 H.M (including contribution from the postdoc to be recruited)
Risks and failback solutions	Medium risk: unexpected technical issues may delay the final setting but at the end the system must be operating because of the expertise and the engagement of the manufacturer.

G.2 INSTALLATION OF THE RGA AND TEST RESULTS

G.2.1. GENERAL TECHNICAL ASPECTS

This part of the project was devoted to the experimental development of the Operando TEM mode for the study of the catalytic materials in conditions as close as possible to that used in catalytic reactions. As explained in the main text of the report, such in-situ TEM studies applied to catalytic materials requires the analysis of the reaction products simultaneously to the acquisition of the TEM images or spectra. To do that, an RGA (Residual Gas Analyzer) system was purchased from the society Pfeiffer©, model QMA200™ (quadripolar analyzer) and installed, in collaboration with Protochips© (the provider of the E-cell holder), at the exhaust line of the Atmosphere gas cell. We mention that this was the first experimental set-up in the world, in combination with a commercial cell, allowing to perform such operando studies using a gas pressure of 1 atm. The general diagram of the interconnections of the RGA with the gas system and the E-cell holder to be inserted in the microscope is shown in **Figure 20**.

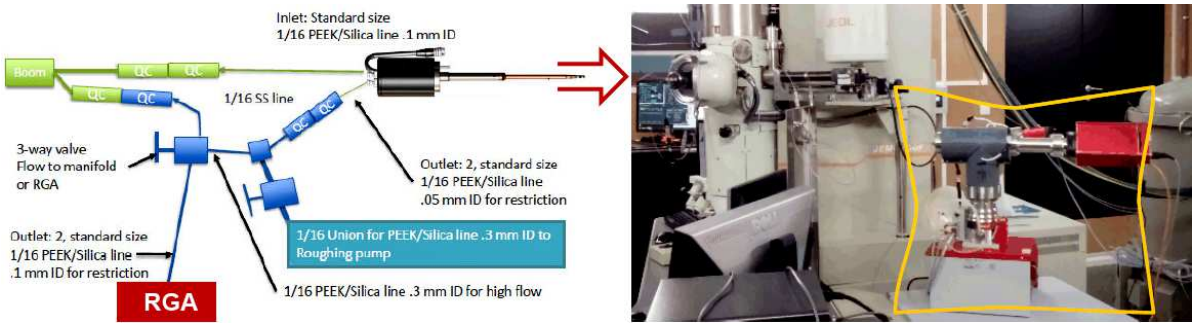

Figure 20: synoptic of the RGA set-up and view of its connection to the microscope (© IPCMS). Note that several positions were tested in order to minimize the vibrations (the quality of imaging in the microscope) due to the pumping system attached to the RGA.

The RGA works on the basis of the following principles: 1) first, atoms from the gas are ionized owing to some ignition filaments; 2): ions are accelerated in the entry tube of the system (the quadrupole part made of 4 rods allowing ion trajectories to be controlled), then detected according to their mass; 3) signal processing: the ionic current is converted into an electric current; 4): analyzed species are display as a mass spectrum, as shown in **Figure 21.**

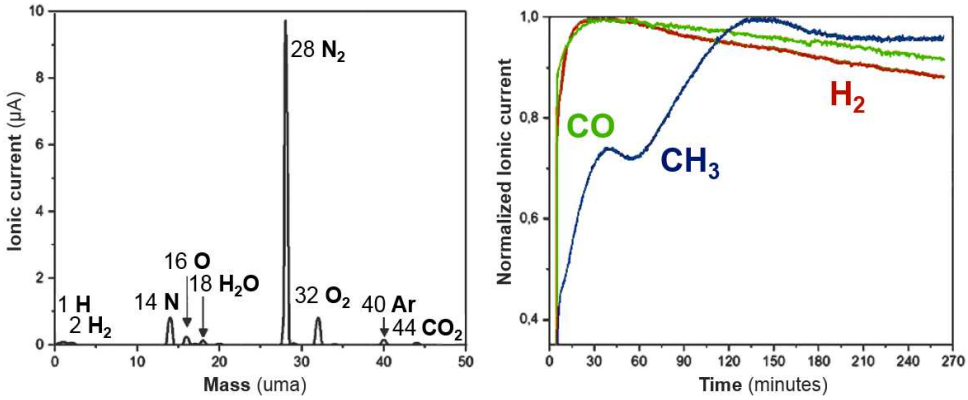

Figure 21: output data form the RGA system: 'analogic scan' and 'detection of multiple ions' modes (respectively left and right; adapted from **[DEM17]**; IPCMS).

The first difficulty of the practical implementation of this experimental set-up originated from the small amount of the catalytic materials which can be deposited in the experimental cell. A considerable number of tests regarding the deposition step was performed in order to maximize the amount of the catalytic material to be inserted in the cell. The second experimental aspect which was considered for the improvement of the experimental conditions was the reduction of the length of the capillary tubes connecting the cell to the RGA system, in order to decrease the time response of the analyzer and to prevent the water condensation phenomena in the tube. A new mechanic detachable support allowing to approach the analyzer close to the cell exhaust lines was developed at this regard during the project (see Figure in the main text of the report).
This experimental set-up was tested using a model system and catalytic reaction, in particular Ni/alumina catalyst and CO_2 methanation reaction. As compared to the FT synthesis, the limited number and the basic type of reaction products we can obtained in this case, facilitate the operando analysis; some typical results are given in the next sub-section (Remark: this study is also part of the 4th Work Package WP4).

G.2.2. Ni nanoparticles used as catalyst in the Sabatier catalytic reaction: operando TEM study in real reaction conditions

In this part of the project, we performed in the context of the operando experiments a typical combined "environmental TEM-RGA" study. By considering the CO_2 methanation as the reaction of interest (Sabatier reaction), one of the most active catalysts is made out of Ni based nanoparticles supported on alumina support. The Ni particles were initially in the oxide state and were thus firstly activated under H_2 at atmospheric pressure (**Figure 22**).

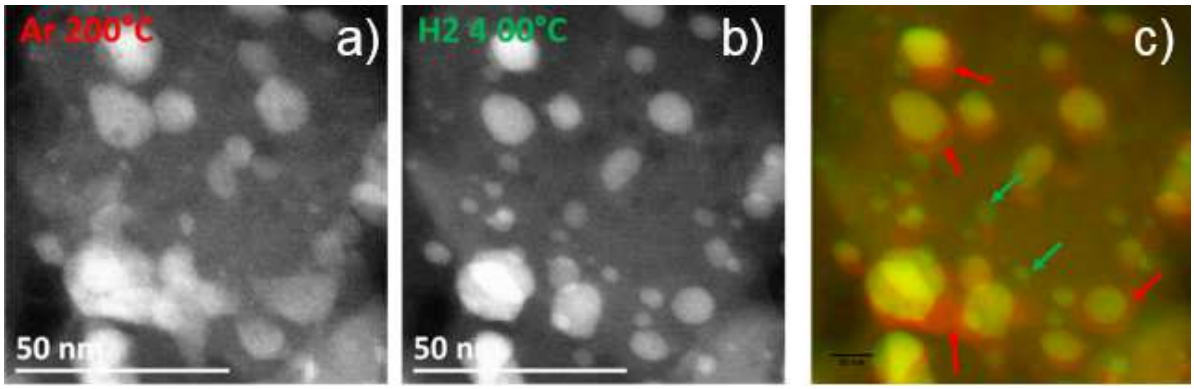

Figure 22: STEM-HAADF analysis of the reduction process of the Ni/Al_2O_3 catalysts: (a) initial state under Ar at 200°C: NiO particles (b) after reduction under H_2 at 400°C: Ni metal particles and (c) the superposition of the two images (a) in red and (b) in green. Red arrows show the oxide phase before reduction and green arrows the particles formed after the reduction step.

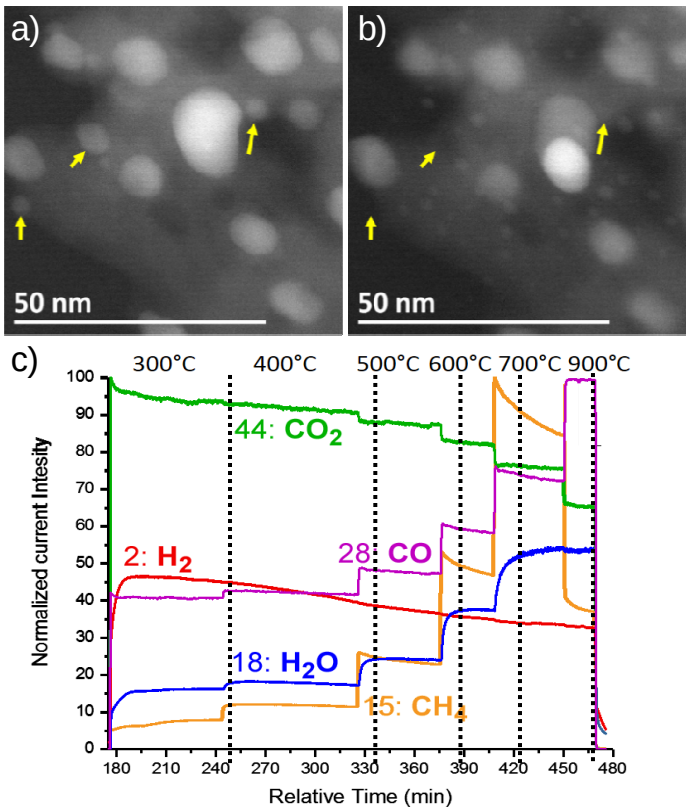

Figure 23: In-situ TEM operando study of Ni catalysts for the CO_2 methanation reaction under a mixture of H_2/CO_2=4 at temperature between 300°C and 900°C. a): STEM-ADF image of one of the typical Ni/Al_2O_3 areas at 400°C. b): STEM-ADF image of the same Ni/Al_2O_3 area at 600°C. Yellow arrows point out the particles fragmentation process from 400°C to 600°C. (c): Monitoring of the main gas compounds using RGA.

By directly following individual NiO particles from 200 to 400°C, we have observed that the oxide to metallic nickel transformation starts at 270°C and that the reduction is accompanied by the Kirkendall effect classically observed **[CHE12]**.
The metallic Ni particles as obtained were then used in the methanation reaction under a mixture of H_2/CO_2 (ratio = 4) at atmospheric pressure with the temperature ranging from 300 to 900°C. In this case, we clearly demonstrated that by combining the TEM in-situ approach with the gas analysis through a mass spectrometer, we are able to measure the reaction products generated by the small amount of catalyst deposited within the cell, to monitor their evolution as a function of the temperature and to correlate them with the microstructural modifications of the catalyst, see **Figure 23**.

These spectroscopic data can be commented in the following way:

(i) The methanation reactions, as introduced in ANNEXE F (§.F.4.3):
$CO_2 + 4H_2 \leftrightarrow CH_4 + 2H_2O$ or $CO + 3H_2 \rightarrow CH_4 + H_2O$
are clearly confirmed according to the continuous decrease of the masses 44 (CO_2) and 2 (H_2), and the associated increase of 15 (fragment of CH_4; the main component of mass 16 for 'CH_4' is also a fragment common to water and also the mass of O) and 18 (H_2O).

(ii) At about 500°C, the increase of mass 28: CO, the accelerated increase of H_2O and decrease of CO_2 indicate that CO_2 conversion occurs through the WGS reaction:
$CO_2 + H_2 \leftrightarrow CO + H_2O$

(iii) A striking relative change in the $CO_2/CO/H_2O$ ratios has been evidenced bear 600°C, assigned to a progressive fragmentation of the particles when increasing the temperature under CO_2/H_2 at atmospheric pressure (see **Figure 23b**).

These results are in very good agreement obtained during ex-situ measurements (operando infrared spectroscopy) reported in ANNEXE F (§.F.4.3, **Figure 18**). This demonstrates the relevance and the interest of a combined TEM and spectroscopy analysis, as permitted by the combination of the RGA system with the environmental close-cell.

G.3 REFERENCES

Note: results obtained during combined ETEM (E-cell) and RGA studies at IPCMS have not yet been published but manuscripts are being prepared at the time of writing this report.

[CHE12] S. Chenna, P. Crozier, *Micron* **43** (2012) 1188.

H APPENDIX 3: WP 3 - ENVIRONMENTAL 2D/3D IMAGE PROCESSING (FAST TOMOGRAPHY AND MORPHOLOGICAL ANALYSIS)

H.1 RECALL OF THE DEFINITION OF THE TASKS

Duration	3 years (PhD thesis)
Objective	. Optimize the TEM nano-tomography in the environmental mode (ETEM); provide methodologies for a routine use of 'fast tomography' for the quantitative 3D characterization of catalysts and beam-sensitive nanomaterials.
Responsable	Voichita Maxim (CREATIS)
Partners	MATEIS (fast tomography in ETEM) and IFPEN (2D / 3D analysis)
Deliverables	. improved acquisition of tomographic tilted series in the ETEM . optimized processing (deblurring / denoising) of the series for further reconstruction. . quantitative morphological analysis of results obtained on catalysts followed in environmental microscopy (ETEM and HPEC).
Contribution	MATEIS/CREATIS/IFPEN internal resources and facilities; 70 H.M with PhD student to be recruited
Risks and failback solutions	*Low risk: feasibility of 3D tomography already demonstrated; good adequation of skills and expertise from all partners involved regarding the challenges of the current task.*

H.2 IMPROVED ACQUISITION OF TOMOGRAPHIC TILTED SERIES IN THE ETEM

H.2.1. SEMI-FAST ELECTRON TOMOGRAPHY

The 3DCLEAN started in a context where the MATEIS partner intended to develop rapid tomography acquisitions in order to follow as much as possible dynamic events during environmental experiments. Under the combined action of temperature and gas, the sample, e.g. a nanocatalytic system, evolves naturally, which implies that any acquisition of tilt series, as required for usual electron tomography analysis, must be performed in a short time to allow meaningful 3D reconstructions.
During the first months of the project, we have improved our preliminary results introduced in our ANR submission, i.e. the 'accelerated' Step-By-Step Electron Tomography' (SBSET) approach. It simply consists in speed up the acquisition in two ways:

- Skipping any adjustment, such as tracking of the object, refocusing, usually performed at each tilt position during the acquisition of a tilt series in conventional ET.
- Furthermore, instead of working in the classical STEM mode which generally requires several tens of seconds to acquire each image, we exclusively work in the Bright Field, where a typical acquisition time for a 2k×2k image is 0.5 seconds or much less. All this allows to decrease the total acquisition time to a couple of minutes, as compared to more than ten, and up to one hour or even more, in usual STEM tomography.

It must be confessed that several drawbacks of this accelerated BF SBSET strategy are generally identified in the specialized literature: out of focus images, diffraction contrast reducing the quality of the reconstruction, it has been demonstrated that these limitations do not totally make any such 3D experiment. Indeed, we can repeat here that during an in situ experiment where the object of interest is possibly constantly evolving, one *has to acquire the tilt series as rapidly as possible*. One of the sine qua none conditions for allowing the reconstruction is to keep the Region Of Interest (ROI) in the field of view during the acquisition of the tilt series. Because of mechanical instabilities, among which the displacements produced by the imperfect eucentric alignment, it is almost impossible to adjust ideally and a priori for high magnification over a tilt amplitude of 140°C. This centering procedure may in fact be performed

manually by a skillful user during a short pause at each tilt position (typically one second). We have developed a simple routine in the form of a script file programmed in Digital Micrograph™, the Gatan © software driving our camera on the Titan ETEM microscope, to drive automatically the rotation of the sample (goniometer) over the whole tilt range together with acquiring each image after a pause as mentioned above. Doing so, it appears that a noticeable fraction of final images remain largely blur because the manual drift correction is not finished when the camera starts recording. Various methods have been tested to at least suppress automatically the worst images post-mortem before the alignment of the acquired series (all needed correction drifts being essentially different, there was no possibility to attempt a deblurring method as it will be tried in the case of the 'rotation blur' present in images during a continuous rotation of the sample, see next sub-section H.2.2). This work was conducted during the master internship of Khanh Tran in 2016 (not financed by the ANR). A typical illustration of this treatment, still imperfect but easy to terminate manually, is given in **Figure 24**.

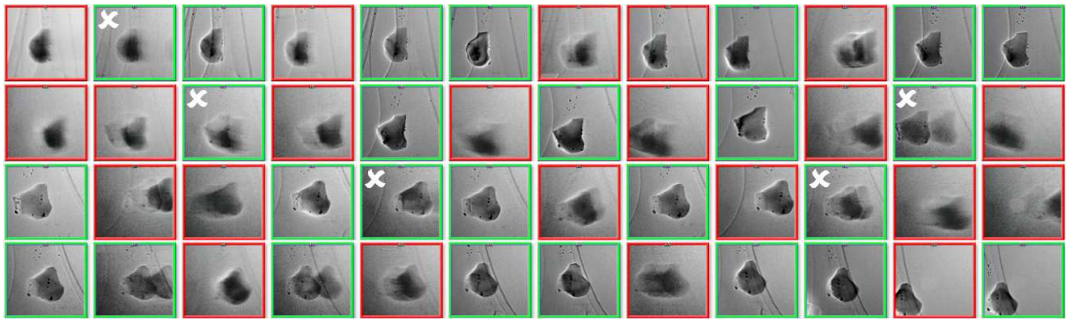

Figure 24 : illustration of the detection of blurred images in a tilt series acquired on the Pd / α-alumina system (to spare space, about one image over 10 is shown here). Green frames show 'sharp' images whereas images considered as blurred as shown in red. Note that few errors marked by white crosses remain.

These elements have been further discussed in **[ROI18, KON19]**, and the method has been used in several studies **[KON17a, KON17b, ROI18, EPI18, EPI19a, KON19]**. Among these works, some were devoted to beam sensitive materials, where the interest to speed up the acquisition is to reduce the irradiation damages, then the morphological evolution of the sample during its exposure to electrons. Indicative illustrations are reported in **Figure 25** and **Figure 26**.

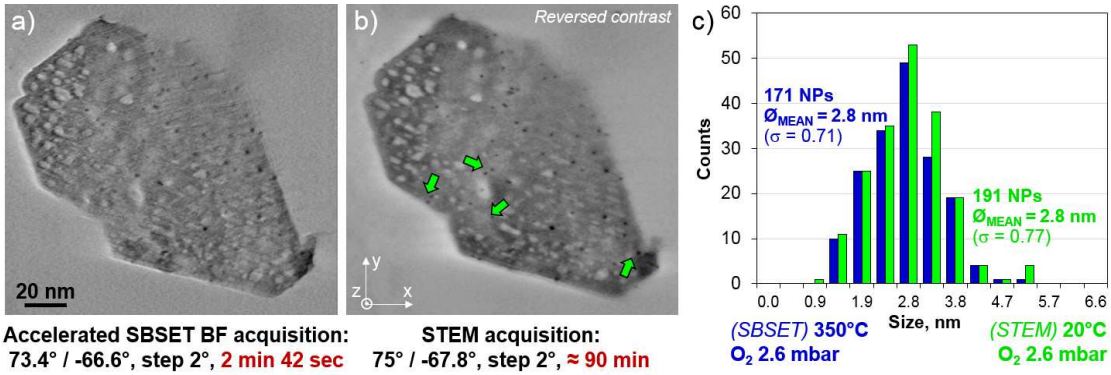

Figure 25: comparison of a fast SBSET tomography acquired on a Pd/δ-Al_2O_3 sample in situ at 350°C under 2.6 mbar of oxygen (a) with a conventional STEM tomography acquired on the same object at 20°C under high vacuum after a rapid cooling under O2 (b). Both images are orthoslices projections near the top surface of the supporting δ-Al_2O_3 sample extracted from the 3D reconstructions (SIRT-FISTA-TV algorithm **[BAN18]**). Note that both microstructures are similar (as expected), except a few more Pd NPs detected (green arrows) in b). c): Histograms of size for the Pd NPs in both cases; their similarity confirm the relevance of the 'accelerated' acquisition performed in situ in a much shorter time than the STEM acquisition (less than 3 minutes as compared to 90 minutes). ETEM 300 kB, MATEIS-CLYM. See more details in **[EPI19a]**.

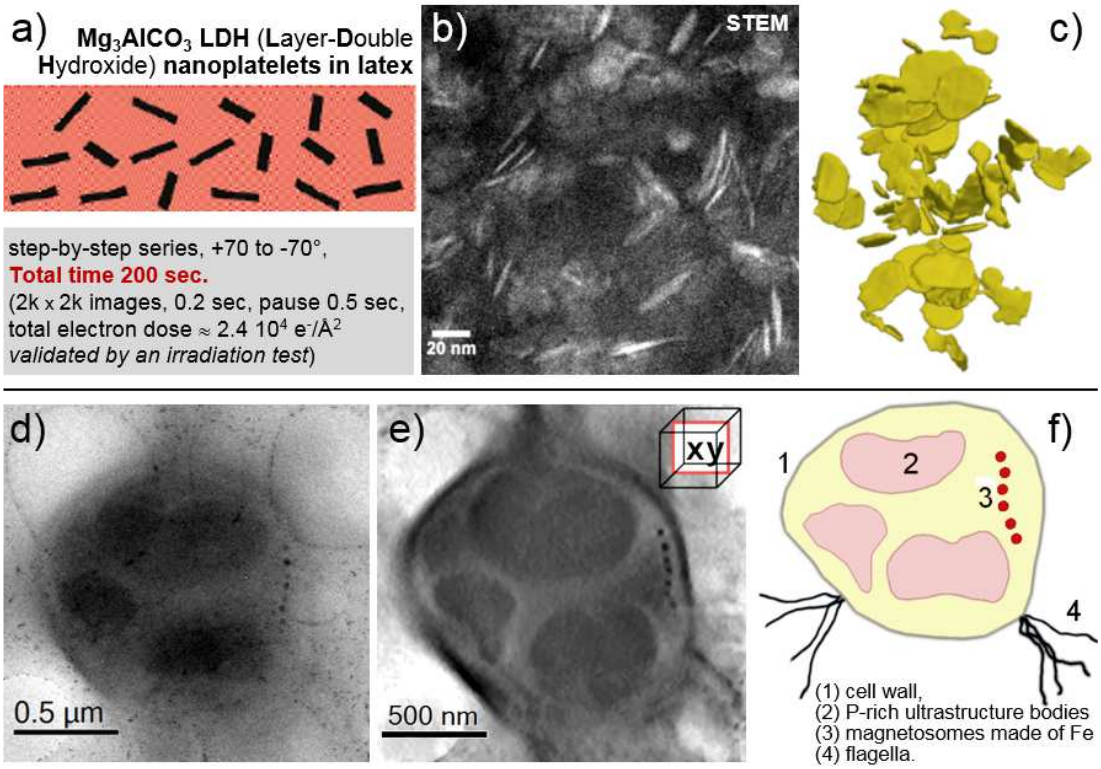

Figure 26: Examples of 'accelerated' SBSET experiments. a-c): Polymer nanocomposite reinforced by LDH platelets; the microstructure sketched in a) is imaged in the STEM mode in b). c): 3D model reconstructed from a tilt series according to the experimental conditions reported in a) (grey frame; ETEM MATEIS-CLYM, 300 kV). d-f): Magnetotactic bacteria studied in the ETEM at 80 kV; a) : bright field image showing a 2D projections with a poor contrast. b) Projection of the reconstructed volume (tilt series acquired in 150 seconds over a tilt range +50 to -50°C. f): Sketch showing various elements identified in b). Reconstruction were performed with the ART algorithm included in the TOMOJ software **[MES07]**. See **[KON19]** for more details.

H.2.2. Continuous rotation and Image deblurring

The idea of acquiring a video, or dynamic sequence of images during a continuous rotation of the sample was already tested in the diffraction mode, where the full rotation of 100° or slightly higher was covered in a few minutes **[NAN14, GEM15]**. Obviously, during this operation, micrographs will integrate a 'rotation blur', that is a blur due to the rotational motion of the sample while acquiring the image in a given time. In addition, additional translational blur may appear because the inaccuracy of the eucentric, meaning that undesirable (x,y) drifts in the image plane. A last cause of blur may be due to corrected drifts applied manually by the user when trying to keep the sample within the field of view.

As planned in the objectives of the project, we have undertaken image processing routine in order to account and correct all these undesirable effects. Although these efforts have been stopped after the acquisition of the fast camera which eliminates roughly the rotation blur (see next sub-section), we summarize here some of the results obtained regarding the deblurring methods. Blur correction was the subject of Yuemeng Feng's master's degree internship started in 2016 (not financed by the ANR). Basically, the blur can be described as the application of a 'blur' function f to an image M, giving a result B:

$$B = M \otimes f + n$$

Where $\otimes$ designates a convolution, and n represents noise.

Direct analytic methods (Wiener filtering, Constrained Least Squares filtering) and iterative methods, including FISTA (a numeric routine favoring convergence, see sub-section H.3.1), where tested. In the case of the rotation blur evoked above, the

convolution filter f is not known. Various tests run on experimental images using other methods, such as one implemented in *Matlab* (the method of SHAN et al. **[Sha08]**, did not gave good results because of the noise in the images. The best results were obtained by implementing a semi-blind deconvolution, where the filter was estimated from a pair of consecutive, or sufficiently close, images within the sequence, one being the blurred one, the other one being a ideally sharp one, as illustrated in **Figure 27**. These results were presented at the European Microscopy Congress EMC2016 **[FEN16]**.

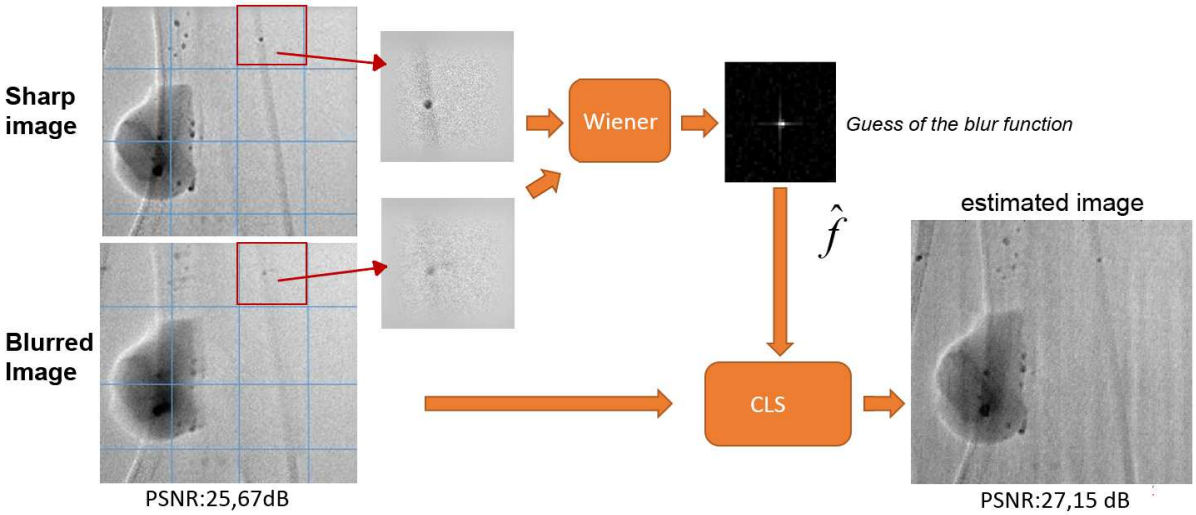

Figure 27 : Methodology for image deblurring (see text for details); illustration with micrographs from a tilt series from the Pd/α-alumina catalyst. Identifying a detail which is not expected to change between both images (like a spherical gold nanoparticle intentionally added as fiducial markers) allows to estimate the blur function f and then produced a deconvoluted, corrected image.

H.2.3. Fast acquisition during continuous rotation with the Oneview camera

Influence of the rotation blur

As previously indicated, the financial support of the project allowed us to by a camera of the last optimized CMOS generation, the Oneview camera form Gatan©. With this device capable of acquisition of 100 fps in a 2kx2k binning mode, it appears that the goniometer of the microscope could be rotated at full speed with any significant rotation blur effect, as it was clearly demonstrated by simulation and reconstruction of a 3D ghost model, including an increasing rotation blur contribution, see **Figure 28**.

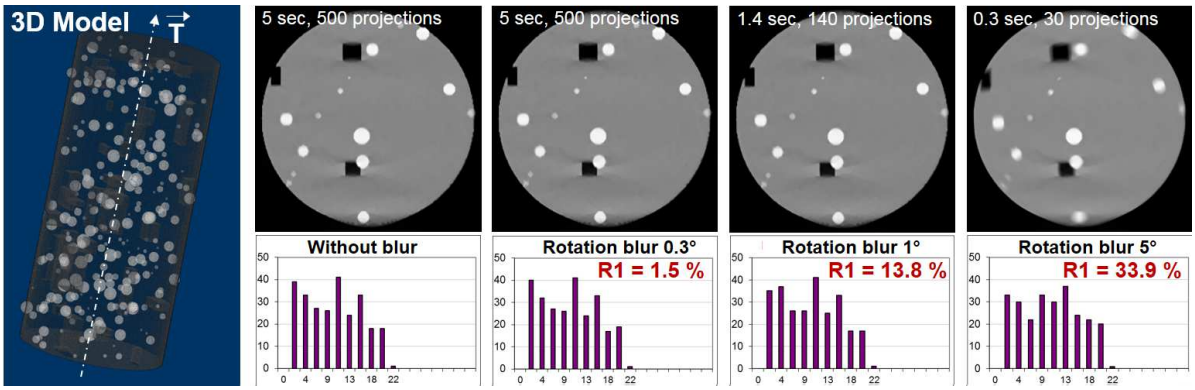

Figure 28 : Simulations of 3D reconstructions of a 3D ghost model (left) for various rotation blurs as produced from rotation conditions expressed in the Table below. The influence of the rotation blur is evaluated through a quantitative comparison of the size histogram of the 'particles' in the model (white circles) of any 'blurred' series with the unblurred one (R1 factor). Reconstructions were obtained with the SIRT-FISTA-TV program developed during the project and described in section H.3.

These simulations have been run under the conditions defined by the Table below, where a 140° rotation amplitude is covered in short times (t_{total}) down to an unrealistic value of 0.3 s.

Rotation angular amplitude: 2α	140°	140°	140°	140°
Total acquisition time: t_{total}	10 sec	5 sec	1 sec	0.3 sec
Angular rotation speed $\omega = 2\alpha/t_{total}$	14°/sec	28°/sec	140°/sec	467°/sec
Number of frames per second: *Fps*	100	100	100	100
Rotation blur / frame: $\Delta\alpha = \frac{2\alpha}{t_{total} \cdot Fps}$	0.14°	0.28°	1.4°	4.7°

According to this, it was shown that the maximum rotation speed available on the microscope Titan ETEM, corresponding to about 5 seconds for a rotation of 140°, did not *intrinsically* produce a rotation blur affecting seriously the quality of both projections and 3D reconstructions. It was then decided to stop our investigations on deblurring methods.
These results were published in the journal *Ultramicroscopy* **[BAN18]**.

Accounting for the inaccuracy of the eucentric alignment and mechanical displacements

While the problem of blur due to the continuous rotation was 'solved' owing to the speed of acquisition of the Oneview camera (100 fps), the very short time of total acquisition made it impossible to correct manually the (x,y) drifts due to any mechanical instabilities, as it was performed in the 'accelerated' SBSET approach described in sub-section H.2.1. Hence, in most fast acquisition of the tilt series, the Region Of Interest (ROI) appeared to exit the field of view, making any 3D experiment meaningless (see **Figure 29**).

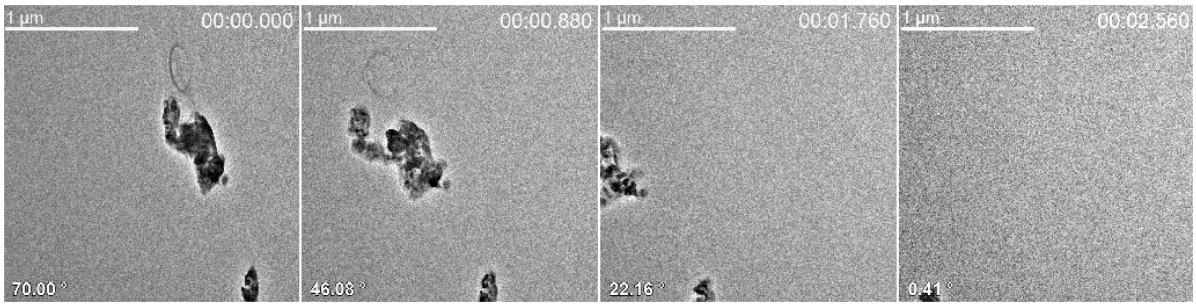

Figure 29: Extraction of a few projections at tilts 70, 46, 22 and 0° from a tilt series recorded with a high rotation speed (time indicated in seconds at the top-right of each image); sample Pd/δ-alumina. Note that the grain of interest exits the field of view after a tilt of only 70°.

We then develop a strategy consisting in:

- (i) Acquiring a 'calibration' tilt series at low mag, from which the trajectory of the ROI was tracked in order to deduce the sets of $\{\delta x(\alpha), \delta y(\alpha)\}$ drifts in any projection acquired at the rotation angle α.
- (ii) Convert the $\{\delta x(\alpha), \delta y(\alpha)\}$ drifts into commands that can be sent to control the image shifts of the microscope, then the in-plane displacements of the ROI to keep it in the field of view during a fast acquisition
- (iii) Record the final tilt series at the desired magnification

It must be confessed that such an approach is not new since acquisition of tilt series using predicted specimen movements has been developed several years ago **[MAS05]**. However, the crucial point here is that our sample is subjected to external solicitations (gas, temperature) and under constant morphological evolution, meaning that not only the acquisition of the final tilt series, but any other operation such as a calibration procedure must be performed as fast as possible in order to reconstruct meaningful data. Our goal was here to stay in the minute range for our calibration routine. A prerequisite for step (i) is that the series of $\{\delta x(\alpha), \delta y(\alpha)\}$ drifts for a given rotation sequence must be reproducible.

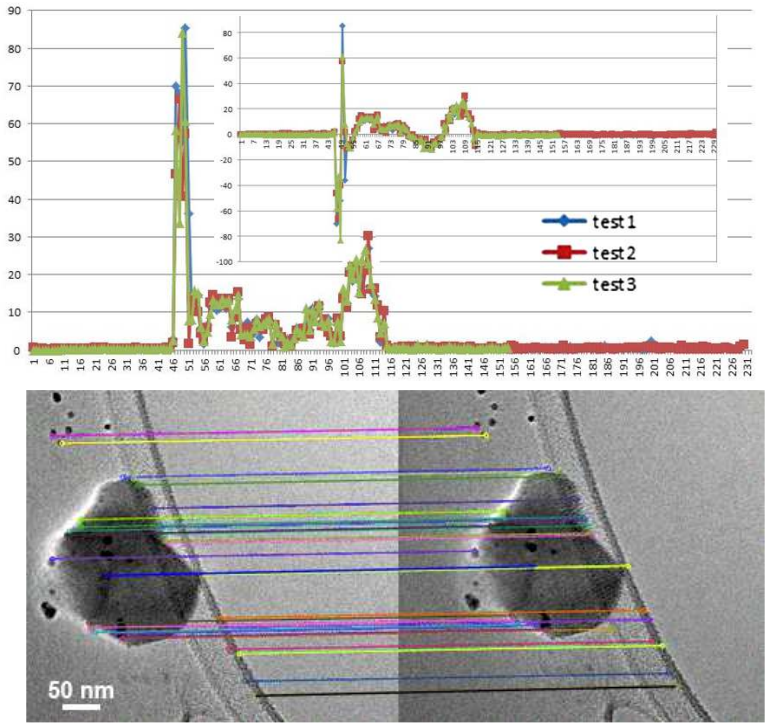

Figure 30: analysis of δx(α) and δy(α) (inset) drifts on 3 repeated tilt experiments, showing that displacements are reproducible. Measurements were performed by tracking dedicated fiducial markers between successive images in each series (bottom).

This was insured through repeated test experiments, as shown in **Figure 30**. To measure the drifts, cross-correlation but also marker-free methods using local descriptors as SIFT, SURF and ORB were tested by Khanh Tran during his master internship in 2016 and partly presented at the EMC2016 conference **[FEN16]**.
The study was pursued from then and a presentation was made at the 19th International Microscopy Congress IMC'19 in 2018 **[GRE18]**.
In addition, Tran's work also dealt with automatic procedures for the selection of blur-free projections, in the spirit of our initial work on blurred/deblurred images.

Image classification was performed according to their sharpness and an algorithm was proposed to remove the blurred images of the sequence by a learning method.
The user has to annotate some images. Features like: contrast, mutual information, mean, standard deviation, number of key points identified by the SIFT algorithm, texture parameters, are used for classification. A first sorting of the characteristics was done on the basis of the ROC (Receiver Operator Curve) curves. Several classifiers were then tested and promising combinations of features were highlighted; although this work was not followed during the continuation of the project.
Regarding the analysis of drift, a fast tracking procedure was developed, based on the Normalized Cross-Correlation in Fourier Space (NCCFS) **[LEW95]** optimizing the following quantity between two images $Im_i(m,n)$ (i=1,2) :

$$\underset{B}{argmax} \frac{\sum_{m,n=1}^{M,N} Im1(m,n).Im2(m,n)}{\sqrt{\sum_{m,n=1}^{M,N} Im2(m,n)^2}}$$

An illustration of the analysis is reported on **Figure 31**. In this case, the original tit series was acquired over a tilt range +71 to -71° at 75% of the maximal rotation speed, leading to 708 (1k)² images acquired in about 7 seconds (acquisition at 100 fps). The full treatment of the series, including decoding the original 'DM4' format of Digital Micrograph™ (the Gatan© software with which images are recorded with the Oneview™ camera), was relatively fast. Adapting the interval between successive images where the analysis is performed, the total duration of the procedure may take less than 10 seconds (40 seconds here with measurements every 5 frames).
This program was developed in C++ and is included in a software suite named 'Fastomo' aiming at proceeding with the next steps (ii) and (iii) previously mentioned: applying corrected drifts during the acquisition of the final tilt series. To achieve this, 'Fastomo' also comprises a routine developed in Visual Basic (Microsoft©) to dialog with

the microscope through the *TEMScripting* protocol provided by the constructor (FEI / Thermo Fischer Scientific©). Its GUI is displayed on **Figure 32**, together with a graph showing the final reduced number of corrected drifts to be applied to the sample.

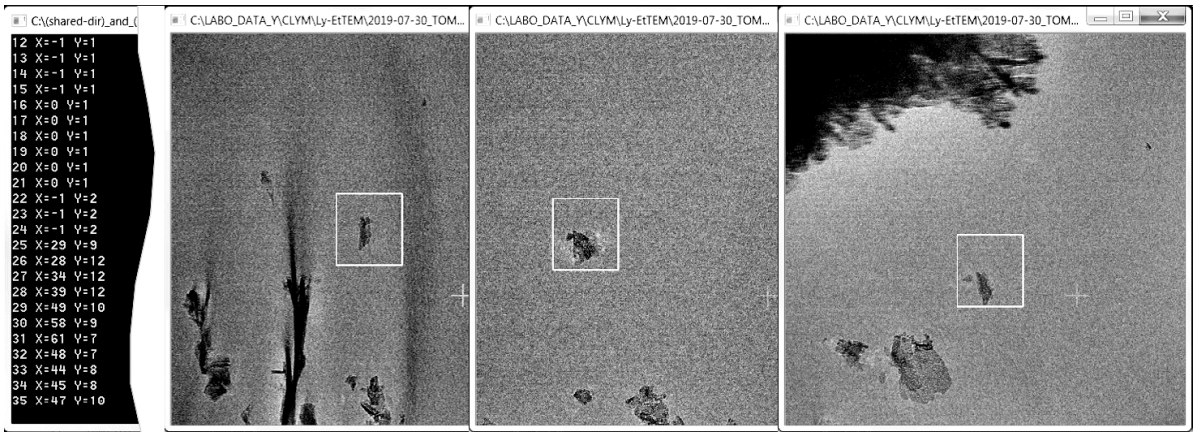

Figure 31 : rapid tracking during the pre-calibration tilt series of the fast tomography process (Pd/δ-alumina sample, ETEM). Examples of a few frames where the ROI (white frame) has been followed (for each frame, X and Y shifts are measured – list on the left, in pixels).

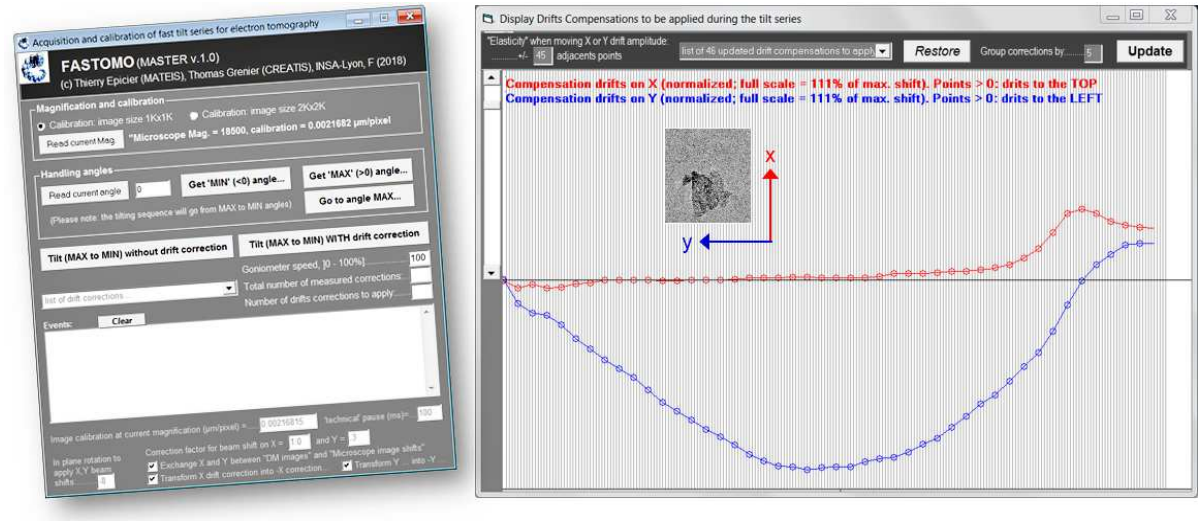

Figure 32 : the 'Fastomo' software developed during the project to keep the ROI in the field of view during fast tilt series acquisitions.

The whole procedure was tested on many examples and is particularly robust with respect to noise (low signal-to-noise ratio) or presence of other objects in the vicinity of the ROI as seen on the frames displayed on **Figure 31**. It was presented in conferences **[GRE18, EPI19b]**. Illustrations of 3D reconstructions performed with the 'Fastomo' approach to characterize the evolution of nanocatalysts under environmental conditions are given in the section H.4 below.

H.3 OPTIMIZED PROCESSING OF THE SERIES FOR FURTHER RECONSTRUCTION

Following the conclusions from sections H.2.2 and H.2.3., the second objective of the WP has been adapted: instead of optimizing the reconstruction algorithm with respect to the presence of potential rotational blur, we focused on penalized iterative reconstruction algorithms that are capable to deal with images presenting a low SNR (including denoising procedures) such as in **Figure 31**. This work was essentially the subject of Hussein Banjak's post-doc stay at CREATIS.

H.3.1. PENALIZED ITERATIVE RECONSTRUCTION ALGORITHMS

Adding a TV prior helps to reduce noise while contours are preserved. This technique, initially proposed for denoising by Rudin et al **[Rud92]**, is widely used in tomography and can significantly reduce artifacts when the number of projections is low and when the tilt angle is limited. The regularized problem consists to solve:

$$\hat{\mathbf{f}} = \underset{\mathbf{f}\in\mathbb{R}^N}{\arg\min} \left\{ \|A\mathbf{f} - \mathbf{p}\|_2^2 + \mu\|\mathbf{f}\|_{TV} \right\}$$

where A is the projection matrix, f is the image of the volume, p is the data volume and mu is the regularization parameter allowing to balance between data-fidelity and prior. During his post-doc, H. Banjak implemented the solution of this problem under the form of the SIRT-FISTA-TV algorithm. Main equations are given below (see details in **[BAN18a]**):

$$\mathbf{f}^{(k)} = \mathbf{f}^{(k-1)} - \lambda \cdot \frac{1}{A^*\mathbf{1}} A^* \left[\frac{A\mathbf{f}^{(k-1)} - \mathbf{p}}{A\mathbf{1}} \right] \quad \textit{(SIRT update)}$$

$$\|\mathbf{f}\|_{TV} = \sum_{i,j,k} \sqrt{(f_{i,j,k} - f_{i-1,j,k})^2 + (f_{i,j,k} - f_{i,j-1,k})^2 + (f_{i,j,k} - f_{i,j,k-1})^2} \quad \textit{(TV regularization)}$$

$$\mathbf{f}^{(k)} = \bar{\mathbf{f}}^{(k)} + \left(\frac{t^{(k-1)} - 1}{t^{(k)}} \right) \left(\bar{\mathbf{f}}^{(k)} - \bar{\mathbf{f}}^{(k-1)} \right)$$

With $t^{(k)} = \dfrac{1 + \sqrt{1 + 4\left(t^{(k-1)}\right)^2}}{2}$ *(FISTA acceleration)*

H. Banjak showed that the total variation prior allows to drastically limit the effect of blur on the final images as illustrated by **Figure 33**. The code was made freely available (https://github.com/CSET-Toolbox/CSET) and is accompanied by a graphical interface.

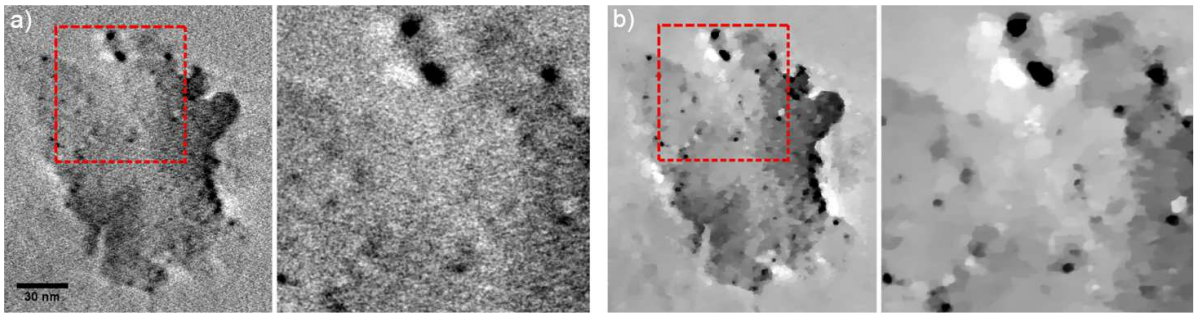

Figure 33 : illustration of the reconstruction of Pd/δ-Al_2O_3 sample using SIRT (a) and SIRT-FISTA-TV (b). XY-plane cross-section in each reconstructed volume is shown first, and a zoom-in on the red rectangular region is illustrated next **[BAN18a]**.

H.3.2. TOMOGRAPHY CODE ON GPU GRID

During the SIRT phase, the iterative algorithm intensively uses the calculation of projections and back-projections. In order to reduce reconstruction time, the use of the GPU is recommended, but owning such a system requires skills, time and budget that are not always available. The Virtual Imaging Platform (VIP, https://www.creatis.insa-lyon.fr/vip/) platform set up at CREATIS allows users, through their own web browser, to run such algorithms on GPUs in cloud computing. A demo version of the code was made available internally on VIP with the help of Sorina Pop (IR, CREATIS) and will be

made publicly available shortly so that any user will then be able to load its own input files (see **Figure 34**) and run his reconstruction.

H.3.3. NEW ALGORITHM FOR TOMOGRAPHIC RECONSTRUCTION AND POISSON NOISY DATA

Electron microscopy data are Poisson distributed, especially for low dose experiments. The problem to solve is thus better modeled by the Poisson likelihood and a penalty that we choose as the TV norm:

$$f^* = \arg\min_f \{\langle Af - p\log(Af), 1\rangle + \mu\|f\|_{TV}\}$$

This problem can be solved with the primal-dual algorithm of Chambolle and Pock **[Cha11]** or one of its accelerated versions. One single loop is then used, and at each iteration first the log-likelihood then the TV norm are decreased. The inconvenient is that a relatively large number of iterations is necessary and each projection/back-projection is relatively expensive. Within the PhD thesis of Y. Feng on single particle emission computed tomography imaging with the Compton camera, we developed a new MAP-EM method, based on two nested loops **[MAX18]**. The external loop is intended to reduce the log-likelihood through MLEM (Maximum Likelihood Expectation Maximization) algorithm. The internal loop is a new Poisson denoising algorithm based on a dual formulation in the spirit of the Chambolle's TV denoising algorithm **[Cha04]**.

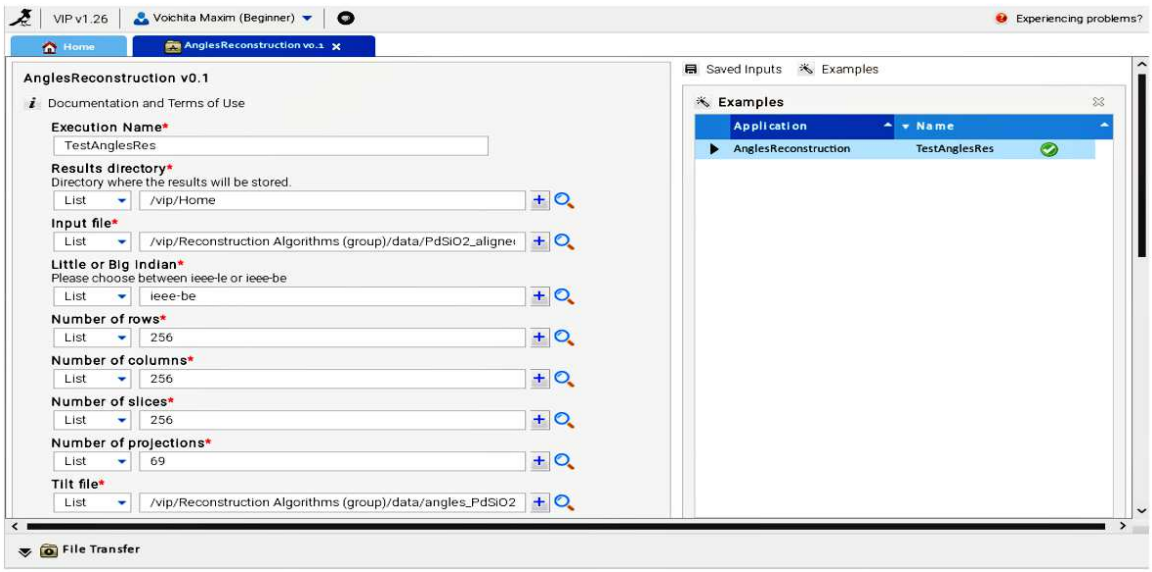

Figure 34: VIP user interface to start using the reconstruction algorithm.

The number of projections/back-projections is reduced with this approach. The method is proven convergent and is numerically fast as FISTA acceleration can be applied. A first attempt of application to TEM data was made during the internship of Benjamin Ganguet, where real data from MATEIS and IPCMS were used (see **Figure 35**). We observed a faster convergence and the missing wedge artefacts seem slightly reduced compared to other iterative algorithms. Due to weaknesses in the evaluation process, the study is restarted within the running short-term post-doc of Y. Feng, and also within the thesis of T. Leuliet (start October 2019). The method was also applied in a more difficult configuration to Monte Carlo simulated data in Compton camera image reconstruction **[FEN19]**. With the new branch that is being added to the code we hope to obtain faster convergence and better agreement with Poisson noise in low-dose acquisitions. As a perspective, this method should be well adapted to direct electron counting detectors and fast tomography.

H.3.4. MACHINE LEARNING APPROACH TO IMPROVE THE 3D RECONSTRUCTION

Convolutional Neuronal Network methods for tomography. Machine-learning approaches were initiated during the last months of Hussein Banjak's post-doc. A convolutional neural network was trained for TV denoising **[BAN18b]**. CNN's allow to fasten the denoising step (see **Figure 36**) and we expect them to learn the regularization parameter. Machine learning methods could bring various improvements in inverse problems resolution. We recently initiated a work on this topic with a main focus on medical applications (thesis of T. Leuliet, started October 2019).

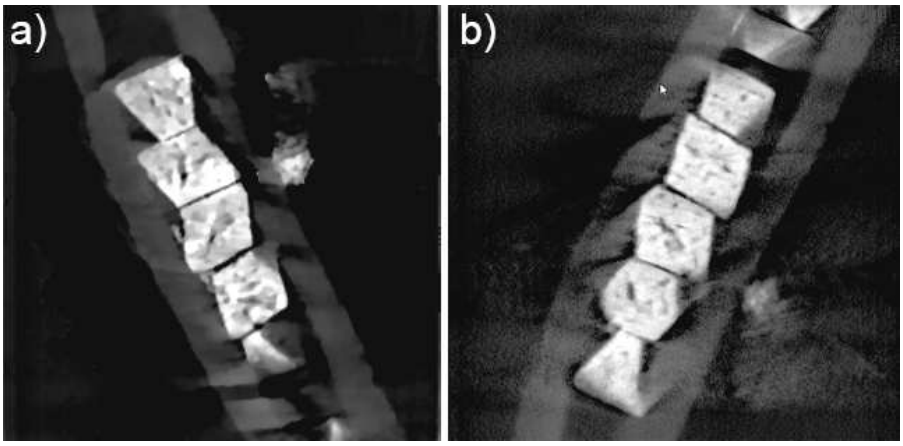

Figure 35 : MAP-EM (left) vs OS-SART (right) reconstruction of a CoOCNT sample (experimental Electron Tomography data provided by IPCMS).

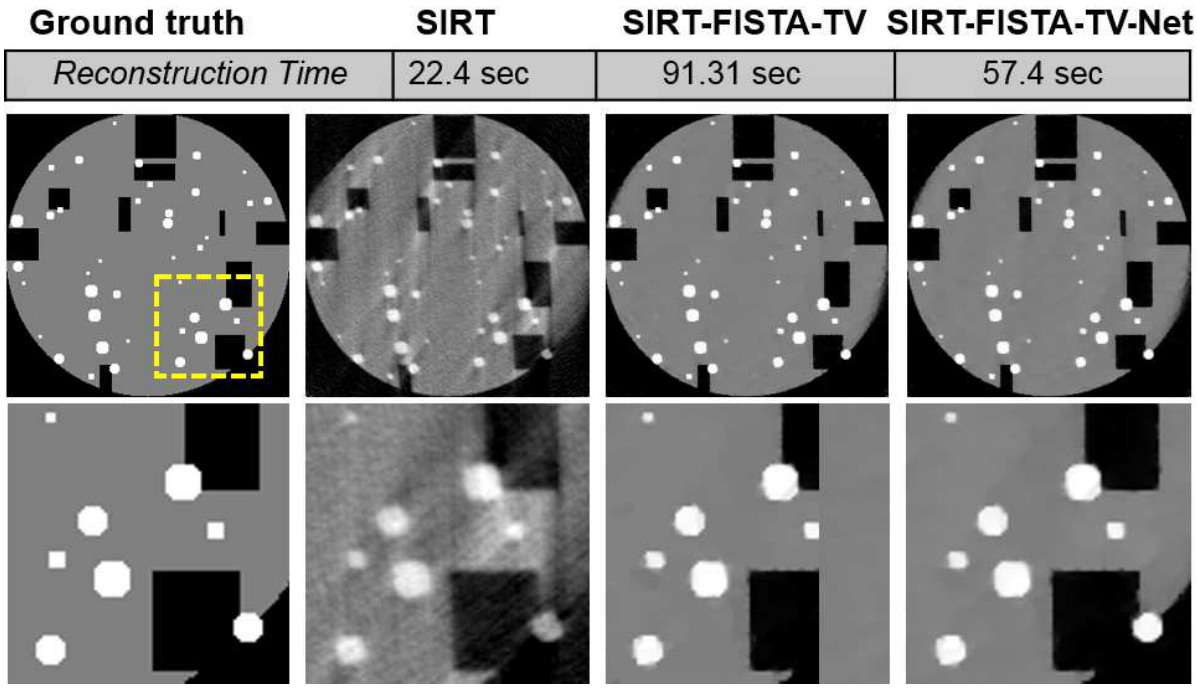

Figure 36 : Illustration of the CNN-aided version of the SIRT-FISTA-TV program introduced on **Figure 28** and **Figure 33**.

H.4 APPLICATIONS OF THE FASTOMO APPROACH TO NANOCATALYSTS

All developments reported in sections H.2 'experimental aspects) and H.3 (reconstruction algorithms) have led MATEIS (with CREATIS and IFPen or with external partners) to perform several experiments where 3D analyses could be made in short

times, down to a few seconds during in situ ETEM experiments. Illustrations of these works can be found in several papers from the semi-fast acquisition approach (**[ROI18, EPI19a, MON19]**) to the fast tomographic approach **[BAN18, ROI18, EPI18a, KON19].**
A typical illustration is given here in the case of the Pd@SiO_2 system presented in ANNEXE F (section F.2.2). **Figure 37** illustrates its microstructure. It is seen that the reduction treatment under hydrogen favors the nucleation of new and very small Pd NPs. This result has also been evidenced during a more complete characterization performed by the partner IPCMS and presented in the ANNEXE I devoted to WP4, section I4). Points out an interesting capability of the Oneview camera acquired during the project. Observing beam sensitive samples, such as silica-based nano-systems, at high resolution is delicate due to the frequent drifts and vibrations induced typically by charging effects and possible irradiation-induced damage (see below for the control of irradiation effects). Recording video sequence at 25 fps in the 4k format, or 100 fps in 2k such as reported in **Figure 38** allows to select the best (sharpest) images, and/or average aligned frames to gain in terms of SNR, as it was done for the micrograph shown in **Figure 37b)**.

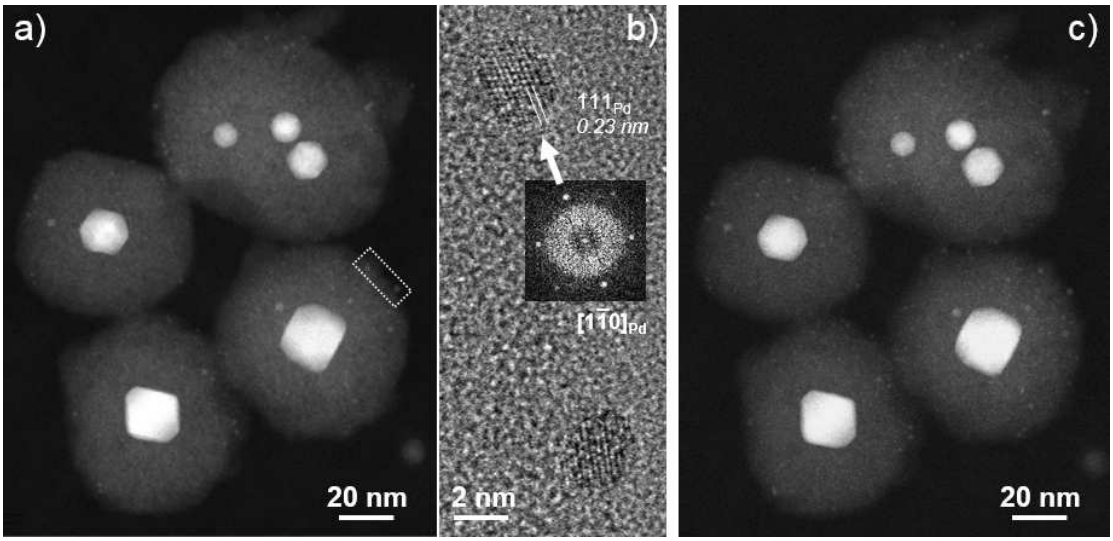

Figure 37: microstructure of several Pd@SiO_2 elementary units (STEM imaging in a) and c), HRTEM in b), ETEM, MATEIS-CLYM). a): Image at 20°C showing large Pd NPs embedded into the silica beads; note the presence of a few small NPs - dotted rectangle enlarged in b) -. b): HRTEM identification of the fcc structure of palladium. c): Same as a) but under 20 mbar at 400°C; note that a few more tiny NPs are detected.

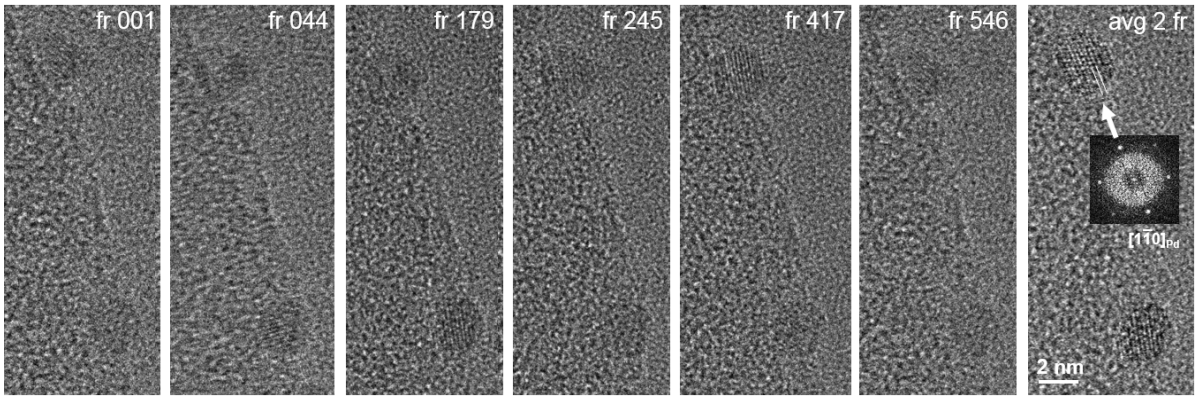

Figure 38: about the interest of a rapid camera for High Resolution imaging of 'unstable samples'. Series of a few frames extracted at random from a 5.46 seconds video sequence recorded in the 2kx2k binning mode at 100 fps. Note that some frames are totally blurred due to uncontrollable movements of the sample, some do not exhibit any lattice fringes due to the probable constant motion of the NPs. Very few of them are 'sharp', which can nevertheless be selected and averaged (2 frames averaged for the image at right, reproduced in **Figure 37b)** (ETEM, MATEIS-CLYM).

We planned to perform a 3D-ETEM experiment to follow in situ the reduction of the system in order to test the efficiency of the silica shell embedding the Pd NPs to their coalescence (or sintering). At this point, the sensitivity of the material to electron irradiation has to be considered: **Figure 39** shows that preserving its integrity during exposure to the electron beam requires a drastic control of the total electron dose, meaning a time limitation depending the electron flux. These constraints were taken into consideration for performing a 3D analysis of the evolution of a Pd@SiO_2 when heated from 20 to 400 and 500°C under 4 mbar of hydrogen. The results **[KON19]** are illustrated by **Figure 40**. It is first seen that the 'fastomo' approaches allowed to keep the sample under a total electron dose lower than that deduced from the irradiation test reported in **Figure 39**. Moreover, acquisitions performed in a few seconds (as indicated) exclude any signification evolution of the aggregate during the tilt series, thus allowing realistic 3D reconstructions, cf. **Figure 40b)**. Despite the SiO_2 'protection', it is further seen that some coalescence occurs since the number of detected NPs decreases, with a slight increase in the average size. Finally, it is seen that rounding of the cuboctahedra-type NPs occurred under reduction at 400 and 500°C, cf. **Figure 40c)**; this means a possible decrease of the active surfaces of the nanocatalysts.
Interestingly, similar experiments on the same system have been performed in the HPEC at IPCMS, but under higher pressure of hydrogen **[BAA18]**. Although the evolution of facets for the cubic NPs is confirmed in both experiments, some difference is found regarding the mean size evolution, see section I.4 in the next ANNEXE and.

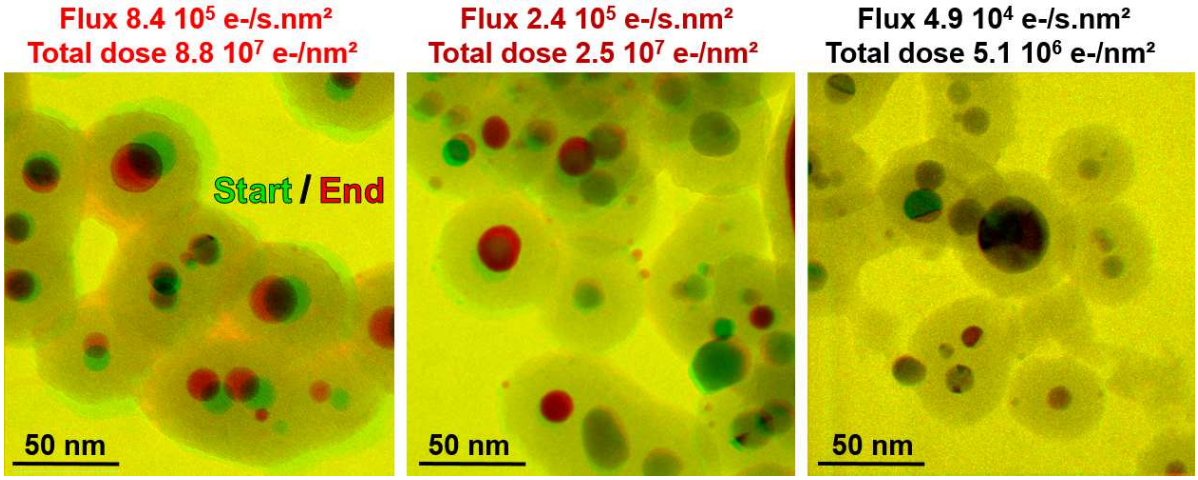

Figure 39: 'accelerated' irradiation test of Pd@SiO_2 aggregates under 4 mbar H_2 at 500°C during 106 seconds under different electron flux (and total cumulative doses). IN each case, the starting and ending frames of image series are superimposed in colors in order to easily visualize any morphological evolution.

H.5 REFERENCES

[BAA18] W. Baaziz, M. Bahri, A S Gay, A. Chaumonnot, D. Uzio, S. Valette, C. Hirlimann, O. Ersen, *Nanoscale*, **10** (2018) 20178.
[BAN18a] H. Banjak, T. Grenier, T. Epicier, S. Koneti, L. Roiban, A-S. Gay, I. Magnin, F. Peyrin, V. Maxim, "Evaluation of noise and blur effects with SIRT-FISTA-TV reconstruction algorithm: Application to fast environmental transmission electron tomography", *Ultramicroscopy*, **189**, (2018), 109. doi.org/10.1016/j.ultramic.2018.03.022; hal.archives-ouvertes.fr/hal-01812662.
[BAN18b] H. Banjak, T. Grenier, T. Epicier, L. Roiban, V. Maxim, Deep Neural Network for Iterative Image Reconstruction with Application to Fast Environmental Transmission Electron Tomography, mini-oral à IMC19, 19th International Microscopy Conference, Sidney, Australia, 9-14 September 2018, imc19.com.
[CHA04] A. Chambolle, *J. of Mathematical imaging and vision*, **20** 1-2 (2004) 89.
[CHA11] A. Chambolle, T. Pock, *J. of Mathematical Imaging and Vision*, 40 1 (2011) 120.

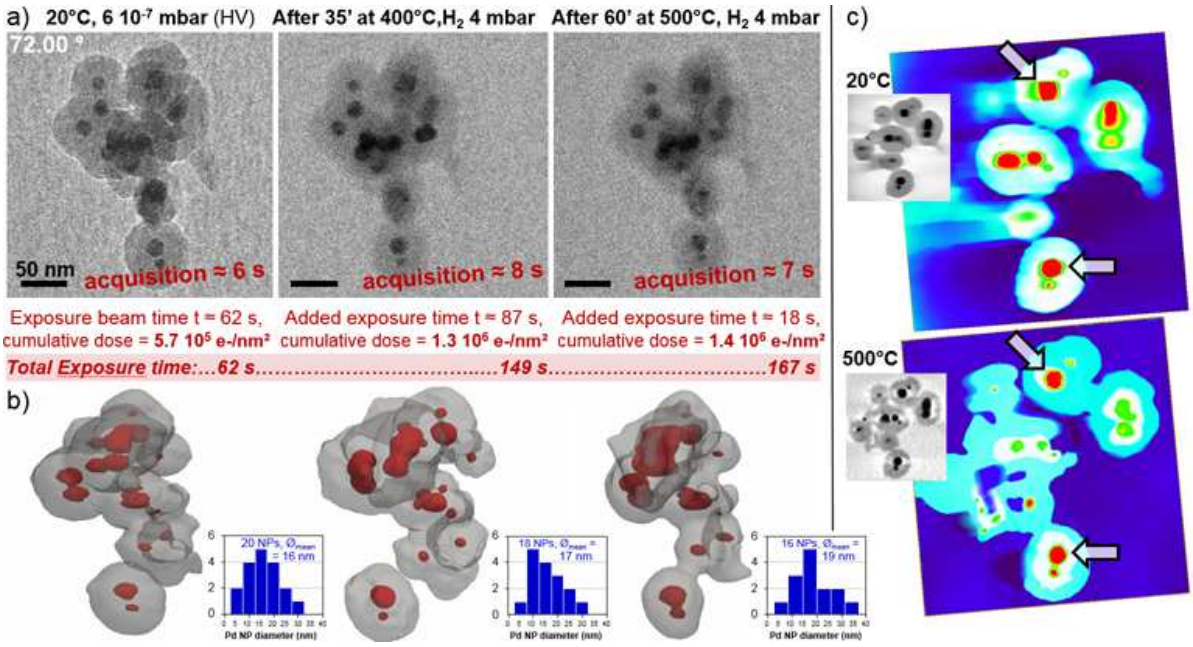

Figure 40: Summary of the in situ 3D analysis of a Pd@SiO2 aggregate during reduction under hydrogen up to 500°C. a): Snapshots of the first frame of the tilt series from +72 to -71°; acquisition time of each 'fastomo' sequence (2k² images, 100 fps) are indicated, as well as the beam exposure and electron dose values (see text for comments). b): Projections of the 3D reconstructed models with the histograms of measured Pd NPs. c): Orthoslices from the volumes at 20 and 500°C oriented in a way to evidence the rounding of facets (arrows) due to the reduction treatment (see text for comments and **[KON19]** for more details; ETEM, MATEIS-CLYM).

[EPI17] T. Epicier, S. Koneti, L. Roiban, D. Lopez-Gonzalez, P. Vernoux, Real time 3D Environmental TEM in-depth study of catalytic soot combustion on Zirconia-based catalysts, presentation orale à MMC2017: Microscience Microscopy Congress 3-7 July 2017, Manchester, UK.
[EPI18a] T. Epicier, H. Banjak, A-S. Gay, T. Grenier, S. Koneti, V. Maxim, L. Roiban, *Microsc. Microanal.* **24**, 1 (2018), 1814. Doi : 10.1017/S1431927618009558
[EPI18b] T. Epicier, S. Koneti, L. Roiban, A-S. Gay, A. Cabiac, 2D and fast 3D in situ calcination and reduction of pd nanocatalysts supported on alumina in Environmental Transmission Electron Microscopy, oral à Matériaux 2018, 19-23 Nov. 2018, www.materiaux2018.fr/, https://hal.archives-ouvertes.fr/hal-01934081v1.
[EPI19a] T. Epicier, S. Koneti, P. Avenier, A. Cabiac, A-S. Gay, L. Roiban, *Catalysis Today*, **334**, 15 (2019), 68; doi.org/10.1016/j.cattod.2019.01.061; hal.archives-ouvertes.fr/hal-02151239.
[EPI19b] T. Epicier, T. Grenier, H. Banjak, V. Maxim, S. Koneti, L. Roiban, Fast acquisition of tilt series in environmental tem tomography: tips and tricks, oral au Colloque 2019 de la Soc. Française des Microscopies (SFμ), 2-5 Juillet 2019, Poitiers, F. hal-02378507.
[FEN16] Y-M. Feng, K. Tran, S. Koneti, L. Roiban, A-S Gay, C. Langlois, T. Epicier, T. Grenier, V. Maxim, Image deconvolution for fast Tomography in Environmental Transmission Electron Microscopy, Proceed. EMC2016, doi: 10.1002/9783527808465.EMC2016.6973.
[GEM15] M. Gemmi et al., J. Appl. Cryst. **48** (2015) 718.
[GRE18] T. Grenier, L. Roiban, H. Banjak,S. Koneti, V. Maxim, T. Epicier, oral à IMC19, 19th International Microscopy Conference, Sidney, Australia, 9-14 September 2018, imc19.com.
[KON17a] S. Koneti, F. Dalmas, L. Roiban, T. Epicier, Fast high resolution 3d microstructural characterization of nanoplatelet-filled polymer nanocomposites, EPFLyon 2017: 16th European Polymer Federation Congress, 02-07 July 2017, Lyon, F.
[KON17b] S. Koneti, L. Roiban, D. Lopez-Gonzalez, P. Vernoux, T. Epicier, Real time 3D Environmental TEM in-depth study of catalytic soot combustion on Zirconia-based catalysts, poster à Microscopy & Microanalysis 2017 in St. Louis, Missouri, USA, August 6-10, 2017.
[KON19] S. Koneti, L. Roiban, F. Dalmas, C. Langlois, A-S Gay, A. Cabiac, T. Grenier, H. Banjak, V. Maxim, T. Epicier, Materials Characterization, 151 (2019) 480; doi.org/10.1016/j.matchar.2019.02.009; https://hal.archives-ouvertes.fr/hal-02151235.
[LEW95] J.P. Lewis, *Vision Interface*, (1995) 120
[MAS05] D. Mastronarde, *J. of Structural Biology* **152** (2005) 36–51.

[MAX18] V. Maxim, Y. Feng, H. Banjak, E. Bretin, *preprint, (2018).*
[MES07] C. Messaoudi, T. Boudier, C. Sorzano, S. Marco, *BMC Bioinformatics 8* (2007) 288.
[MON19] A. Monpezat, S. Topin, V. Thomas, C. Pagis, M. Aouine, L. Burel, L. Cardenas, A. Tuel, A. Malchère, T. Epicier, D. Farrusseng, L. Roiban, *ACS Appl. Nano Mater.* **2**, 10, (2019), 6452. DOI : 10.1021/acsanm.9b01407; https://hal.archives-ouvertes.fr/hal-02354958.
[NAN14] B.L. Nannenga et al., *Nature Methods* **11** (2014) 927-930.
[ROI18] L. Roiban, S. Li, M. Aouine, A. Tuel, D. Farrusseng, T. Epicier, J. of Microscopy, 269, 2 (2018), 117, https://doi.org/10.1111/jmi.12557; https://hal.archives-ouvertes.fr/hal-01612818.
[RUD92] L.I. Rudin, S. Osher, E. Fatemi, *Physica D: Nonlinear Phenomena*, **60** 1-4 (1992) 259.
[Sha08] Q. Shan, J. Jia, and A. Agarwala, *ACM Trans. Graph*., **27** 3 (2008) 73.

I APPENDIX 4: WP 4 - ENVIRONMENTAL MICROSCOPY ON SELECTED CATALYTIC SYSTEMS

I.1 RECALL OF THE DEFINITION OF THE TASKS

Duration	2.5 years
Objective	- perform an operando characterization of catalysts "in function" at the finest scale permitted by environmental approaches within Cs-corrected environmental microscopes (ETEM and HPEC) - compare in situ results to ex situ 'before' / 'after' results - bring new insights in the understand of the behaviour of catalysts during the calcination an activation phases; correlate the results with catalytic performances of the studied systems - provide new quantitative tools in environmental 3D / gas analysis
Responsible	Thierry Epicier (MATEIS)
Partners	Ovidiu Ersen (IPCMS) + Anne-Sophie Gay (IFPEN)
Deliverables	. Environmental TEM experiments: report and publications . Computer routines for the optimized processing (deblurring / denoising) of the series for further reconstruction. . Quantitative morphological analysis of results obtained on catalysts followed in environmental microscopy (ETEM and HPEC).
Contribution	MATEIS/IPCMS internal resources and facilities; about 72 H.M (including non-permanent staff)
Risks and failback solutions	*Low risk: from the point of view of environmental TEM, MATEIS-CLYM will have already a 2 and a half years feedback on conducting such experiments; IPCMS will have almost a one year expertise; the additional expertise of IFPEN in the field of catalysis will insure good interpretation skills. CREATIS is a specialist in image processing and analysis especially in complex cases of 3D approaches of "dynamic objects" (breathing patients, organs in function).*

I.2 PD/DELTA-ALUMINA CATALYSTS

1.2.1. SIZE DISTRIBUTION DURING CONDITIONING

We only present results obtained on the Pd / δ-alumina system introduced in ANNEXE F (section F.2.2.). The first objective of the ETEM experiments performed at MATEIS were to compare size distributions at each state of the conditioning treatments when performed either ex situ or in situ in the microscope under environmental conditions. For the latter observations, typical microstructures are reported in **Figure 41**.

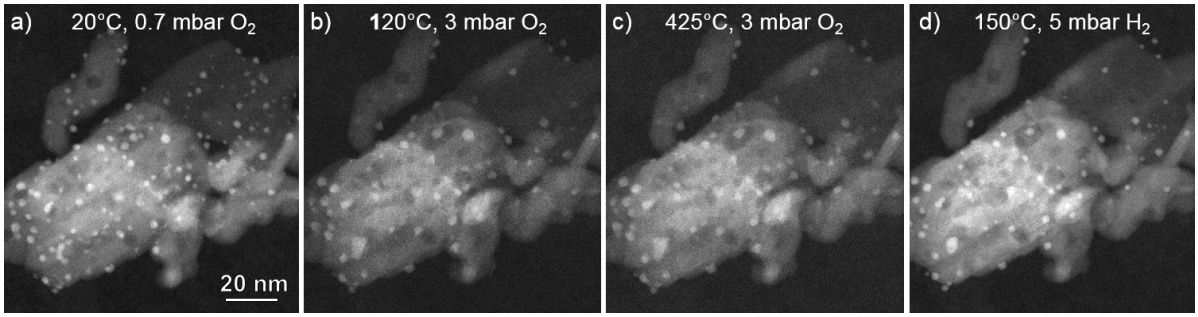

Figure 41 : Evolution of the population of Pd NPs supported on d-alumina in the IMPREGNATED, DRY, CALCINED and REDUCED states as obtained during in situ treatments in the ETEM microscope (STEM images, 300 kV).

A size evolution is clearly visible by eye inspection: at first, Pd NPs grow slightly from the IMPR to the DRY and CALC state, which is consistent with the occurrence of some

coalescence as mentioned in section F.2.2 after ex situ treatments. Moreover, a size increase due to the re-oxidation of particles that have undergone an undesirable reduction under the high vacuum of the microscope just after the introduction of the sample cannot be ruled out (a 15% volume increase is expected according to crystallography during oxidation of Pd into PdO **[EPI19]**. This point will be re-discussed briefly in the next sub-section.

In a second step, NPs clearly decrease in size during the reduction process (from c) to d) in **Figure 41**, owing to the volume variation evoked above. Regarding size determination, we have performed several measurements under ETEM conditions during the oxidation processes (drying, calcination), in both TEM and STEM imaging mode, as well as under high vacuum under samples treated ex situ. Results are shown on **Figure 42**.

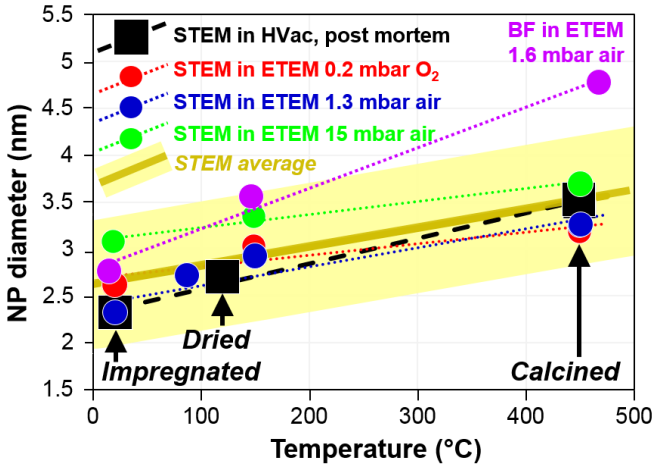

Figure 42: ETEM Size measurements of the Pd NPs

Generally speaking, all measurements give the same (expected) evolution, but it is seen that TEM measurements significantly over-estimated the sizes in the DRY and CALC states. This was mainly attributed to irradiation effects that favor coalescence of NPs under the electron beam, as it has been posted on the web site of the project (top illustration on the page http://www.clym.fr/3DCLEAN_web/3DCLEAN-gallery.html). Taking the average of the STEM measurements, we found the following evolution of the Pd NPs diameter $Ø_{Pd}$:

$Ø_{Pd}$(IMPR) = 2.57 ± 0.5 → $Ø_{Pd}$(DRY) = 3.0 ± 0.5 → $Ø_{Pd}$(CALC) = 3.41 ± 0.5 nm

These values are slightly higher than those reported in ANNEXE F (Table in F.2.2) after ex situ treatments, but the relative increase is very similar (about 19 % from the DRY to the CALC state in the Table in ANNEXE F, 14 % here).

I.2.2. Atomic resolution imaging of Pd transformations

Other results on the Pd / δ-Al_2O_3 system concern the structural evolution by atomic imaging in both TEM and STEM modes as reported on **Figure 43**. Taking care of irradiation effects, the reduction of PdO_x oxides into metallic fcc Pd has been followed in situ under environmental conditions. Note that in each case, the *same* NP has been characterized, which is one of the advantages offered by in situ ETEM observations.

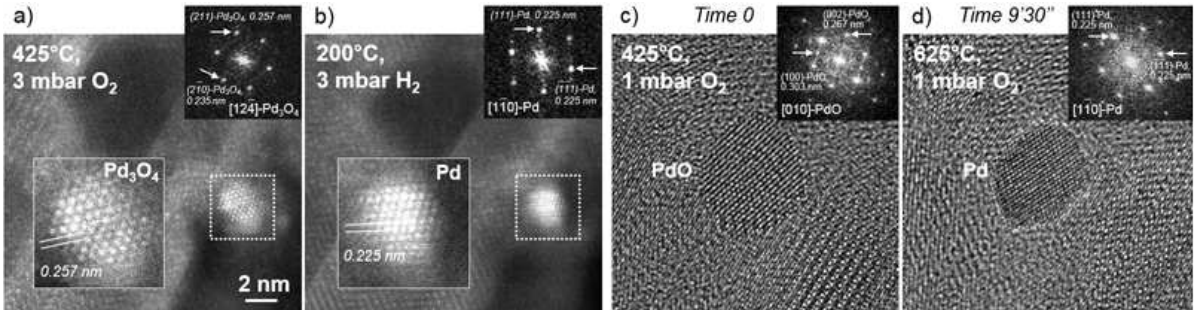

Figure 43: High Resolution imaging of the reduction of Pd oxides: a-b) in STEM mode, c-d) in TEM mode (ETEM 300 kV, MATEIS-CLYM).

Interestingly, the PdO structure is known to easily destabilize even under an oxidizing atmosphere: according to KETTELER et al. **[KET15]**, PdO decomposes around 600°C under an oxygen partial pressure of 1 Torr (see **Figure 44**). A spectacular demonstration of this effect has been obtained in the ETEM

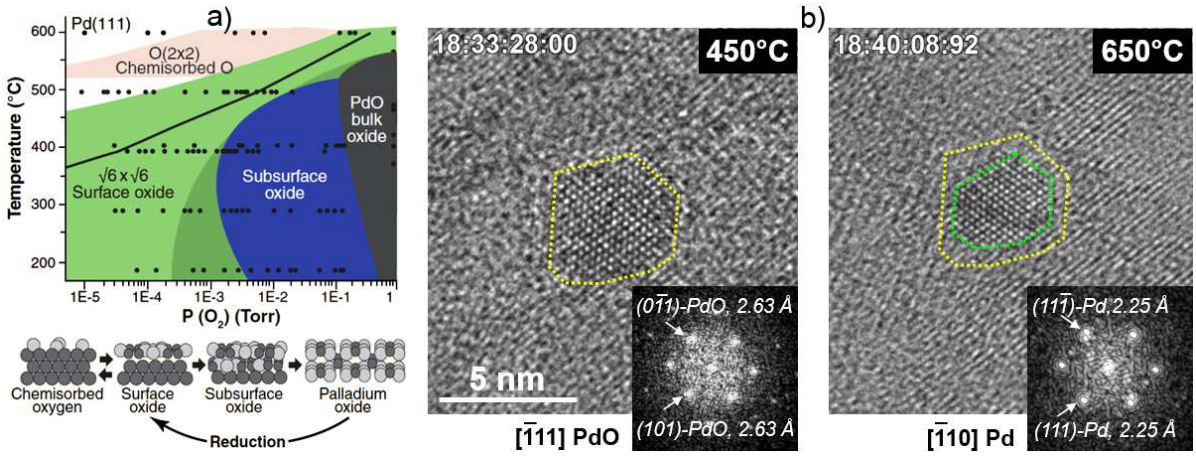

Figure 44: Decomposition of PdO under oxygen. a) Graph of the Pd/PdO equilibrium as a function of temperature and oxygen partial pressure (from [KET15]). b-c): Tracking of the evolution of a PdO NP between 450 and 650°C under 1 mbar of oxygen. During a continuous temperature ramp performed in 7 minutes, a tetragonal PdO NP (b), left) gets 'reduced' into metallic fcc Pd (b), right). The beam is kept blank about half of the time; irradiation experiments performed with the same electron flux but keeping the temperature equal to 450°C confirm that no 'reduction' occurs. (ETEM 300 kV, MATEIS-CLYM).

I.3 CO NANOCATALYSTS FOR THE FISCHER-TROPSCH REACTION

I.3.1. CONTEXT OF THE APPROACH

The Fischer-Tropsch (FT) synthesis is an efficient process to produce high quality hydrocarbon molecules from the conversion of natural gas, biomass or coal. The generic reaction given in ANNEXE F (section F.3.1) is recalled here:

$$(2n+1)\,H_2 + n\,CO \rightarrow C_nH_{2n+2} + n\,H_2O$$

In this synthesis, heterogeneous catalysts, made out of metallic nanoparticles (Fe, Co, Ni, Ru) dispersed onto alumina, silica or titania supports, are generally used. To improve the catalytic performances (activity, selectivity, stability), there is a need to better understand their behaviour during the time on stream. To understand mechanisms such as the catalysts activation and stability/deactivation, numerous studies using *in situ* and *ex situ* techniques have been used. Here, we present an *operando* TEM approach that associates an *in situ* TEM and a residual gas analyzer (RGA), to probe catalysts under experimental conditions simulating their activation, operation, and deactivation.

I.3.2. RESULTS

Urchin-like Co nanostructures

During Kassiogé Dembelé thesis **[DEM17]** involving IFPEN and IPCMS and partly concerned in the 3DCLEANB project, several original Co-based nanostructures have been tested and tried in various gaseous environments, in the perspective of their potential use for the FT synthesis. Main results have been gathered in **[DEM18]** and are briefly illustrated by **Figure 45**.

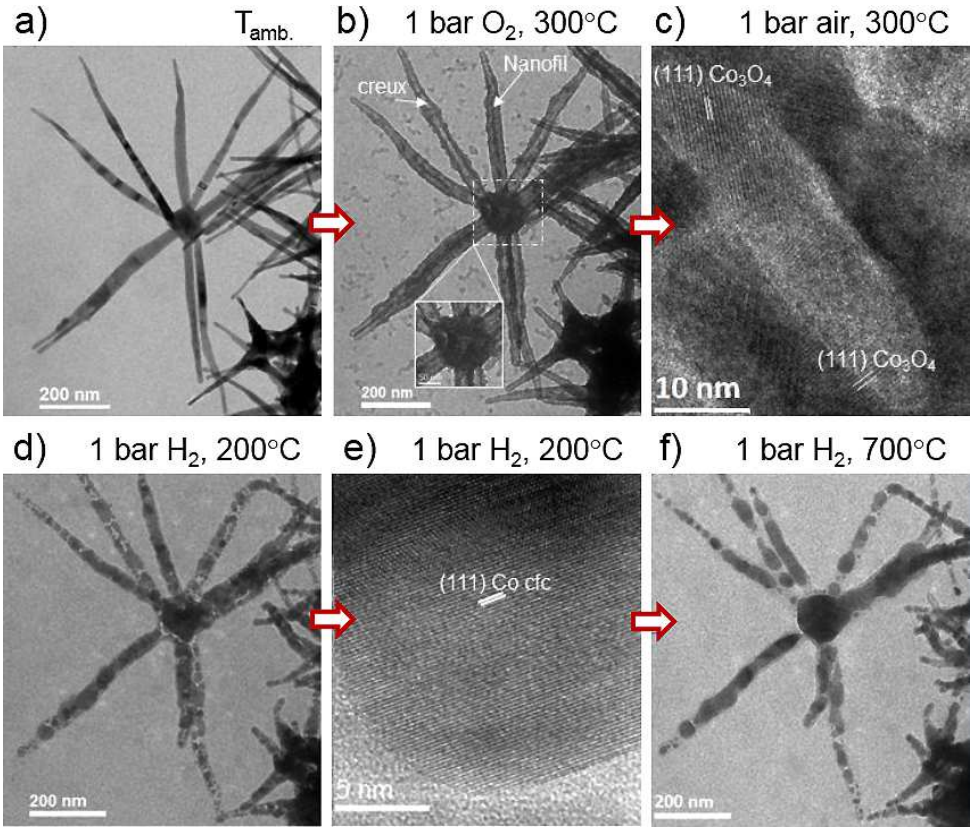

Figure 45: evolution of the Urchin-like Co nanostructures under different gases in the Environmental Cell (E-cell at IPCMS, 200 kV; **[DEM17]**). a-c): Under oxygen at atmospheric pressure; cavities form within the branches of the urchins (Kirkendall effect) before the formation of the oxide Co_3O_4. d-f): Under hydrogen at 1 bar; reduction and tendency to form chains of Co nanoparticles.

Co NPs supported on Al_2O_3 or SiO_2

Using the *operando* tools, cobalt oxide nanoparticles (NPs) supported onto alumina and silica supports have been submitted to different atmospheres and temperatures for gathering a complete knowledge of their stability during the reaction time and to perform a mass spectrometry analysis of the resulting gases. To this end, the systems are firstly observed under the inert argon atmosphere at 200 °C, then activated under pure hydrogen at a temperature up to 430 °C, followed by the operation under syngas (CO/H_2 = 2) at 220 °C and 300-650 °C.

During the catalysts activation, different processes simultaneously occurred as a result of the oxygen removal: the disappearance of the cavity in the Co aggregates; the NPs densification with the decrease of the global size. In addition, the reduction phenomena were faster in the silica support compared to the alumina one, due to a weaker NPs-support interaction with silica support. In the subsequent operation under syngas, we have shown that with the silica support the Co active phase is relatively stable in the FT regime (220°C) for 2h. However, in the alumina support, the NPs reduction was ongoing. By increasing the temperature above 350°C, the NPs were encapsulated by graphitic carbon layers. This was related to the high dissociation of CO which can lead to the CO disproportionation reaction as observed by the mass spectrometry, see **Figure 46**. An additional increase of the temperature to 450 -650 °C showed the catalysts activation toward the growth of carbon nanotubes as reported in **Figure 47**.

In conclusion, by using the *operando* TEM, we have developed a novel approach to follow the reactivity behaviour of Co-based FT catalysts under different atmospheres and temperatures. Thus, this has allowed us to correlate the catalysts modifications to the synthesised products. More generally, this method can be extended to the study of others important catalytic reactions such as the CO_2 methanation, the CO oxidation by *operando* TEM.

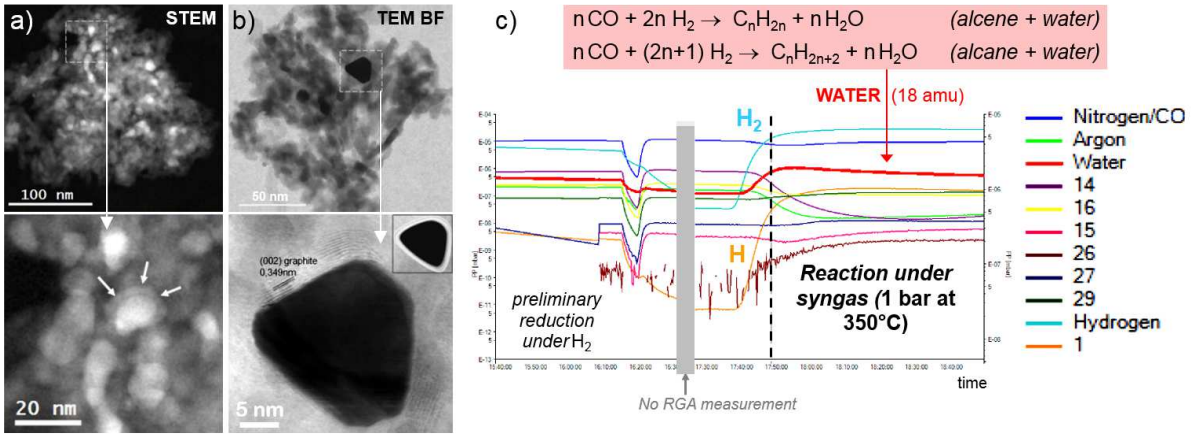

Figure 46: Co / Al_2O_3+SiO_2 catalyst under syngas (1 bar, E-cell, IPCMS). a): STEM image at 350°C; b): TEM bright field image at 450°C: both micrographs show evidence for NP coking. c): RGA analysis showing numerous fragments from hydrocarbon gases as accepted form the reactions shown in insert (adapted from **[DEM17]**).

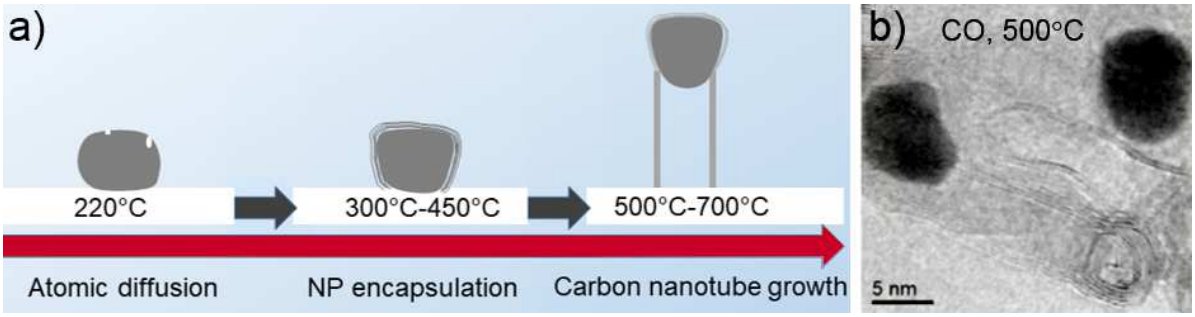

Figure 47: Schematic representation (a) of the reactivity and dynamic behavior of the Co-based catalysts under syngas (mix of CO and H_2 molecules) up to the formation of carbon nanotubes (b) as deduced by environmental gas TEM (E-cell, IPCMS).

I.4 THE PD@SIO2 CATALYTIC SYSTEM

I.4.1. COMBINATION OF IN-SITU ENVIRONMENTAL TEM IN E-CELL AND ELECTRON TOMOGRAPHY ("IDENTICAL LOCATION" TEM APPROACH)

The second system of interest in the WP4 was the core-shell Pd@SiO_2 in which Pd particles with size between 15 and 20 nm and shapes octahedral or icosahedral, are confined inside a porous silica shell (see ANNEXE F, section F2.2). The main idea of this study was to put the basis of an identical location TEM approach allowing to identify some subtle changes at the surface of a catalyst during an in-situ treatment; from a practical point of view, such a study requires to combine the environmental gas TEM at atmospheric pressure with electron tomography performed on the chosen particles before and after the thermal treatment under the reactive gas at atmospheric pressure. The measurements were done on a JEOL 2100 F microscope equipped with tomography capabilities and an Atmosphere™ gas cell from the Protochips Company.

Figure 48 summarizes the main results. Some typical areas containing such nanostructures were followed under H_2 gas at atmospheric pressure during a thermal heating up to 400°C with tomographic data acquired before and after the thermal treatment. The first observation was the formation of new Pd particles with a size of 1±0.5 nm inside the silica shell due to a diffusion mechanism activated around 300°C. One of the original findings was the evidence of a very strong thermal dependence of the shape and faceting parameters depending on the initial crystallographic structure of the particles. The monocrystalline octahedral NPs were found to be quite unstable and get rounded after the heat treatment (see central micrographs in **Figure 48**); the

thermally activated atomic diffusion leads to a decrease in the particle size and induces a high migration kinetic towards the silica shell. As a consequence, new palladium particles have been formed inside the shell and also on their outer surface. The icosahedral-polycrystalline NPs showed a better thermal stability with morphology and faceting globally unchanged: this can be explained by a significant diffusion effect "within" the particle, in agreement with the higher amount of crystallographic defects compared to the single crystal NPs. In this last case, new particles were observed only inside the silica shell and no additional sintering was evidenced.

I.4.2. 3D QUANTIFICATION OF THE CRYSTALLOGRAPHIC FACETS

In the context of this project, we developed also a methodological approach allowing for the identification and the subsequent quantification of nanoparticles crystallographic facets by using as input the 3D data obtained by electron tomography and corresponding 2D high resolution images. In particular, the quantitative analysis of faceting is carried out on the particles 3D model using a geometrical approach that automatically detects planar regions on particle boundaries.

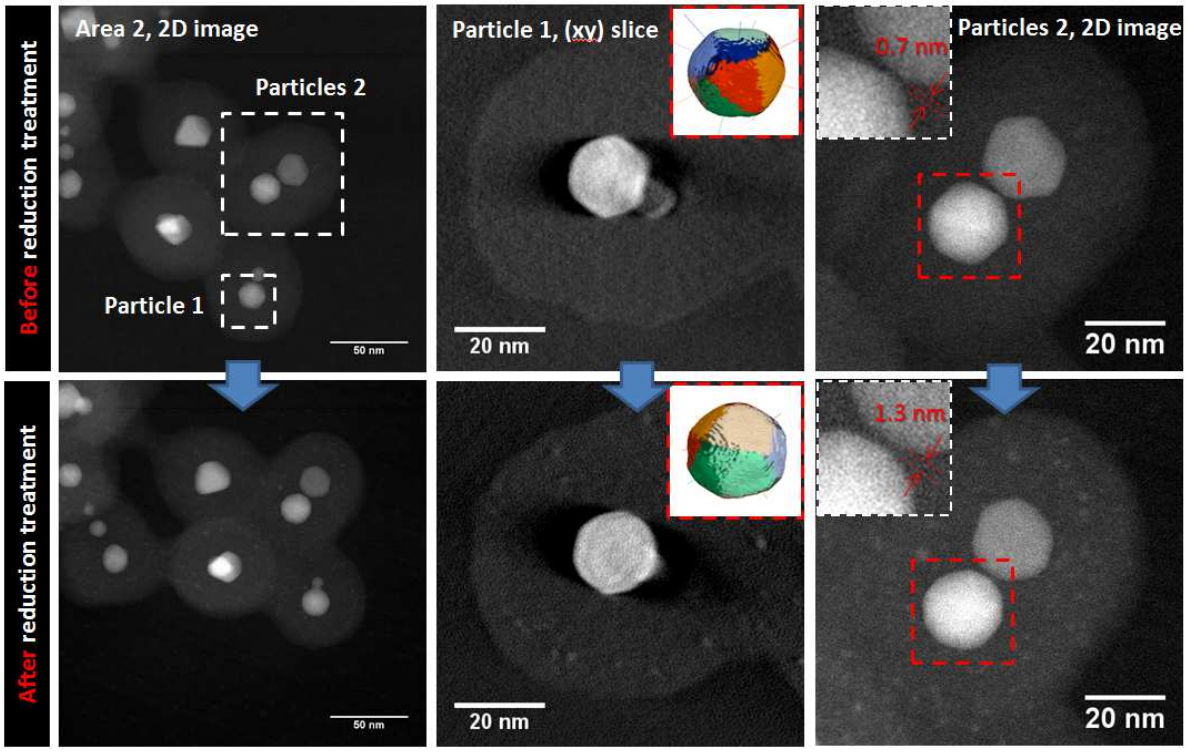

Figure 48: Illustration of the combined environmental TEM – electron tomography approach as applied to the second type of Pd@SiO_2 nanostructures containing icosahedral multiply twinned Pd particles. *Top:* TEM data before the reduction treatment; *Bottom:* same areas and data, after the treatment under hydrogen. *Left:* chosen area for the combined analysis, with the squares denoting the particles analyzed more in detail. *Middle:* corresponding slices extracted from the volume reconstructions of the same nanostructure, before and after the treatment, illustrating similar faceting (inset) as well as the formation of new small Pd nanoparticles in the silica shell after the treatment. *Right:* The thermal evolution of the nanostructure containing two Pd nanoparticles within the same shell.

Quantitative analysis of particle faceting is carried out as follows, using the DESK framework **[JAC12]**: first, each particle surface is extracted from its 3D volume and meshed using the ACVD software **[VAL08]**. The result is a uniform triangular mesh with the number of vertices set to 10000, which provides a good trade-off between smoothness and accuracy given our sampling conditions. A normal is estimated for each vertex by averaging the normals of the triangles around the vertex. Then vertex normals are

clustered in 20 classes using the K-means algorithm. In order to remove small non-planar regions, only the biggest clusters are kept which provides a well identified set of large planar regions. Finally, for each planar region, only the vertices with a normal deviating less than 20 degrees from the region average are considered as belonging to the flat region. This gives a robust vertex count for each planar region, and as the mesh is uniform, the number of vertices inside each planar region is a good approximation of the region area.
In order to check the reliability of our approach, we analyzed palladium particles confined inside a mesoporous silica shell ($Pd@SiO_2$) and at its external surface after an annealing treatment at 250°C under H_2 for 12 h. The application to this system of the as-developed approach is schematically summarized in **Figure 49** below.

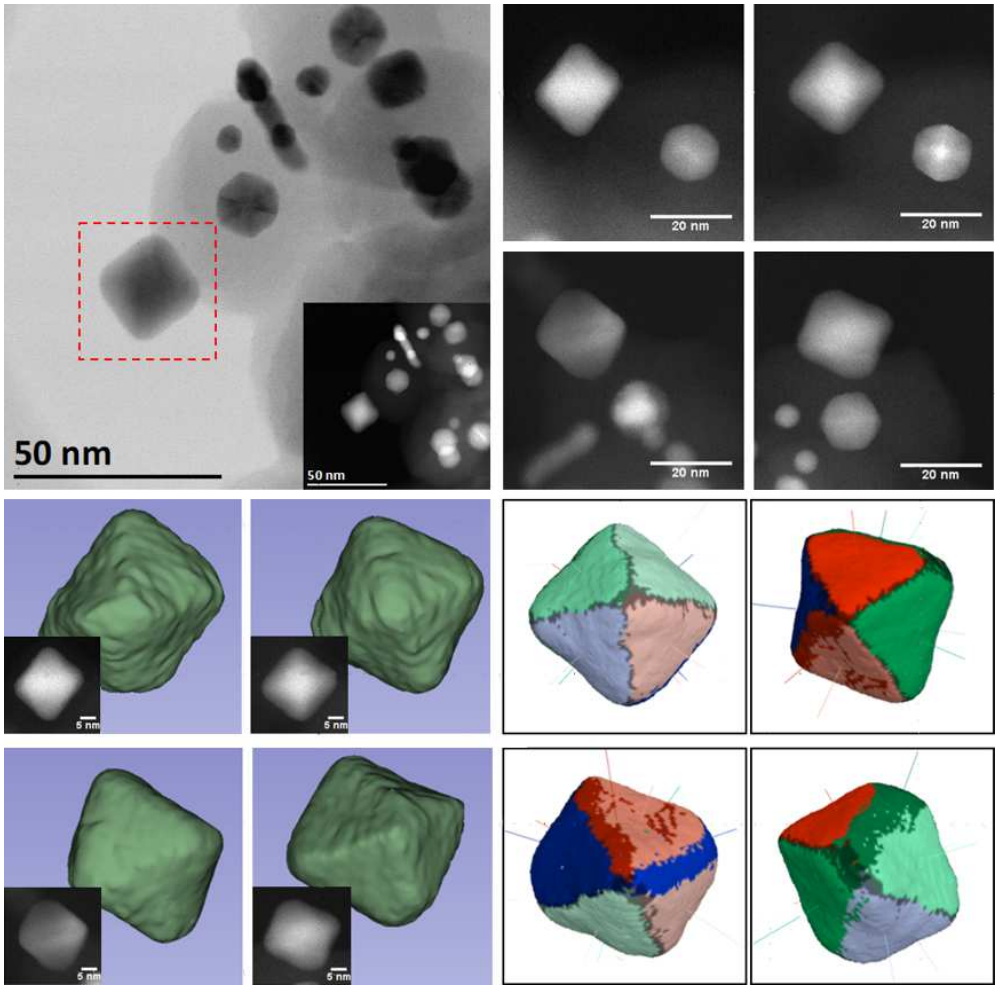

Figure 49 : *Top:* STEM-BF (in inset STEM-ADF) image of a typical Pd particle localized at the outer surface of a silica shell *(left)* and several STEM-ADF images extracted from the tilt series of the chosen area *(right)*. *Bottom:* 3D model obtained by electron tomography, using a data segmentation procedure, of the particle highlighted in the first image *(left)* and the decomposition of the 3D model in crystallographic facets *(right)*.

I.5 2D-IMAGE PROCESSING FOR MORPHOLOGICAL ASPECTS

Apart from the numeric treatments performed in 2D for the projections series required for tomography (ANNEXE H), or for the 3D analysis of facets presented in the previous section, a large number of usual morphological operations and analysis were performed especially on all dynamic sequences acquires on all systems, in order to quantify size distributions for example as reported in section H.2.1.
In addition, it is interesting to mention preliminary works performed in order to track the trajectories of NPs, essentially during the calcination process, in order to quantify the size evolution but also events such as NPs coalescence or disappearance. Such measurements

and statistics are relevant for the identification of possible mechanisms leading to a growth of NPs, such as Ostwald ripening and/or coalescence (for a review, see for example **[DEL13]**).
In this context, specific actions have been initiated through the development of the platform PLUG-IM (https://www.plugim.fr) by Maxim Moreaud and co-workers at IFPen, see **Figure 50**). In parallel, MATEIS and CREATIS started to work on the same problematic in collaboration with the team of Prof. Christophe Ducottet at LaHC, University Jean Monnet of Saint-Etienne. This initiative was launched in the frame of local projects supported by Ingé'LySe, the Federation of Research in Engineering from Lyon and Saint-Etienne (ingelyse.com) and by MANUTECH-SLEIGHT, the graduate school of research on the Surfaces Light EngineerinG Health and SocieTy (https://eur-manutech-sleight.universite-lyon.fr/).
Although in both cases no definitive and conclusive results were obtained in the course of the 3DCLEAN, this approach is a promising one for future studies which present a high interest for heterogeneous catalysis, since quantifying and understanding the motion of NPs on their support is essential to prevent extensive NPs growth by coalescence and/or Ostwald ripening process.

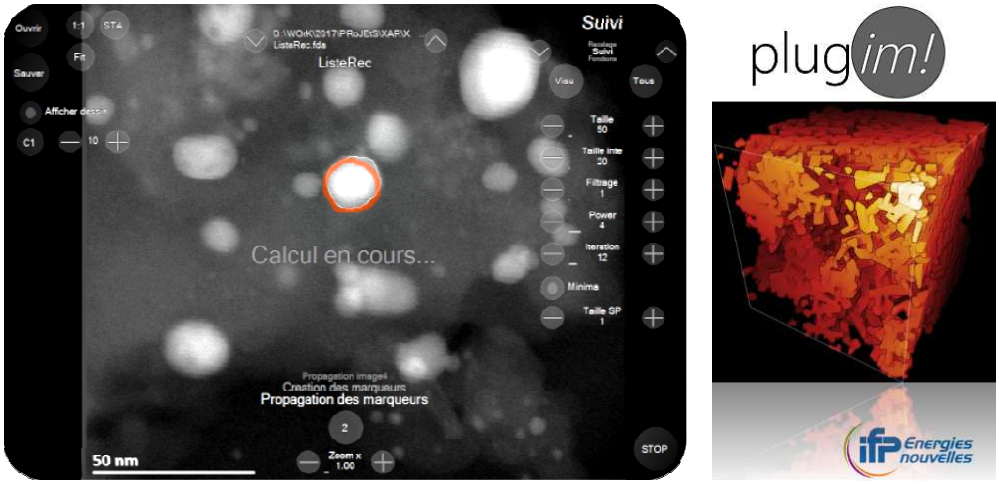

Figure 50: Preliminary work on the automatic identification and tracking of NPs from dynamic sequences of (2D) images during in situ ETEM experiments. *Left:* indicative illustration (case of the Pd / δ-Al_2O_3 system). *Right*: visual of the Plug-IMTM web-platform made available by IFPen for image processing.

I.6 COMBINED ETEM / E-CELL ENVIRONMENTAL APPROACH

I.6.1. CONTEXT AND AIMS OF A COMPARATIVE STUDY

The purpose of this part was to perform a complementary study on the same nanocatalytic material, i.e. Ni NPs on delta-alumina, using both ETEM and E-Cell approach. From an experimental point of view, the consortium has access to a dedicated objective Cs-corrected 300 kV FEI-TITAN ETEM equipped with a DENS Solutions 'Wildlfire' heating specimen holder, for ETEM, and a Protochips 'Atmosphere' E-cell mounted on a probe Cs-corrected 200 kV JEOL 2100F, for E-cell. Both microscopes are also equipped with a Tridiem GIF (Gatan Imaging Filter) and EDX (Energy-Dispersive X-ray spectroscopy) analyzers. From a material perspective, the aim of the study was (i) use each instrument on the best of its own capabilities, under common experimental conditions and oxidizing and reduction atmospheres to study the oxidation and reduction steps of Ni(O).
So, in this combined approach, we intended to compare directly the results in imaging, and chemical analysis (EDX and EELS) obtained under pressure and temperature conditions adjusted to the same values in both the ETEM and the E-cell (i.e. 10 mbar of gases - H_2 or O_2 - and temperatures up to 500°C).

As a remember, the demonstration of the use of the RGA coupled with the E-cell to follow the evolution of the system under a gas mixture H2/CO_2 to study the methanation of CO_2 was presented in ANNEXE G (WP2).

I.6.2. RESULTS ON THE NI / δ-AL_2O_3 SYSTEM

Two systems presented in the previous ANNEXES have been extensively studied on both 'dedicated ETEM' and E-Cell TEM instruments, respectively at MATEIS-CLYM and IPCMS: Pd or Ni NPs on δ-alumina. Although comparative results were obtained on both systems, we only report here the results of the investigation on the Ni / δ-Al_2O_3 system.
The first illustration (**Figure 51**) concerns the reduction, under 10 mbar of hydrogen, of NPs previously properly oxidized in situ. It is seen that both results are consistent, showing a clear reduction at 500°C, evidenced by the densification of the particles **[CHE12]**, as well as crystallographic data (not reported here) and EELS analysis as reported on **Figure 52**. Chemical analyses were also made by EDX and very similar maps were obtained at 400°C under 10 mbar of hydrogen in both cases.

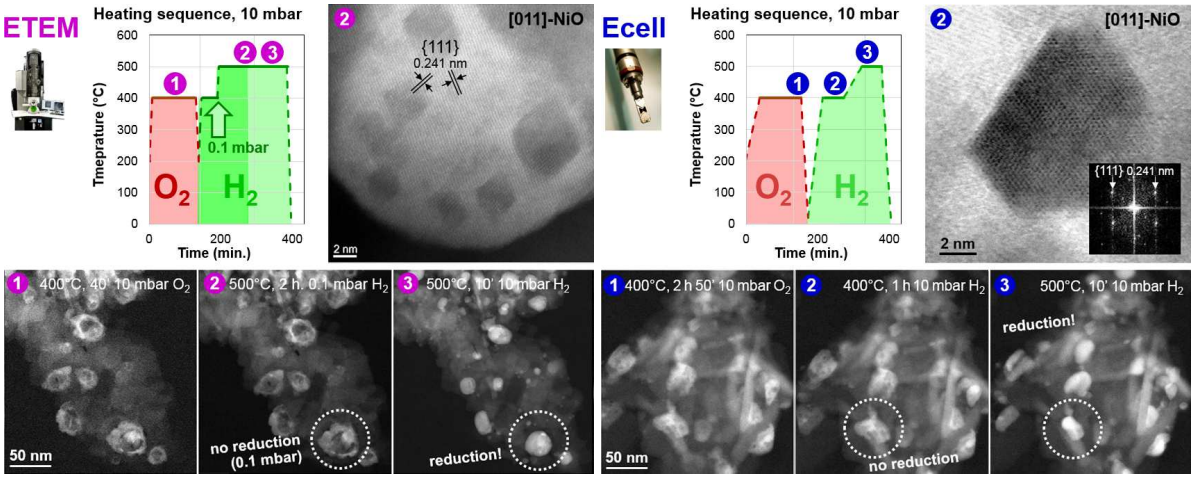

Figure 51: Comparison ETEM (MATEIS-CLYM, 300 kV) vs. E-cell (IPCMS, 200 kV). In situ reduction of pre-oxidized Ni NPs on Al_2O_3. *Left:* ETEM result; the heating sequence is shown, and 3 states (labelled 1, 2, 3) respectively are shown to illustrate the advancement of the reaction. The high resolution STEM image (2) confirms the lattice planes of the NiO cubic phase. *Right:* same presentation as a) for the E-cell results.

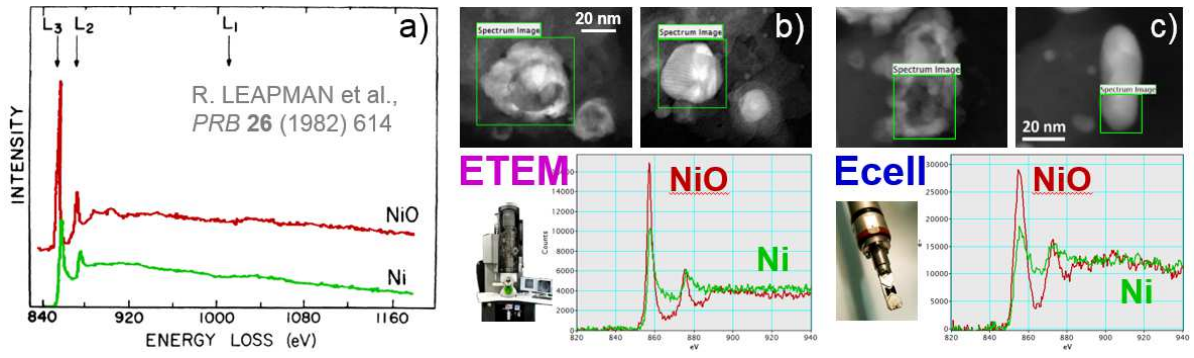

Figure 52: EELS analysis of the Ni-$L_{2,3}$ edge allowing to distinguish the metallic and oxidized states of Ni through the ratio between the L_3 and L_2 lines as reported in the previous literature (a) **[LEA82]** and as measured in both NiO and Ni states in the ETEM (b) and E-cell (c) experiments under 10 mbar of oxygen and hydrogen (left and right micrographs respectively in each case).

Figure 53 concerns the re-oxidation of well reduced samples. Here a difference is evidenced since oxidation is clearly detected at 200°C in the ETEM and seems to start only around 300°C in the Ecell. It is very difficult to evaluate properly the reason of this

discrepancy according to the very different setups used in both experiments; however, a possible explanation could be linked the energy of incident electrons (300 kV in the ETEM and 200 kV with the E-cell, which may favor more reactive conditions in the ETEM.

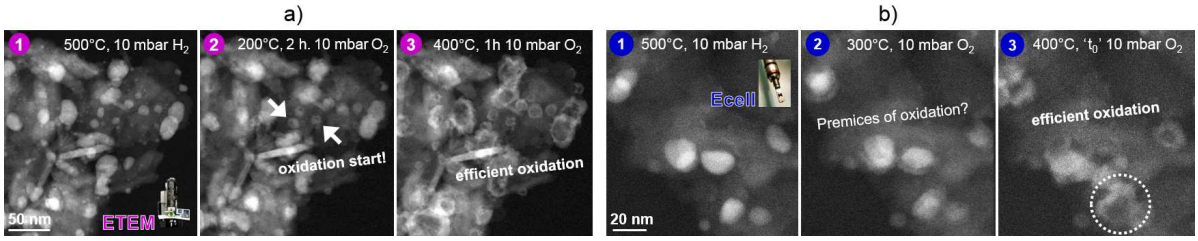

Figure 53: Comparison ETEM in a) (MATEIS-CLYM, 300 kV) vs. E-cell in b) (IPCMS, 200 kV). In situ oxidation under 10 mbar of oxygen of Ni NPs reduced at 500°C (under 10 mbar of H_2).

In parallel to these in situ sequences performed under similar pressures, further experiments (not reported here) were made at 0.1 mbar in the ETEM and 1 bar with the E-cell, conditions that cannot be reproduced respectively on both instruments. At 0.1 mbar, no RedOx reaction was observed within reasonable times of analysis at the temperature previously used. Under atmosphere pressure, it is seen that reduction operates at 200°C (500°C for both instruments at 10 mbar; the oxidation was not checked under 1 bar).

Considering all performances and opportunities offered by one of the two systems, or both of them (high resolution imaging, very low or high - controlled - pressures, tilt capabilities, available space for the specimen), it can be concluded that the dedicated ETEM and the E-cell are really complementary tools for in environmental in situ experiments.
This collaborative work between IPCMS, MATEIS and IFPEN work was presented at the International Microscopy Conference (imc19.com) in 2018 **[BAH18]**.

I.7 REFERENCES

[BAH18] M. Bahri, L Roiban, A.-S. Gay, O. Ersen, T. Epicier, Gaseous Environmental TEM: a complementary study of nanocatalysts using a combined "dedicated ETEM vs E-cell" approach, oral à IMC19, 19th International Microscopy Conference, Sidney, Australia, 9-14 September 2018.
[CHE12] S. Chenna, P. Crozier, *Micron* **43** (2012) 1188.
[DEL13] A.T. DeLaRiva et al., *J. of Catalysis*, **308** (2013) 291.
[DEM17] K. Dembelé, thesis, U. Strasbourg, F, 20/12/20187. http://www.theses.fr/2017STRAE008
[DEM18] K. Dembelé et al., *J. of Microscopy*, **269**, 2 (2018), 168.
[EPI19] T. Epicier et al., *Catalysis Today*, **334**, 15 (2019), 68.
[JAC12] H. Jacinto, R. Kéchichian, M. Desvignes, R. Prost, S. Valette, *A Web Interface for 3D Visualization and Interactive Segmentation of Medical Images, in 17th International Conference on 3D Web Technology (Web 3D 2012), Los-Angeles, USA*, **2012,** 51.
[KET15] G. Ketteler et al., *JACS.*, **127** 51 (2015) 18269.
[LEA82] R. Leapman et al., *PRB* **26** (1982) 614.
[VAL08] S. Valette, J. M. Chassery, R. Prost, *IEEE Trans Visu Comp Grap,* **2008,** 14, 369.

J APPENDIX 5: WP 5 - COMMON MEETINGS, PRESENTATIONS IN CONGRESSES, REPORTS / PUBLICATIONS / PATENTS

J.1 RECALL OF THE DEFINITION OF THE TASKS

Duration	The whole project but reinforced in the second half
Objective	Animation of the consortium; dissemination of results
Responsable	Thierry Epicier (INSA)
Partners	Ovidiu Ersen (IPCMS) + Anne-Sophie Gay (IFPEN) + Voichita Maxim - CREATIS)
Detailed program	Common meetings, reports; National meeting around the IWETEM workshop in 2016
Deliverable	Scientific papers and communications to conferences
Contribution	Internal resources: contribution from all partners; about 24 H.M
Risks and failback solutions	*None; a minor risk exists regarding the arranging and organization of the IWETEM workshop but (i) such an event was already successfully organized by the coordinator in 2013, (ii) it may benefit from the dynamism impelled in France by the 16th European Microscopy Congress held in Lyon in 2016 (EMC2016).*

J.2 SCIENTIFIC MEETINGS IN THE FRAME OF AND AROUND 3DCLEAN

J.2.1. LIST OF INTERNAL MEETINGS WITH PARTNERS.

3DCLEAN meeting in Lyon, 25/07/2017 *(invited in italic)*

The Table below lists all meetings of the 3DCLEAN consortium, excluding frequent exchanges between one or two partners especially those based in the vicinity of Lyon (IFPEN, MATEIS and CREATIS).

Date	Lieu	Partenaires présents	Thème de la réunion
30/11/2015	Lyon	Tous (IPCMS en visio)	Réunion de lancement
13/06/2016	Solaize	Tous	Réunion d'avancement et présentation du post-doc IFPEN
17/01/2017	Strasbourg	Tous	Réunion d'avancement et présentation du post-doc CREATIS
25/01/2018	Solaize	Tous	Réunion d'avancement
22/11/2018	Strasbourg	Tous	Réunion d'avancement
28/02/2019	-	Responsables d'équipe (visio + échanges de mails)	Discussion autour d'une demande de prolongation de 6 mois
02/10/2019	-		Réunion préparatoire à la rédaction du rapport final

J.2.2. GLEEM WORKSHOP (DÉFI CNRS 'INSTRUMENTATION AUX LIMITES', 2016)

In parallel with our scientific program, the initial project was planning to organize an international workshop 'IWETEM' aiming at promoting environmental microscopy, a growing topic in the field of nanomaterials characterization, in the French community. The financial support for this event was cut by the ANR and it could not be organized under the desired form. Dr. O. Ersen and T. Epicier decided then to 'convert' their initiative by depositing a project of Workshop in the CNRS 'DEFI' *Instrumentation aux Limites*, which was indeed accepted and held at CNRS Michel-Ange in Paris on December 13th and 14th (www.cnrs.fr/mi/spip.php?article953). This workshop entitled 'GLEEM' for 'Gas and Liquid Environmental Electron Microscopy' gathered 100 participants in a multi-disciplinary field from medicine to chemistry, nanotechnologies and earth sciences (see illustrations on **Figure 54**). This event allowed to establish a snapshot of the community and its intentions at that time, and further act as a seed for the creation of national GDR 'NanOperando' briefly described in the next sub-section.

Figure 54: photographs from the GLEEM meeting. From top to bottom and left to right: view of the audience (CNRS amphitheater, Michel-Ange site, Paris); invited speakers : Bénédicte Ménez (IPGP), David Portehault (UPMC), Michel Daudon (*Collège de France*) and Dominique Bazin (hospital Tenon), Philippe Vernoux (IRCELYON); wrap-up during the round table (© T. Epicier).

J.2.3. CONTRIBUTION TO THE ACTIVITIES OF THE NATIONAL GDR 'NANOPERANDO'

In 2018, the CNRS (INP) has validated the creation of a GDR devoted to operando studies of nanomaterials concerning hot scientific topics such as (i) the synthesis, structuration and self-assembly of nanocrystals, (ii) the reactivity of nanocatalysts (involving directly the activity of 3DCLEAN), (iii) electrochemistry, (iv) biological materials and (v) life cycle of nanomaterials in biological environments (www.nanoperando.com). Techniques involved in the GDR are synchrotron-based approach and all types of microscopies: optical, near-field or electron techniques. Both IPCMS and MATEIS are active members of this GDR which gather almost 200 researchers from 60 French laboratories. Linked to several contribution form 3DCLEAN, the first national meeting of this GDR was organized in Lyon in 2018 (**Figure 55**).

Figure 55 : Welcome page of the web site of the first Colloque of the GDR NanOperando held in Lyon in November 2018. More than 120 participants (https://nanoperando.sciencesconf.org/).

J.3 OTHER ACTIONS

J.3.1 3DCLEAN WEB SITE

To accompany the project during these last 3 years, a public web site (see **Figure 56**) was maintained by the coordinator, with a 'Members' section dedicated to internal documents such as scientific reports or minutes of meetings.

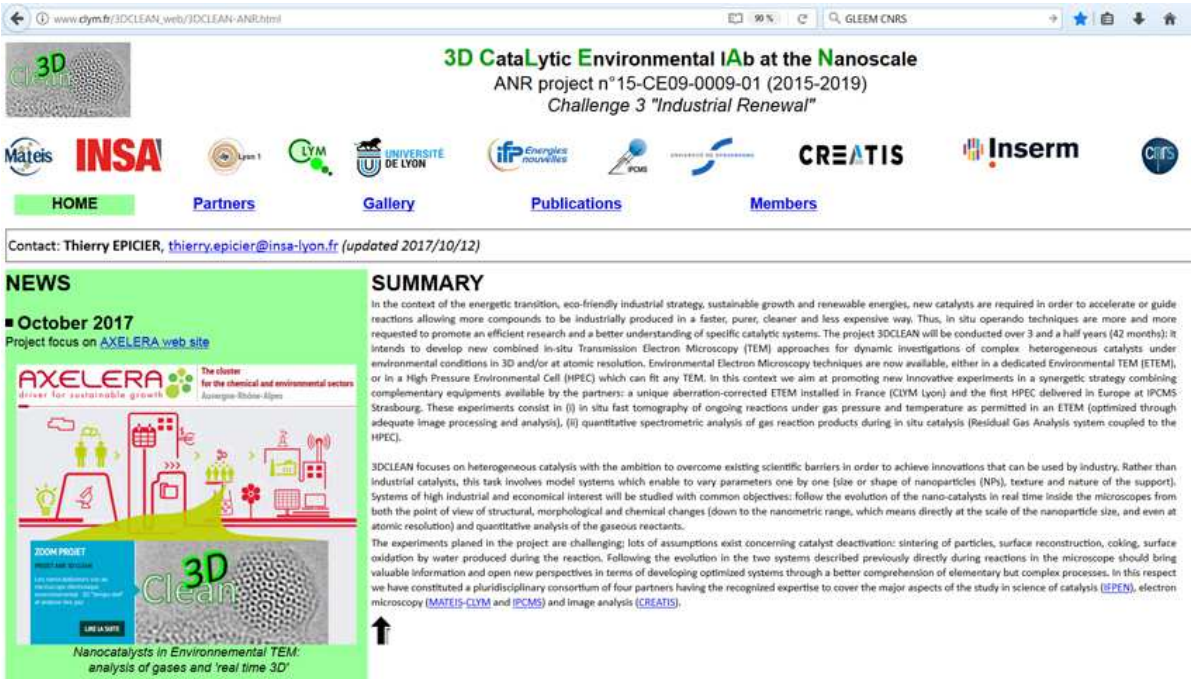

Figure 56 : 3DCLEAN website http://www.clym.fr/3DCLEAN_web/3DCLEAN-ANR.html.

J.3.2 OTHER PUBLICATIONS

To complete the mention of a scientific production induced by the equipments that have been acquired through the project (cf. section C.5; in particular, the Oneview™ camera installed on the ETEM microscope at CLYM on Lyon), we list below 12 publications not directly linked to 3DCLEAN thematics but having used this equipment since it was operating in 2016.

1) I. Trenque, G.C. Magnano, M.A. Bolzinger, L. Roiban, F. Chaput, I. Pitault, S. Briancon, T. Devers, K. Masenelli-Varlot, M. Bugnet, D. Amans. *Shape-selective*

synthesis of nanoceria for degradation of paraoxon as a chemical warfare simulant. *Physical Chemistry Chemical Physics*, **21**, 10 (2019) 5455. DOI: 10.1039/c9cp00179d.
2) I.Z. Jenei, F. Dassenoy, T. Epicier, A. Khajeh, A. Martini, D. Uy, H. Ghaednia, A. Gangopadhyay. *Mechanical response of gasoline soot nanoparticles under compression: An in situ TEM study*. *Tribology International*, **131** (2019) 446.
3) C. Dessal, A. Sangnier, C. Chizallet, C. Dujardin, F. Morfin, J.L. Rousset, M. Aouine, M. Bugnet, P. Afanasiev, L. Piccolo. *Atmosphere-dependent stability and mobility of catalytic Pt single atoms and clusters on γ-Al2O3*. *Nanoscale* **11** (2019) 6897.
4) E. Aneggi, J. Llorca, A. Trovarelli, M. Aouine, P. Vernoux. *In situ environmental HRTEM discloses low temperature carbon soot oxidation by ceria-zirconia at the nanoscale*. *Chemical Communications* **55** (2019) 3876. DOI: 10.1039/C8CC09011D.
5) M. Bugnet, S. Overbury, Z. Wu, F. Aires, Frédéric Meunier, T. Epicier. *Visualizing and Quantifying the Cationic Mobility at 100 Surfaces of Ceria: Application to CO2 Adsorption/Desorption Phenomena in the Environmental Transmission Electron Microscope. Microscopy and Microanalysis,* **24**, S1 (2018) 1940. DOI: 10.1017/S1431927618010188
6) T. Epicier, M. Aouine, F.J. Cadete Santos Aires, L. Massin, P. Gélin. *Experimental Evidence for the Existence of an Iridium Sesquioxide Metastable Phase during ETEM Studies of Methane Steam Reforming on an Ir/$Ce_{0.9}Gd_{0.1}O_{2-x}$ Catalyst*. *Microscopy and Microanalysis* **24**, S1, (2018) 1648.
7) S.K. Cheah, L. Massin, M. Aouine, M.C. Steil, J. Fouletier, P. Gelin. *Methane steam reforming in water deficient conditions on Ir/Ce0.9Gd0.1O2-x catalyst: Metal-support interactions and catalytic activity enhancement*. *Appl. Catal. B-Environ.* **234** (2018) 279. DOI: 10.1016/j.apcatb.2018.04.048
8) Z. Liu, J. Siegel, M. Garcia-Lechuga, T. Epicier, Y. Lefkir, S. Reynaud, M. Bugnet, F. Vocanson, J. Solis, G. Vitrant, N. Destouches. *3D self-organization in nanocomposite layered systems by ultrafast laser pulses*. *ACS Nano* **11**, 5 (2017) 5031.
9) M. Bugnet, S. H. Overbury, Z. Wu, F. J. C. S. Aires, T. Epicier. *Atomic scale environmental transmission electron microscopy study of the surface mobility of ceria nanocubes*. *Microscopy and Microanalysis* **23**, S1 (2017) 898.
10) M. Bugnet, S.H. Overbury, Z. Wu, T. Epicier. *Direct visualization and control of atomic mobility at {100} surfaces of ceria in the environmental transmission electron microscope*. *Nano letters* **17**, 12 (2017) 7652.
11) M. Tonelli, M. Aouine, L. Massin, V.B. Baca, J.M.M. Millet. *Selective oxidation of propene to acrolein on FeMoTeO catalysts: determination of active phase and enhancement of catalytic activity and stability*. *Catal. Sci. Technol.* **7**, 20 (2017) 4629. DOI: 10.1039/c7cy01574g
12) A. Caravaca, S. Picart, M. Aouine, B. Arab-Chapelet, P. Vernoux, T. Delahaye. *Development of highly nano-dispersed NiO/GDC catalysts from ion exchange resin templates*. *Catalysts* **7,** 12 (2017) 368. DOI: 10.3390/catal7120368